7-2-2011

Trends and interannual variability in snowpack and spring season hydroclimatology in the southwestern United States

Sarah J. Keller

Sarah Keller
Candidate

Earth and Planetary Sciences
Department

This thesis is approved, and it is acceptable in quality and form for publication:

Approved by the Thesis Committee:

David A. Fuentes, Chairperson

TRENDS AND INTERANNUAL VARIABILITY IN SNOWPACK AND SPRING SEASON HYDROCLIMATOLOGY IN THE SOUTHWESTERN UNITED STATES

BY

SARAH J. KELLER

B.A., BIOLOGY
UNIVERSITY OF MONTANA, 2005

THESIS

Submitted in Partial Fulfillment of the
Requirements for the Degree of

Master of Science
Earth and Planetdary Sciences

The University of New Mexico
Albuquerque, New Mexico

May 2011

ACKNOWLEDGEMENTS

This thesis would not have been possible, nor the work as pleasant, without contributions from a number of individuals and institutions. I am extremely grateful for support from the New Mexico Experimental Program to Stimulate Competitive Research (NM-EPSCoR), the UNM Department of Earth and Planetary Sciences and the Alfred and Geraldine Wanek Scholarship.

I owe a great deal of gratitude to my advisor, Dave Gutzler. Without Dave's willingness to put a field biologist in front of a computer, I would have been denied the intellectual growth that I found in this work. I appreciate that Dave gave me the freedom to find my own way, but also patiently guided me back on track when I strayed towards the precipice of data analysis despair. Dave's humanity, his genuine interest in my success, and carrot, rather than stick-based, pedagogical style contributed greatly to my quality of life as a graduate student.

It was a joy to work with my committee. They were an efficient group that supported my career goals and I learned much from their individual approaches to science questions.

I am grateful for Joe Galewsky's contributions to my professional and scientific development. Joe's availability to impart facts, philosophy and formal training about numerical modeling enriched my perspective on my own research and scientific prediction in general.

I am thankful for Marcy Litvak's perspective as a biologist and as a field scientist. Marcy ensured that I occasionally emerged from my MATLAB-induced stupor to remember that real plants, not simulated ones, grow in the ground.

My thesis was based almost entirely on output from a single data product and literally would not have been possible without the multi-institution North American Land Data Assimilation System (NLDAS). David Mocko was especially helpful in answering my questions about the data. Dennis Lettenmaier and Brian Cosgrove were also helpful in their correspondence about NLDAS-2 and soil moisture.

Mark Fleharty provided valuable support for using the Department of Planetary Sciences LINUX system and he provided advice that expedited my data processing.

Finally, Jim Curry's unflagging support, incredible patience and empathy for his often-distracted spouse was more than anyone could hope for while earning a graduate degree.

TRENDS AND INTERANNUAL VARIABILITY IN SNOWPACK AND SPRING SEASON HYDROCLIMATOLOGY IN THE SOUTHWESTERN UNITED STATES

BY

SARAH J. KELLER

ABSTRACT OF THESIS

Submitted in Partial Fulfillment of the
Requirements for the Degree of

Master of Science

Earth and Planetary Sciences

The University of New Mexico
Albuquerque, New Mexico

May, 2011

TRENDS AND INTERANNUAL VARIABILITY IN SNOWPACK AND SPRING SEASON HYDROCLIMATOLOGY IN THE SOUTHWESTERN UNITED STATES

by

Sarah J. Keller

B.A., Biology, University of Montana, 2005

M.S., Earth and Planetary Sciences, University of New Mexico, 2011

ABSTRACT

By virtue of its relatively low latitude and already marginal snowpack, especially in Arizona and much of New Mexico, the southwestern U.S. is a compelling location in which to study how temperature and seasonal snowpack interact to affect spring hydroclimatology. Understanding snowpack-mediated spring soil moisture and how observed, current changes in the regional climate affect the snowpack-soil moisture relationship will provide important insights into the current and future hydrology of the southwestern U.S.

In this study, we use newly available data from the North American Land Data Assimilation System (NLDAS-2) Phase 2, run with the Mosaic land surface model, to investigate the effects of recent historical trends and interannual variability (1979-2009) on land surface hydroclimatology in the Southwest U.S. There are multiple feedback mechanisms by which snowpack in the southwestern U.S. may indirectly influence short term and/or long-term climate variability. This study represents the first attempt to use

newly available land surface data to describe the processes by which snowpack alters soil moisture and surface energy fluxes, thus characterizing the potential for land surface-atmosphere interactions to proceed in the southwestern U.S.

We study the period between snow ablation and monsoon onset and find positive linear trends in spring temperature, decreasing linear trends in total precipitation, linear trends towards earlier snowmelt, decreasing linear trends in soil moisture and latent heat flux and increasing linear trends in sensible heat flux and the Bowen Ratio. We find that snowpack alters the magnitude and timing of soil moisture and the surface energy balance, though our sample sizes are small and the sizes of the uncertainties in the means are large. While monsoon onset negates these effects later in the year, decreased snowpack will likely exacerbate temperature-driven warming and drying, months after the complete ablation of snowpack.

NLDAS-2 provides a unique opportunity to consider potential large-scale interactions of land surface hydrologic variables. With additional quantification of how the land surface behaves under changing climate conditions, we may be better able to anticipate future land surface variability and feedbacks and assess model projections with a better foundation of results from current climate change.

Table of Contents

1. INTRODUCTION 1

Research Questions 4

2. DATA AND METHODS 5

North American Land Data Assimilation System Phase 2 (NLDAS-2) 5

SNOwpack TELemetry (SNOTEL) 7

NCDC Climate Data 7

3. TRENDS, VARIABILITY AND CLIMATOLOGIES 13

Introduction 13

Maximum SWE 13

Melt-out day 13

Temperature 24

Precipitation 31

Soil moisture 39

Latent Heat Flux 44

Sensible Heat Flux 49

Bowen Ratio 53

Summary of results 56

4. SNOW WATER EQUIVALENT PREDICTORS 60

Temperature 60

Precipitation 62

Melt date vs. maximum SWE 64

5. SOIL MOISTURE PREDICTORS 66

Monthly mean lagged soil moisture 66

Temperature vs. soil moisture 68

Correlations 68

SWE vs. soil moisture 70

Correlations 70

Precipitation vs. soil moisture 74

Composite analysis of soil moisture 76

Summary of results....82

6. ENERGY BUDGET PREDICTORS.... 84

Soil moisture versus latent heat flux 84

SWE versus latent heat flux 85

SWE versus sensible heat flux....88

Bowen Ratio....90

Energy budget analysis 96

Summary of results....98

7. DISCUSSION AND CONCLUSIONS 100

REFERENCES 109

1. INTRODUCTION

Two major processes, cold season snow accumulation and warm season precipitation, dominate the hydroclimatology of the southwestern United States, with natural interannual and decadal variability influencing both. While the causes of recent and historical droughts in the region remain unresolved, it is clear that temperature has increased in the region during the 20th century, and that alone has had consequences for regional hydroclimatology. Numerous studies have documented rising temperature and altered characteristics of snowpack in the western United States. These changes include the amount and timing of snowpack (Stewart et al. 2004), more precipitation falling as rain rather than snow (Knowles et al. 2003, Barnett et al. 2008) and earlier peak runoff (Stewart et al. 2004, Barnett et al. 2008). Additionally, a growing body of climate projections for the region suggests that the western United States will become more arid with longer drought recovery times (Cayan 2010, Gutzler and Robbins, 2010).

By virtue of its relatively low latitude and already marginal snowpack, especially in Arizona and much of New Mexico, the southwestern U.S. is a compelling location in which to study how temperature and seasonal snowpack interact to affect spring hydroclimatology. The most visible role of snowpack in the hydrology of arid systems is in generating runoff that is crucial to society. A less obvious, though important, role of snowpack is its influence on seasonal soil water content. Through moistening a large area, snowpack enhances soil moisture, thus generating “memory” in the land surface that may persist long after winter storms have passed and the snowpack has ablated. Snowpack-

mediated soil moisture memory may be a source of potential seasonal predictability of subsequent weather. This hydroclimatological aspect of the southwestern U.S. is less well-understood and more difficult to measure than the runoff component of the water budget. Nevertheless, snowpack-mediated soil moisture likely provides an important bridge in surface moisture during the dry period between snow ablation and monsoon onset. Understanding snowpack-mediated spring soil moisture and how observed, current changes in the regional climate affect the snowpack-soil moisture relationship, will provide important insights into the current and future hydrology of the southwestern U.S.

A handful of studies have attempted to address the region's snowpack-mediated soil moisture in the context of seasonal prediction of the North American monsoon (Gutzler and Preston 1997, Gutzler 2000, Lo and Clark 2001, Zhu et al. 2005). Initial interest in the problem arose from the work of Gutzler and Preston (1997) and Gutzler (2000). Gutzler (2000) found a negative, time-period dependent linkage between antecedent land surface condition, specifically 1 April snow water equivalent (SWE) anomalies, and July-August precipitation in New Mexico. The author proposed that surface soil moisture anomalies modulate the surface energy budget, thus altering the land-sea temperature contrast hypothesized to drive the monsoon circulation. Later work (Zhu et al. 2005) examined the proposed snowpack-monsoon feedback mechanism using data from the LDAS land surface model. While the complexity of factors controlling the North American monsoon dictates that an explanation for the role of the land surface in monsoon prediction remains elusive, Zhu et al. (2005) did establish a relationship between winter and early spring SWE and early spring and summer soil moisture.

Even fewer studies have attempted to assess the impact of rising temperature and declining snowpack on regional soil moisture. This likely results from a dearth of long-term soil moisture observations and the difficulties associated with modeling the large-scale evolution of soil moisture. Cayan et al. (2010) simulate future snowpack and soil moisture, identifying possible future decreases in soil moisture and snowpack as well as prolonged drought periods. However, there are still very few studies addressing the processes by which temperature and snowpack interact to modulate interannual variability in surface soil moisture, especially at long temporal and/or large spatial scales.

A reduction in snowpack-mediated soil moisture is also likely to change the surface energy budget of the southwestern U.S. Assuming that there is sufficient moisture for evaporation, energy at the surface will evaporate water rather than heat the surface. Since the southwestern U.S. is usually not sunlight limited, a water deficit at the surface can result in the transfer of more net surface radiation into sensible heat rather than latent heat. Through this process, a positive feedback that acts to increase local temperature may develop. By prescribing multiple levels of depleted soil moisture, and thus reducing evaporative cooling in modeling experiments, Fischer et al. (2007) found that land-atmosphere interaction played an important role increasing maximum daily temperature and European heat wave duration.

The potential for 21st century, long-term, temperature and snowpack-modulated soil moisture declines in the southwest U.S. is alarming from a water resource perspective, as well as from a local warming and drought persistence perspective. While many studies have addressed the potential for soil moisture to generate land-atmosphere precipitation

feedbacks through the surface energy budget (Pal and Eltahir 2001, Zheng and Eltahir 1998, Eltahir and Bras 1996), there is a dearth of studies addressing how projected declines in snowpack might affect that process in already semi-arid or arid regions.

Research Questions

In this study, we use newly available data from the North American Land Data Assimilation System (NLDAS-2) Phase 2, run with the Mosaic land surface model (Koster and Suarez 1996), to investigate the effects of recent historical trends and interannual variability (1979-2009) in snowpack, temperature and precipitation on trends and variability in surface soil moisture and surface turbulent fluxes of sensible and latent heat. There are multiple feedback mechanisms by which snowpack in southwestern U.S. may indirectly influence short term and/or long-term climate variability. This study represents the first attempt to use newly available land surface data to describe the processes by which snowpack alters soil moisture and surface energy fluxes, thus characterizing the potential for land surface-atmosphere interactions to proceed in the southwestern U.S.

We ask the following research questions to examine the indirect consequences of variability in snowpack on climate variability in the southwestern U.S.:

1) **What was the spatial and temporal variability in southwestern U.S. spring land surface condition during 1979-2009?**
2) **How does interannual variability of spring snowpack affect the amount and timing of warm season soil moisture in the southwestern U.S.?**
3) **How do snowpack anomalies influence the surface energy budget throughout the warm season?**

2. DATA AND METHODS

Data Sets

North American Land Data Assimilation System Phase 2 (NLDAS-2)

Studies of trends and variability in land surface hydrology, especially in mountainous regions, are difficult largely because there are few multi-decadal data sets available and spatial coverage is limited. One solution is to use derived quantities of soil moisture and surface fluxes, specifically in the form of output from a land surface model (LSM). Accurate land surface fields are also very important in the initialization of general circulation models (GCMs). In general, land surface models attempt to represent the features and processes of the land surface and possibly sub-surface, with varying degrees of complexity; they may or may not be interactively coupled to an atmospheric model.

NASA's North American Land Data Assimilation System Phase 2 (subsequently referred to as NLDAS-2) is a relatively high resolution (0.125°, 3-hourly) dataset derived from the ingestion of observational data into a LSM via data assimilation. NLDAS-2 was run uncoupled from an atmospheric model, retrospectively, starting in January of 1979 and is now run in near real time. In this study, we use data from January 1979 – December 2009. Parallel versions of NLDAS-2 are based on four different LSMs; we use output from the Mosaic LSM (Koster and Suarez 1996). Ground, satellite and radar based observations of temperature and precipitation initialize NLDAS-2, as well model reanalysis data (Mitchell et al 2004). The model domain focuses on the continental United States where meteorological observations are dense relative to other geographic areas.

NLDAS-2 is a data product in the sense that it ingests a set of observations (forcing data) for each time step and interpolates them over the model domain. In theory, the interpolation of temperature and precipitation observations in NLDAS-2 should provide better spatial representations of those fields than surface observations do. NLDAS-2 is a simulation in the sense that ingested observations are used to force a land surface model that generates fields that were not ingested as observations, such as soil moisture. However, rather than being generated from simulated precipitation and temperature, modeled fields are generated from observations at each time step, theoretically improving the estimates of variables from the LSM.

NLDAS-2 elevation (0.125° resolution) is derived from the U.S. Geological Survey's GTOPO30 Global 30 Arc Second (~1-km) Elevation Dataset (Figure 1). The Mosaic LSM uses sub-grid vegetation tiles with vegetation classification derived from University of Maryland's (UMD) global, 1-km, Advanced High Resolution Radiometer (AVHRR)-based, 13-class vegetation database (Hansen et al., 2000). Detailed information about the application of these vegetation data in the Mosaic model are found in Mitchell et al. (2004).

The snowpack module used in the Mosaic land surface model, as in the other three NDLAS LSM's, balances snowfall input, snowmelt output and snow sublimation. Heat flux through the snowpack is used to change snowpack temperature, phase composition and amount (Pan et al. 2003). Snow energy process in Mosaic is coupled to the energy transfer of the entire LSM so the temperature of soil layers, snowpack layers, and the soil surface is solved from heat balance equations for the entire soil, snowpack, vegetation and air system, along with the water balance equations (Pan et al. 2003). One simplifying

assumption of Mosaic is that rain falling directly onto snowpack is routed directly to the soil surface where it infiltrates or runs off (Koster and Suarez, 1996).

Mosaic has three soil moisture layers to a depth of 200 cm. The first two are in the root zone. We use the 0 - 10 cm layer throughout this study. Mosaic was designed to account for subgrid scale vegetation variability, so each surface layer is divided into a maximum of 10 vegetation tiles, and each tile has its own energy and water balance as well as soil moisture, soil type and temperature. The energy and water balances for each tile are simulated independently, using the one dimensional Richard's equations for the water balance.

SNOwpack TELemetry (SNOTEL)

We compared NLDAS-2 snow water equivalent (SWE) in our study region to SWE from a selection of the Natural Resources Conservation Service's (NRCS) SNOwpack TELemetry (SNOTEL) snowpack and climate monitoring stations. Quality control of SNOTEL data was based on procedures from Serreze et al. (1999).

NCDC Climate Data

We compared NLDAS-2 temperature and precipitation to monthly divisional climate data compiled from co-operative weather stations by the National Climatic Data Center (NCDC) (Guttman and Quayle 1996). NCDC and NLDAS-2 were compared as state-wide (New Mexico and Colorado) means of area-weighted climate divisions and grid cells. NLDAS-2 and NCDC data are not independent because NLDAS-2 aggregates measures of temperature and precipitation, including weather stations that are also used in the NCDC divisional data. However, comparing NCDC and NLDAS-2 provides assurance that the temperature and precipitation fields were not corrupted during model spin-up or data assimilation.

Development of indices and analysis regions

We use empirical orthogonal function (EOF) analysis to identify snowpack-based analysis regions within the Four Corners domain and to develop indices of snowpack variability for the 1979-2009 analysis period. EOF analysis provides an objective means to identify coherent spatial patterns of variability. We develop two snowpack indices, one of snow water equivalent (SWE) amount and one of SWE timing, because it is not readily apparent which of these characteristics of snowpack is more important for climate change detection or for modulating post-snow ablation variability in land surface hydrology.

SWE on April 1 is a commonly employed snowpack index because it coincides with maximum SWE in most high elevation regions of the western U.S (e.g. Cayan 1996). In warmer regions, an earlier measurement of SWE may be a more appropriate proxy for maximum SWE. Rather than use a fixed date throughout the analysis domain, we calculated maximum SWE for each grid cell over the region. Figure 2a shows the 1979 -2009 maximum SWE climatology map for the Four Corners analysis region. NLDAS-2 SWE climatology represents snow distribution in the high elevations of Arizona and New Mexico and shows regions of highest SWE in Colorado's San Juan Mountains and Utah's La Sal Mountains. We used the annual anomaly maps of maximum SWE, without de-trending, to generate a map of the first empirical orthogonal function (EOF1) and a time series of the first principal component (PC1) of maximum SWE (figure 2c and figure 3, respectively).

We selected two major regions of coherent variability from the EOF1 map in figure 2c to generate spatially averaged time series. We call the region encompassing Northern New Mexico and Southern Colorado and a small portion of Utah, "NM" (northern mountains or New Mexico) for the remainder of this document. We call the averaging region that

encompasses much of the Mogollon Rim and the Arizona high elevations the “AZ” averaging region. The entire analysis domain is called the Four Corners, or “FC” region (Figure 1). These regions were selected based on their coherent variability in the EOF1 map, their geographic coherence and because they may be important regions for snowpack – monsoon feedbacks (Gutzler 2000).

We define the snowpack melt out day as the number of days into the water year (WY), starting in Oct 1, at which snowpack is no longer present in any specific grid cell or observation site, and remains absent for seven days. The criterion for snowpack presence was not checked until February 1 (123 days into the water year) to ensure that true spring snow ablation would be detected. We applied EOF analysis to the SWE melt day in the FC region (WY 1980-2008) to develop an index of SWE melt timing.

Throughout this study, we refer to variables averaged during the period between snow ablation and monsoon onset as “interim”. The interim period was calculated for each year using the snow ablation index discussed above, and a monsoon onset index. Monsoon onset is defined as three consecutive days at the Albuquerque airport with a dew point greater than 47°F, after May 15 (Higgins 2008). The snow ablation and monsoon onset indices were then used to extract and composite daily values from the variables of interest. Seasonal mean values for each year of soil moisture, turbulent fluxes and precipitation were calculated from the time series of these interim daily values. We compare the time series of land surface hydrologic variables to temperature and precipitation, and to each other, using correlation analysis. We reference the Pearson correlation coefficient (r-value) throughout the study. Correlation coefficients are referred to throughout as weak ($r = |0 - 0.40|$),

moderate (r =|0.40-0.70|) or strong (r =|0.70-1.0|). Spatial averages are compared, as well as the leading PCs of the variables of interest. References to correlations of spatial averages refer to the temporal correlation between two spatially averaged time series.

We focus throughout the study on the leading covariance-based EOF (EOF1) and its corresponding PC (PC1), as these explain the largest amount of the variance in the data. When trend maps of NLDAS-2 data are referenced, they refer to the map of the linear least squares regression estimate of the slope at each grid cell. When statistical significance is referenced, it refers to a two-tailed t-test at $\alpha = 0.05$.

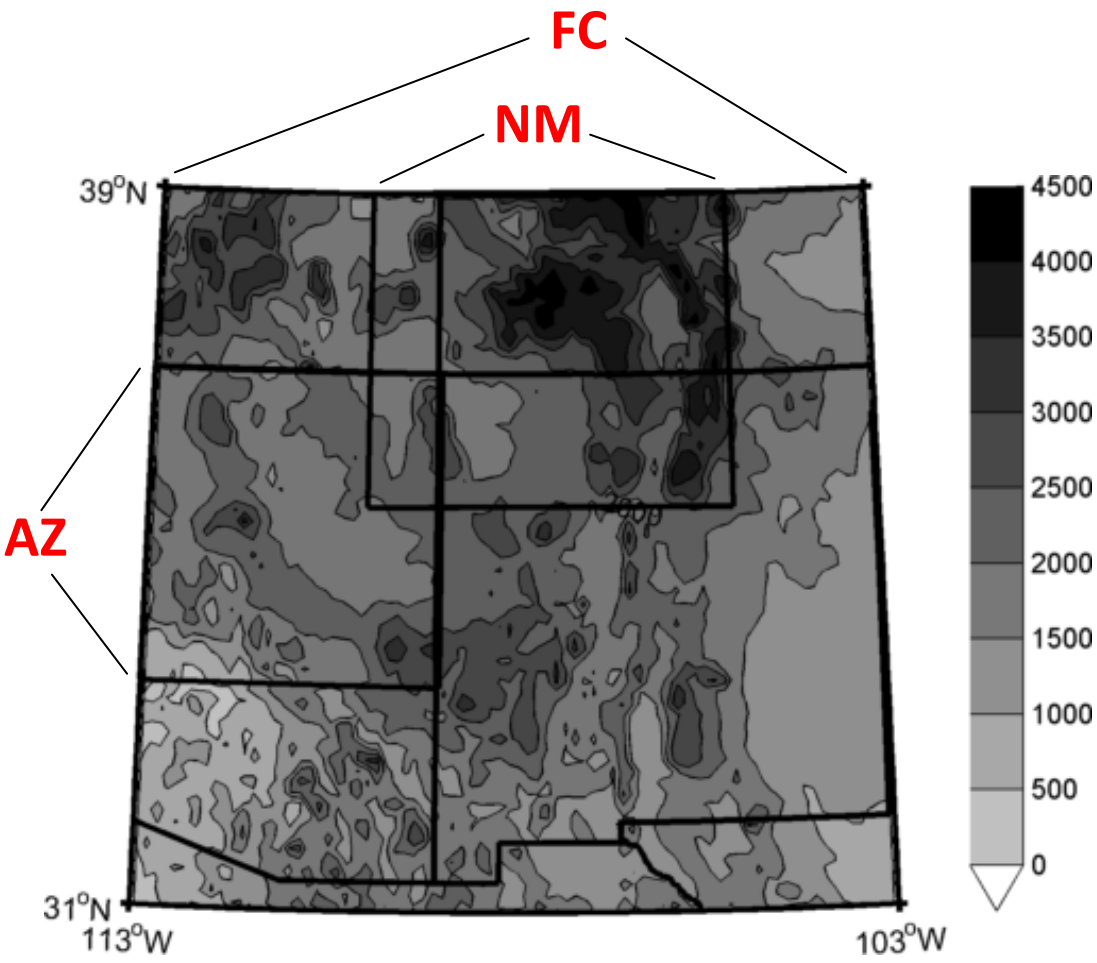

Figure 1. NLDAS-2 0.125° elevation (meters) map for the Four Corners region, based on the USGS GTOPO30 Global 30 Arc Second Elevation Dataset from NLDAS-2. Boundaries for the FC, NM and AZ averaging regions are shown.

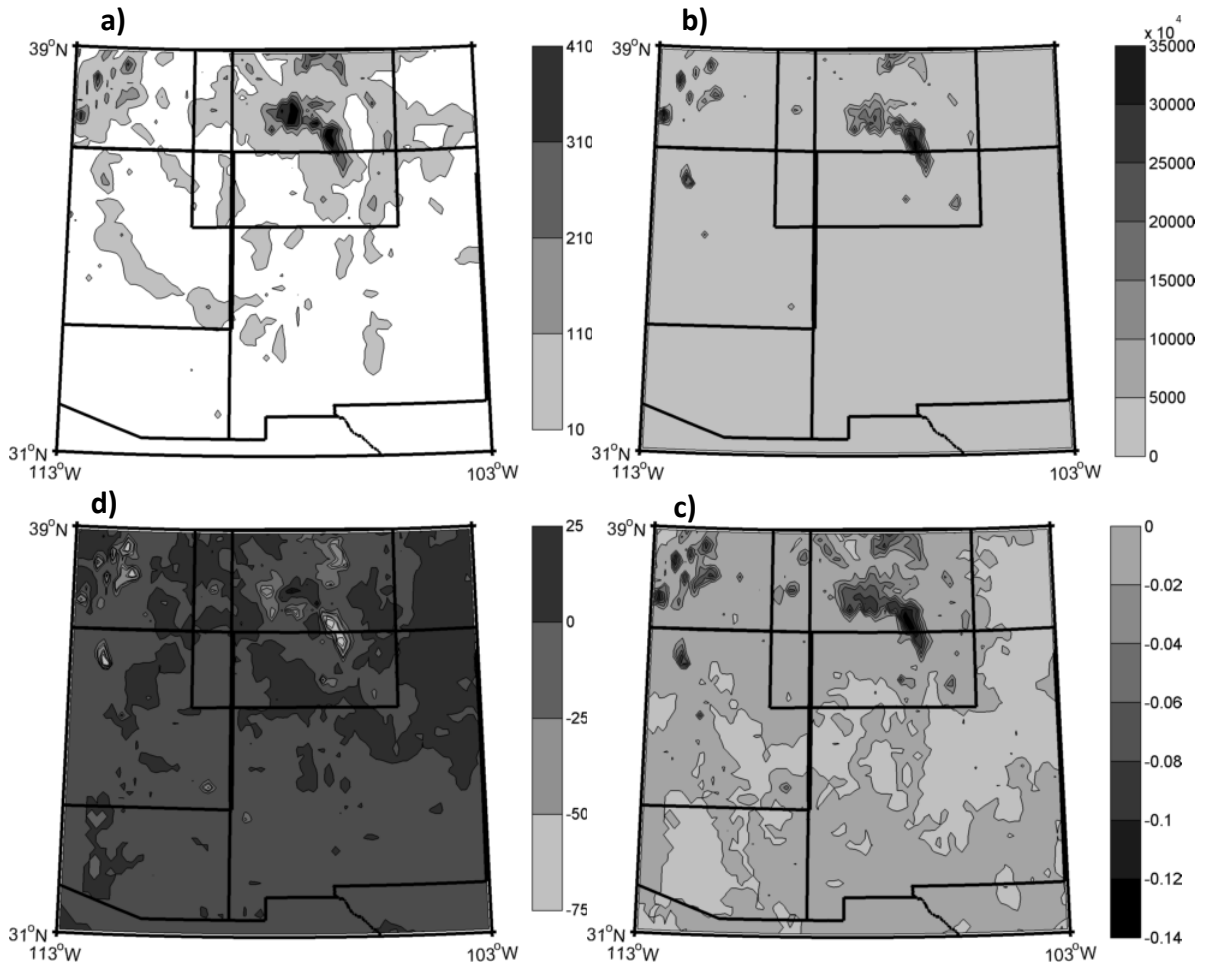

Figure 2. Climatology (kg/m^2) (1979-2009) (a), interannual variance (kg^2/m^4) (b), the first empirical orthogonal function (unitless) (c), and the linear trend (kg/m^2/decade) (d) of maximum NLDAS-2 SWE.

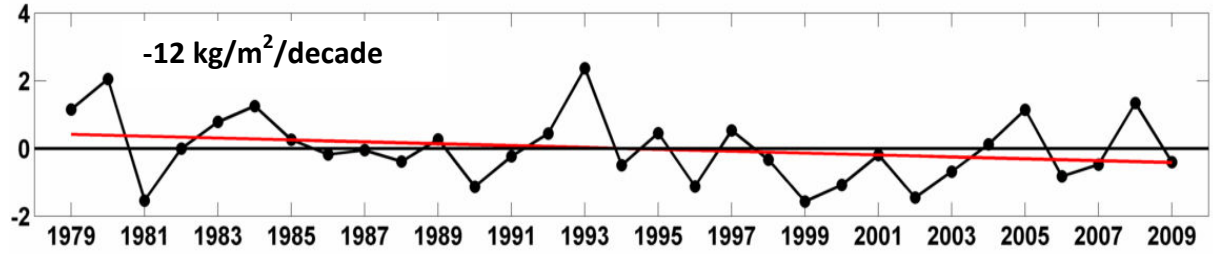

Figure 3. Normalized (unitless) PC1 of NLDAS-2 maximum SWE over the FC region.

3. TRENDS, VARIABILITY AND CLIMATOLOGIES

Introduction

This section describes the trends, variability and distributions of each of the variables of interest in this study: annual maximum SWE, SWE melt day, temperature, precipitation, soil moisture, latent heat flux, sensible heat flux and the Bowen ratio. For each variable, we analyze trends in first principal component (PC1) of the variable, trends in the interim period values of the variable for the FC, NM and AZ averaging regions and trends in the monthly means of the variable, for each of the three averaging regions. We also examine the first empirical orthogonal function (EOF1) and distributions of the means, variances, and linear trends for each of the variables in this section.

Maximum SWE

There is no significant trend in PC1 of NLDAS-2 maximum SWE for the FC region; the time series is dominated by variability (Figure 3). The leading EOF of maximum SWE (Figure 2c) accounts for 57% of the variance in the data. The maps of interannual variance, linear trends and EOF1 are similar in distribution, with regions of strongest trends coincident with the largest values of maximum SWE (Figure 2b, c, d).

Melt-out day

The first principal component of NLDAS-2 SWE melt day (WY 1980-2008) does have a significant linear trend towards earlier snowmelt, explaining 51% of the variance in last day of SWE (-17 days/decade, $p = 0.00$, in Figure 4). All three of the spatially averaged regions also have significant linear trends towards earlier snowmelt (Figure 5). The strongest linear

trend is in the FC region (-9.0 days/decade, p = 0.00), followed by the AZ averaging region (-6.4 days/decade, p = 0.00), then the NM averaging region (-5.0 days/decade, p=0.01).

The leading EOF of SWE melt day (Figure 6c) explains 23% of the interannual variance (PCTV) in the data, across the FC analysis domain. Most of the low frequency variance in SWE melt day is spread throughout the analysis region with a region of highly concentrated high interannual variance in Colorado (Figure 6b). The variance in SWE melt day in Figure 6b is not coincident with the distribution of climatological maximum SWE or the interannual variance of maximum SWE in Figure 2. The map of EOF1 largely captures the spatial pattern generated by the trends of melt day (Figure 6d). The regions of latest melt, which coincide broadly with increases of highest maximum SWE, do not exhibit the strongest trend in melt day or largest interannual variance.

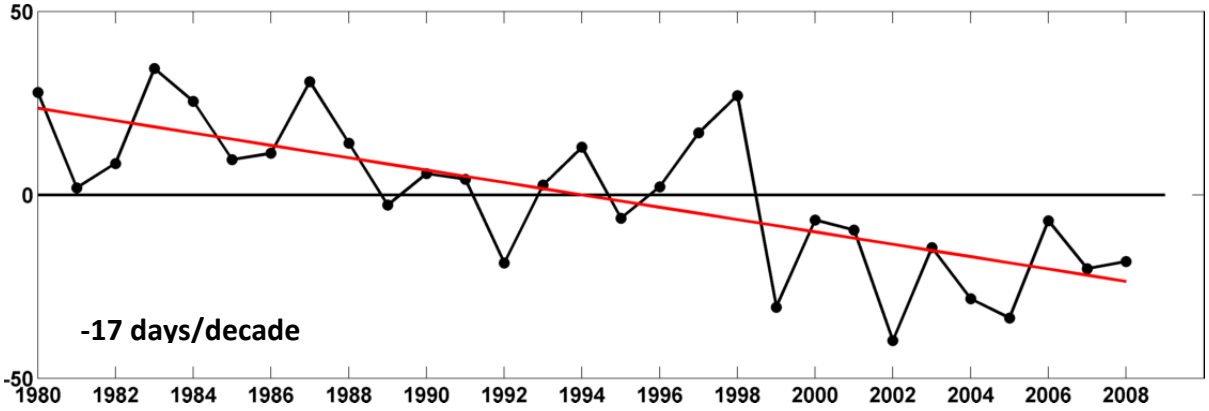

Figure 4. Normalized first principal component of the last day of NLDAS-2 snow water equivalent (SWE) presence (days since Oct 1). Significant linear trend at α = 0.05 (p = 0.00).

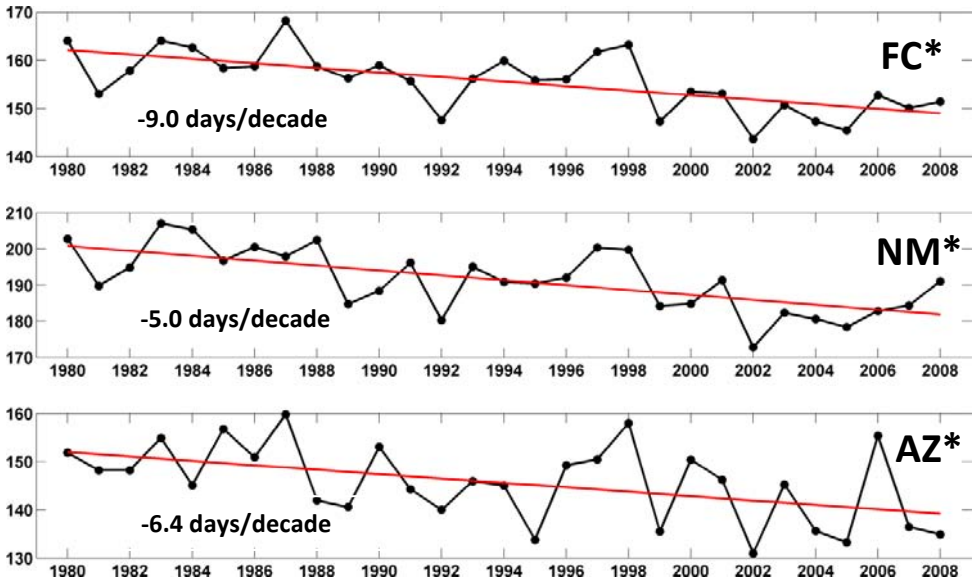

Figure 5. Spatially averaged time series of last day of NLDAS-2 snow water equivalent (SWE) presence (days into WY since Oct1) for the FC, NM* and AZ* averaging regions. *Indicates statistically significant linear trend at α = 0.05.*

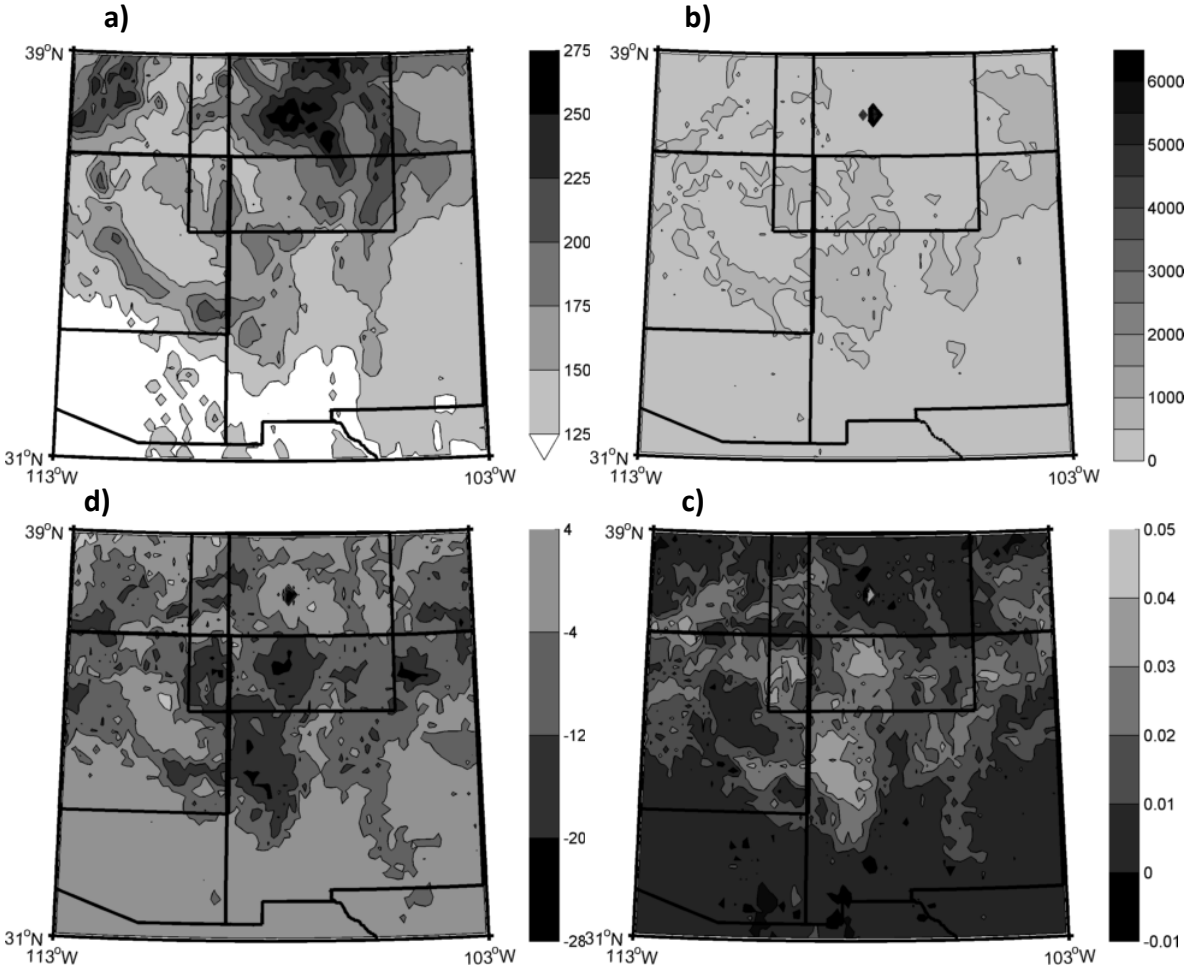

Figure 6. Climatology (days since Oct1) (WY 1980-2008) (a), interannual variance (days since Oct1^2) (b), the first empirical orthogonal function (unitless) (c), and the linear trend (days since Oct1/decade) (d) of SWE melt out day in NLDAS-2 SWE.

NLDAS-2 SWE indices and surface observation comparisons

We compared the NLDAS-2 maximum SWE index with snowpack observations, by correlating maximum NLDAS-2 SWE with a large scale, 1 April SWE index originally developed by Gutzler (2000). The Gutzler (2000) index is derived from four Natural Resources Conservation Service (NRCS) manual snow course observation sites in New

Mexico and Arizona. While our study area also includes parts of Utah and Colorado, the first EOF of maximum SWE indicates coherent variability within our entire study area. Therefore, we expect reasonable agreement in interannual variability between the two data sets, even given their differences. Indeed, the first PC of NLDAS-2 maximum SWE and the Gutzler (2000) index do agree in many, but not all years, during 1979-2009 (r = 0.70) (Figure 7). Considering the large inherent differences between the SWE indices, we consider this to be satisfactory agreement between a land surface product and a very small set of surface observations.

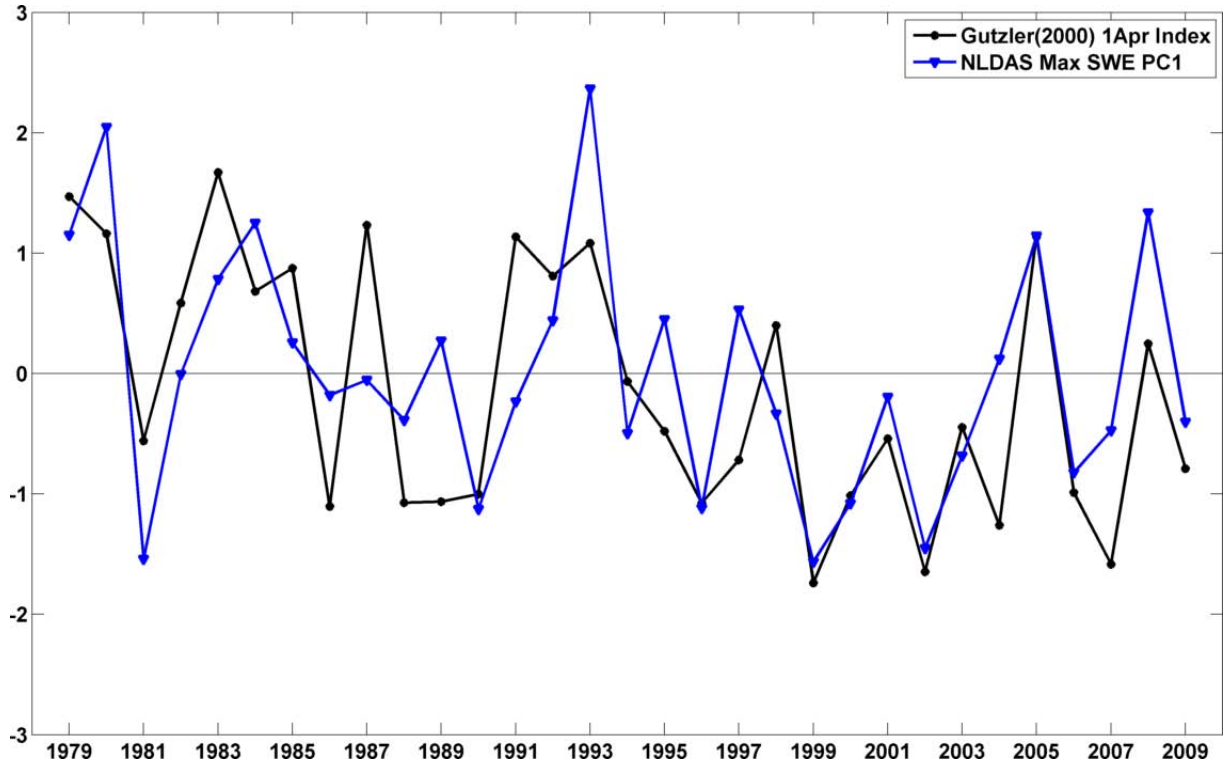

Figure 7. Normalized 1 April SWE index Gutzler (2000) and normalized first principal component of NLDAS-2 SWE (r = 0.70).

NLDAS-2 and SNOTEL trend and elevation analysis

To validate the NLDAS-2 SWE melt out days and trends we compare the NLDAS-2 data with spatially averaged SNOTEL station observations that fall within the NLDAS-2 AZ and NM study regions. Twenty stations that passed our quality control procedures (Serreze 1999) were included in the NM averaging region. Thirteen stations included in the average were from Colorado, 10 stations were from New Mexico and one station was from Utah. Seven stations from Arizona were included in the AZ average.

Comparing melt dates in NLDAS-2 and SNOTEL, the two values are uncorrelated (AZ, r = 0.00) to moderately, positively correlated (NM, r = 0.42) (Figure 8). NLDAS-2 linear trends in melt day for NM and AZ are significant, but linear trends in SNOTEL stations from the NM and AZ regions are non-significant (Figure 9, Figure 10). This is not surprising, as we are comparing gridded data over a large region to point data. More importantly, melt day exhibits greater large-scale, coherent interannual variance than does maximum SWE (Figure 1b and Figure 3b), but it does not necessarily coincide with the mountainous areas where SNOTEL observations are made, perhaps explaining why melt day is more poorly correlated with surface observations than maximum SWE.

Not only are the melt days weakly correlated, but there is a large mean bias between NLDAS-2 and SNOTEL melt day. For example NM NLDAS-2 melts out, on average, at 191 days into the WY compared to 256 days into the WY for the NM SNOTEL average (mean bias = 65 days). The mean bias for the AZ region is 58 days with NLDAS-2 melting out at 146 days into the water year and SNOTEL sites melting out at 204 days into the water year. SNOTEL data are not entirely representative of our spatial averages due to their

selective placement in high elevations, possibly explaining the discrepancy between melt day in NLDAS-2 and SNOTEL.

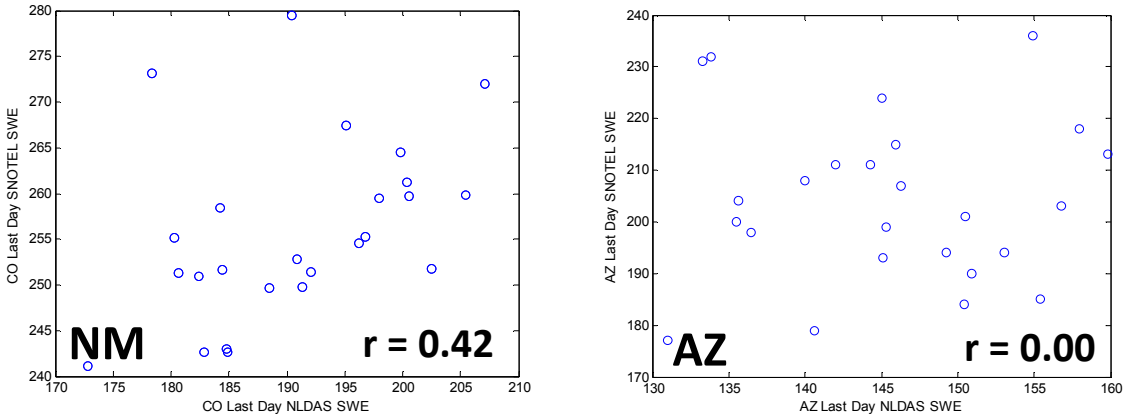

Figure 8. Right: Spatially averaged NM NLDAS-2 SWE melt out day (days since Oct 1, abscissa) versus NM SNOTEL station aggregate melt out days (days since Oct 1, ordinate) for 1983-2007 (r = 0.42, n = 25). Left: Spatially averaged AZ NLDAS-2 SWE melt out day (days since Oct 1, abscissa) versus AZ SNOTEL station aggregate melt out days for 1983-2007 (days since Oct 1, ordinate) (r = 0.00, n = 25).

We examined SWE melt day in regions with elevations that are more similar to the SNOTEL elevation distribution (Figure 13), to investigate if elevation bias in the SNOTEL data explains the discrepancy between means and variability of melt date in NLDAS-2 and SNOTEL (Figure 8). By spatially averaging NLDAS-2 SWE from southern Colorado, the last day of NLDAS-2 SWE linear trend was reduced, to a non-significant -3.2 days/decade (Figure 11) from a significant -5.8 days/decade (Figure 10). The correlation between SNOTEL and NLDAS-2 was also improved with the high elevation comparison (r = 0.58) (Figure 12), as was the mean bias between NLDAS-2 and SNOTEL (mean bias = 20 days).

Comparing the elevation map (Figure 1) and the map of NLDAS-2 SWE melt day trends (Figure 6d), the highest elevations on the map, in Colorado, do not have strong trends

toward earlier melt, with one localized spot excepted. Most of the trends in last day of SWE reside in western New Mexico, eastern Arizona and southeastern Utah, all places where the SNOTEL network is relatively sparse. It is nearly impossible to ground truth the trends in NLDAS-2 SWE melt because snow-measuring stations are generally biased towards the highest elevations; the observing network was not designed for detecting snowpack changes in marginal areas.

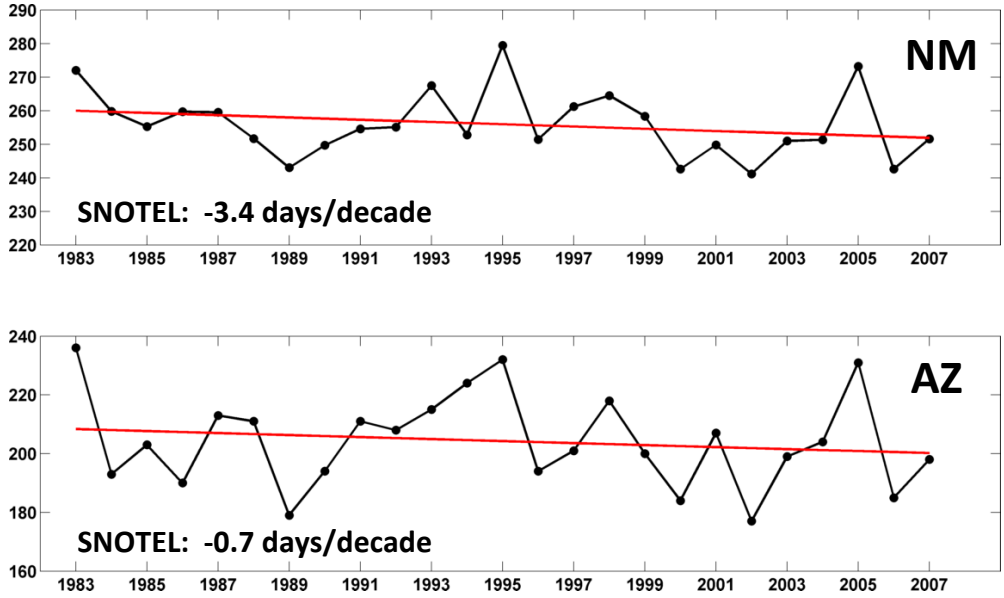

Figure 9. SNOTEL last day SWE (days since Oct 1) time series and linear trends for aggregated SNOTEL stations corresponding to the NM and AZ averaging regions. Trends are not statistically significant at α = 0.05.

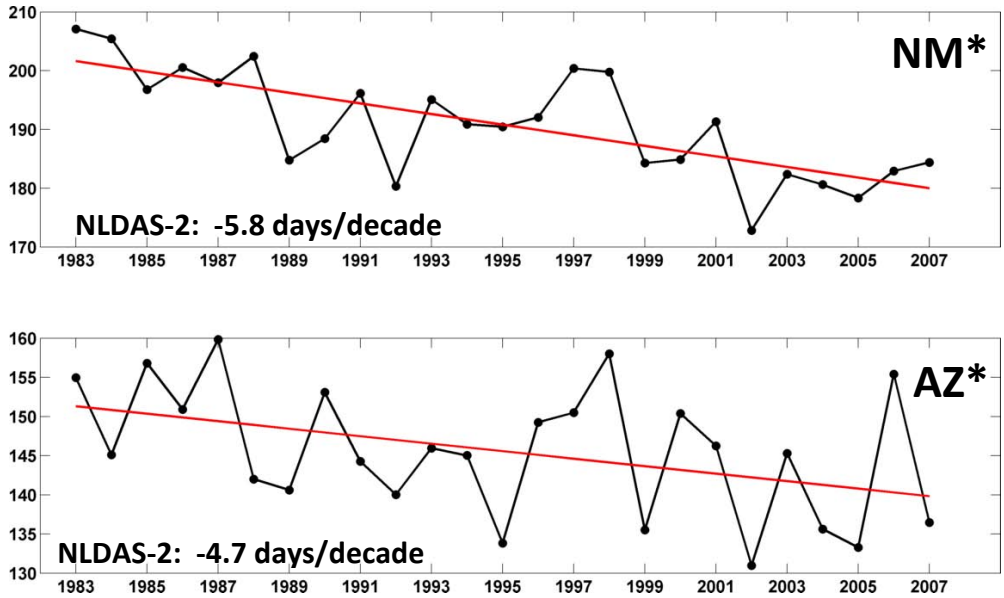

*Figure 10. NLDAS-2 last day SWE (days since Oct1) time series and linear trends for NM and AZ averaging regions. *Indicates statistical significance at α = 0.05.*

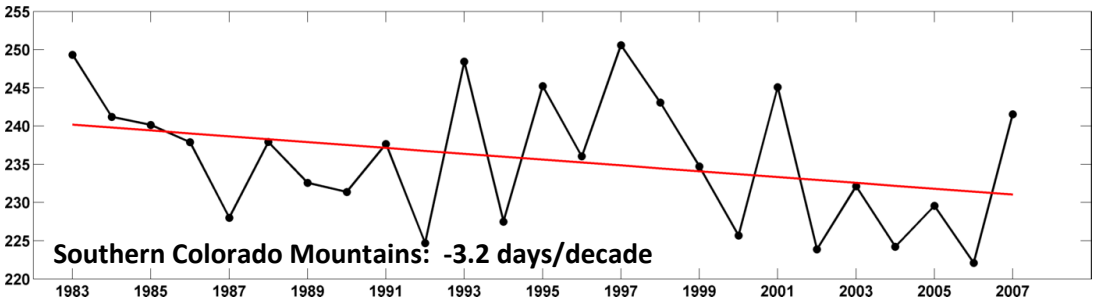

Figure 11. NLDAS-2 last day of SWE (days since Oct 1), spatially averaged, restricted to high elevations in Colorado. Trend is not statistically significant at α = 0.05.

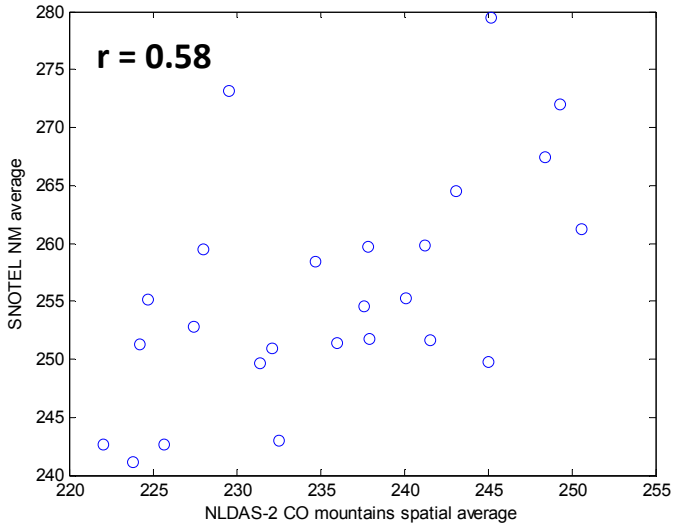

Figure 12. Correlation of NLDAS-2 last day SWE restricted to high elevations in southern Colorado (abscissa) and SNOTEL NM spatial average (ordinate) for 1983-2007 (r = 0.58, n=25).

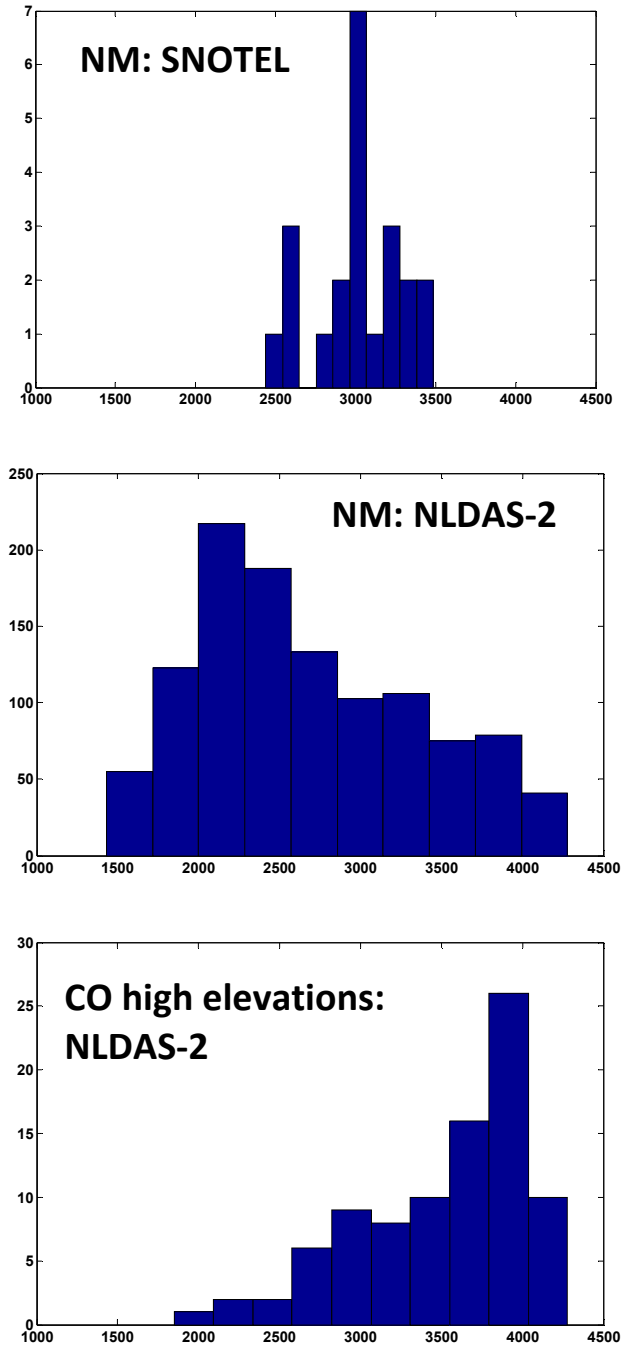

Figure 13. Elevation distributions for NM aggregated SNOTEL stations, NM NLDAS-2 spatial average and an NLDAS-2 spatial average restricted to high elevations in Colorado.

Temperature

We analyzed trends and interannual variability of January-February-March (JFM) and March-April-May (MAM) mean temperature as well as individual monthly mean temperature. JFM mean temperature (Figure 14) is used for correlation with snow indices and MAM temperature (Figure 15) is used as an index of temperature between the time of snow ablation and monsoon onset. Monthly mean temperature was analyzed to identify the most critical warming months in the regions. We also analyzed the leading PC of MAM temperature anomalies, to be used as an index for temperature during the time between snow ablation and monsoon onset.

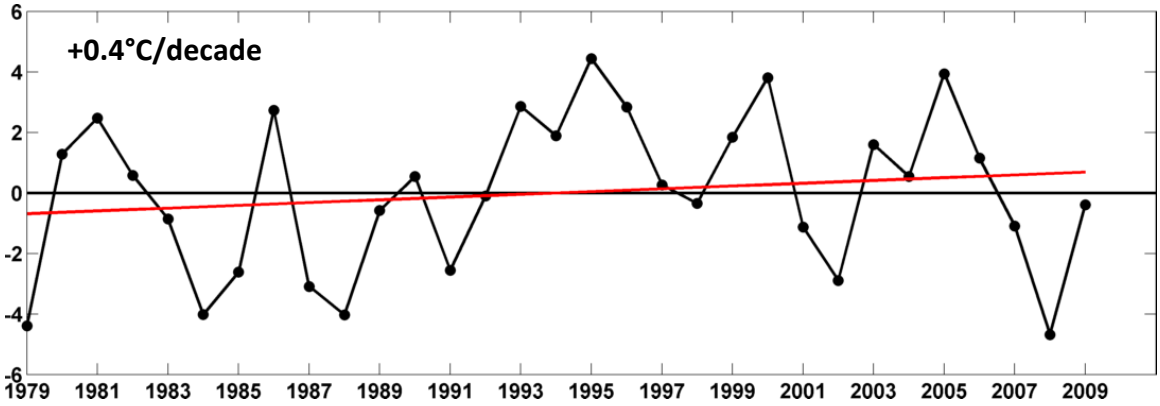

Figure 14. First principal component of JFM mean temperature anomaly (°C) for FC region. Trend is not statistically significant at α = 0.05.

MAM temperature trends

The first principal component of MAM temperature has a non-significant positive linear trend (slope = +0.8°C/decade) (Figure 15). Examining the spatial averages, the FC, NM and AZ regions have positive non - significant linear trends in MAM temperature (+0.3 °C/decade, +0.2 °C/decade, +0.4 °C/decade, in Figure 16).

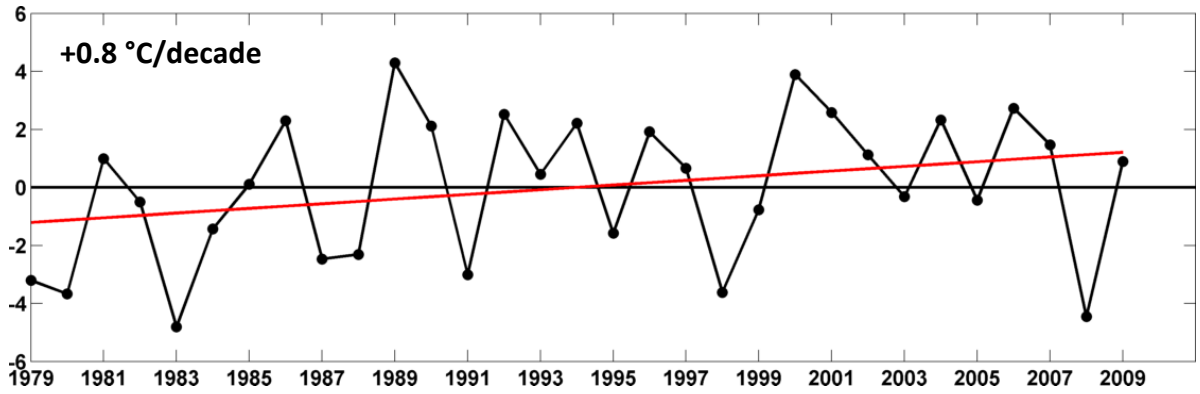

Figure 15. First principal component of MAM mean temperature anomaly (°C) for FC region. Trend is not statistically significant at α = 0.05.

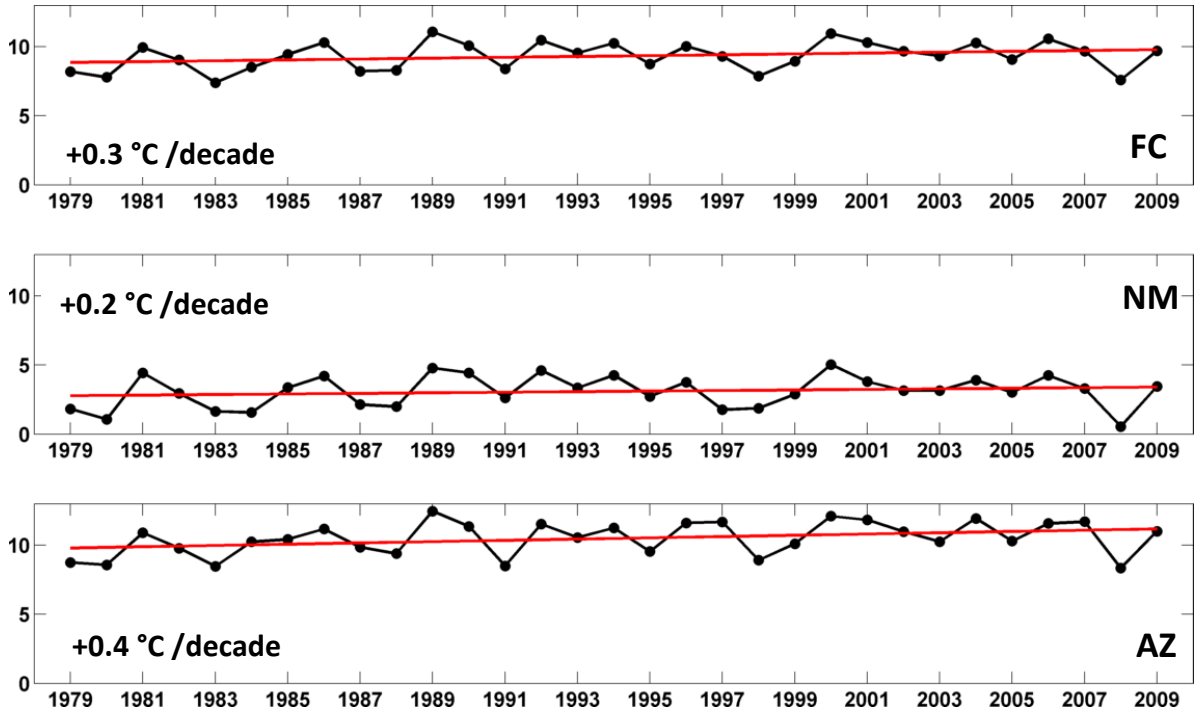

*Figure 16. NLDAS-2 MAM mean temperature (°C) time series and linear trends for FC, NM and AZ averaging regions. *Indicates statistical significance at α = 0.05.*

Monthly Mean Temperature Trends

We examined linear trends in monthly mean temperature and the variance accounted for by those trends for all months in the FC, NM and AZ averaging regions (Table 1). In the FC averaging region, May has the strongest linear trend in temperature (+0.52 °C/decade) followed by November (+0.30°C/decade). The remaining months have linear trends between +0.26 °C/decade (February and March) and -0.40°C/decade (December). In the FC averaging region, the greatest percentage of variance (PCTV) accounted for by the trend occurs in May (17.8%), followed by December (14.9%, negative trend). The remaining months have PCTV's between 0.79% (April) to 4.66% (March) (Table 1).

In the NM averaging region, May (+0.42 °C/decade) and then July (+0.23 °C/decade), have the two strongest linear trends in temperature (Table 1). The remaining months have trends between +0.15 °C/decade (April) to -0.09 °C/decade (October). Compared to other months, the May trend accounts for the greatest PCTV in temperature (10.2%), followed by December (14.1%, negative trend). The rest of the months have variances accounted for by the trend between 0 % (June) and 1.2% (February).

In the AZ averaging region, May (+0.65 °C/decade) and March (+0.47 °C/decade) have the strongest linear trends (Table 1). The remaining months have trends ranging from 0 °C/decade (September) to +0.43 °C/decade (July). Compared to other months, the July trend accounts for the greatest PCTV in temperature (15.8%), followed by May (14.4%), then March (11.2%). The remaining months have values between 0.38% (January) and 4.1% (February).

Table 1. Linear trends (°C/decade) (1979-2009) and percentage of interannual variance explained by the trends in monthly mean NLDAS-2 temperature for the FC, NM and AZ averaging regions.

	FC		NM		AZ	
Temp. (°C)	**Trend**	**PCTV**	**Trend**	**PCTV**	**Trend**	**PCTV**
Jan	0.16	1.33	0.11	0.36	0.10	0.38
Feb	0.26	3.05	0.22	1.2	0.35	4.1
Mar	0.26	4.66	0.05	0.08	**0.47**	11.2
Apr	0.14	0.79	0.15	0.78	0.26	2.09
May	**0.52**	**17.8**	**0.42**	**10.2**	**0.65**	**14.4**
Jun	0.24	1.88	0.01	0.00	0.18	1.5
Jul	0.16	7.34	0.23	4.9	0.43	**15.7**
Aug	0.16	2.55	-0.01	0.01	0.14	1.9
Sep	0.00	0.00	-0.20	1.9	0.00	0.00
Oct	0.05	0.22	-0.09	0.67	0.04	0.11
Nov	0.30	4.96	0.07	0.25	0.40	8.9
Dec	**-0.40**	**14.9**	**-0.50**	**14.1**	-0.40	12.5

MAM temperature maps

MAM climatological temperature (1979 -2009) generally decreases with increasing elevation (Figure 17a). MAM temperature trends are distributed with the strongest linear trends in increasing temperature in northern New Mexico, the high elevations of Arizona and southern Utah (Figure 17d). The pattern abruptly changes with decreasing trends in the high elevations of southern Colorado (Figure 17d). EOF1 (Figure 17c) of MAM temperature exhibits regions of strongest spatial coherence in the northwest corner of New Mexico into southern Utah and the high elevations of Arizona, coincident with the regions of strongest positive linear trends in temperature (Figure 17d).

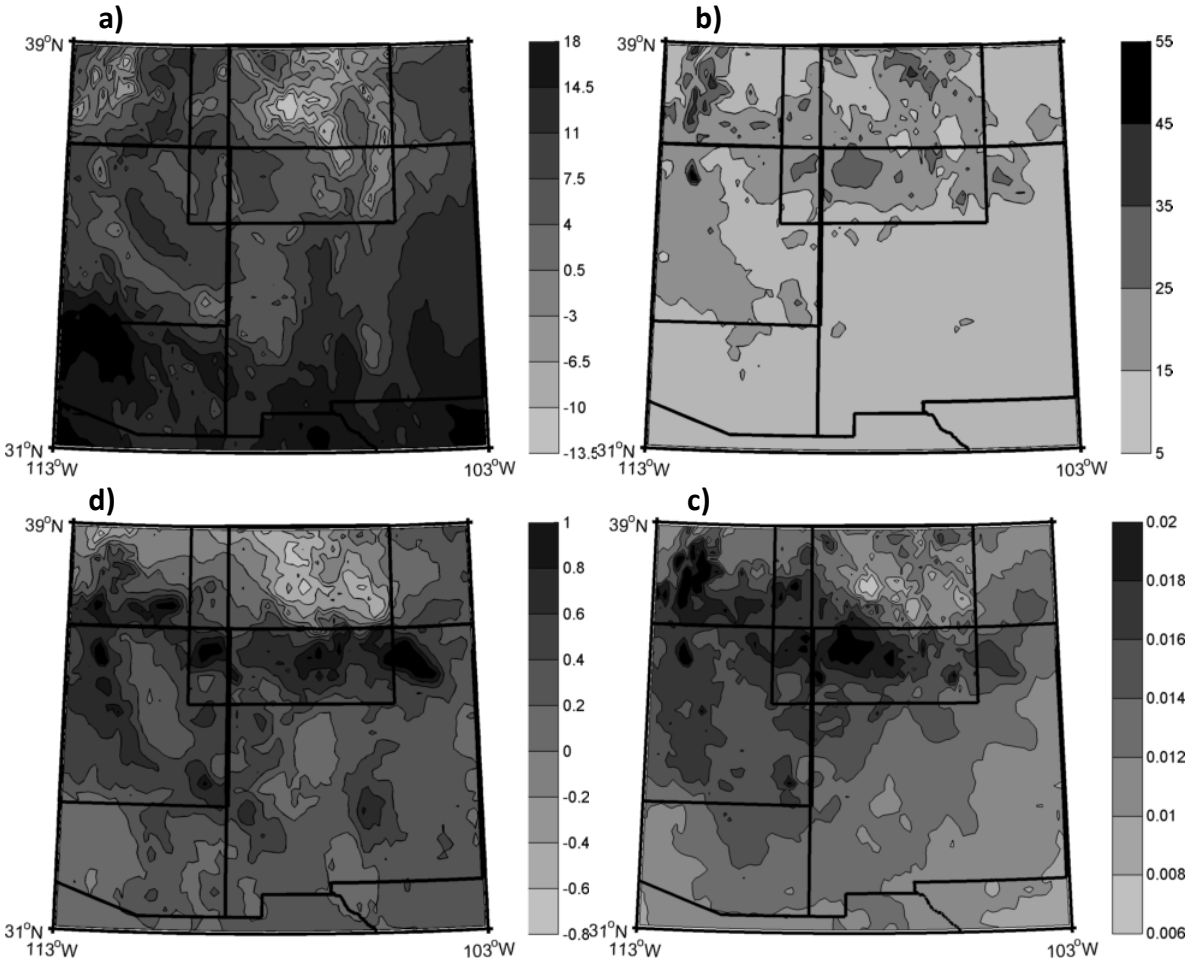

Figure 17. Climatology(°C) (1979-2009)(a), interannual variance (°C^2)(b), the first empirical orthogonal function (unitless) (c) and the linear trend (°C /decade) (d) of NLDAS-2 MAM mean temperature.

Temperature comparisons with surface observations

We compared monthly mean NLDAS-2 temperature with monthly mean temperature observations from the National Climate Data Center's (NCDC) climate divisions for 1979-2009 (Figure 18). Area-weighted averages were calculated for divisional temperature data for the state of New Mexico and compared with spatially averaged values of NLDAS-2 temperature for New Mexico. In general, NLDAS-2 temperature and NCDC temperature are strongly-correlated (r = 0.73 - 0.95) (Figure 18, Table 2). We show January, February, March

and April comparisons here (Figure 18). While NLDAS-2 and NCDC temperatures are generally well-correlated, the relationship departs from a 1:1 relationship, especially in the winter months (Figure 18). Mean bias between NCDC and NLDAS-2 ranges from -0.4°C to 5.9 °C, with the largest biases in the winter months and a smaller negative bias in June (Table 1).

We suspect that the temperature biases may be related to the placement of the co-operative weather stations that comprise the NCDC divisional averages. In general, the stations are located near places of human habitation and thus do not represent the full complement of variability in elevation, especially high elevations, found in the NLDAS-2 data. In theory, NLDAS-2 should provide better averaged estimates of surface temperature than divisional data, because NLDAS-2 temperatures are evenly interpolated across all elevations rather than simple arithmetic averages of available observations. For this reason, we suspect that NCDC climate division data may overestimate winter spatially averaged temperature.

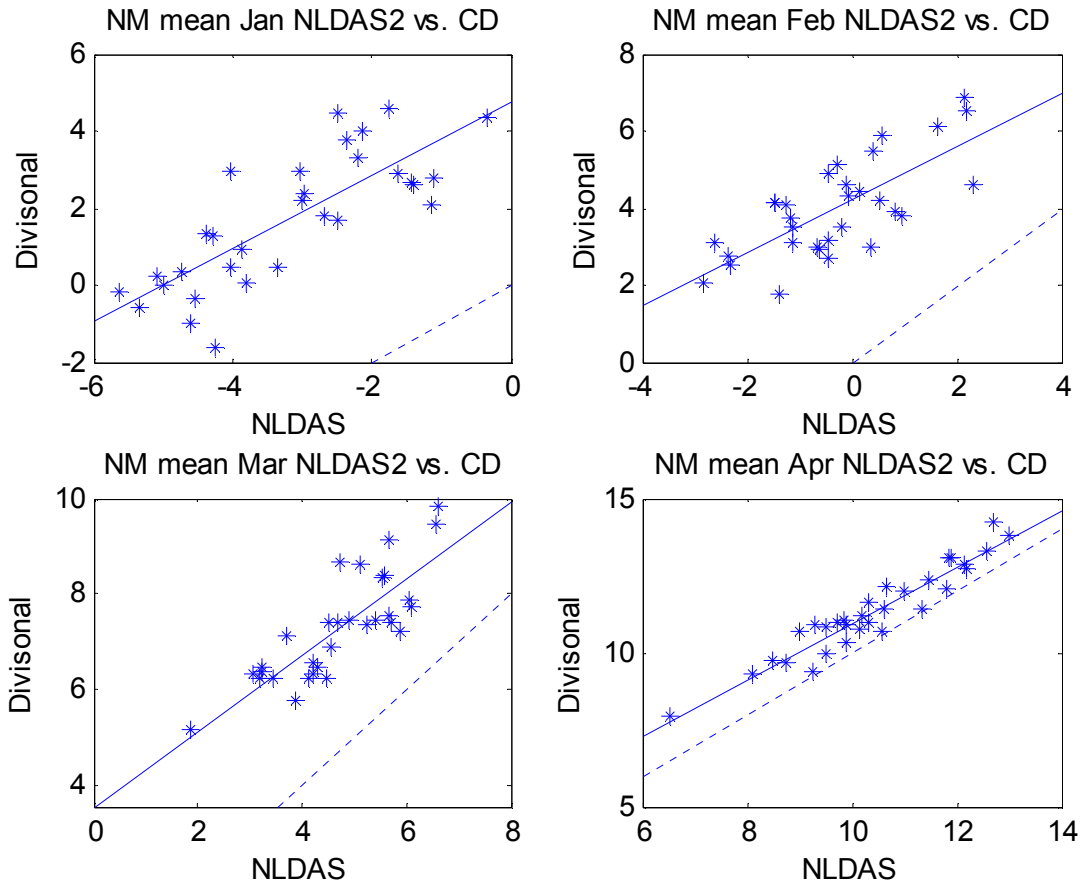

Figure 18. NLDAS-2 monthly mean temperature (abscissa) (°C) versus NCDC climate division monthly mean temperature (ordinate) (°C). Dashed line is a 1:1 line, solid line is a linear regression line.

Table 2. New Mexico mean temperature values, biases and interannual r-values from NLDAS-2 and NCDC comparisons, averaged over 1979-2009.

Month	NCDC Temp (°C)	NLDAS-2 Temp (°C)	Mean bias(°C) (NCDC-NLDAS2)	Pearson's r-value
Jan	1.7	-4.2	5.9	0.79
Feb	4.0	-1.4	5.3	0.73
Mar	7.3	3.7	3.6	0.82
Apr	11.3	9.4	1.9	0.95
May	16.4	16.0	0.4	0.92
Jun	21.2	21.7	-0.5	0.95

Precipitation

Spatially averaged interim precipitation

The first principal component of interim period total precipitation has a non-significant decreasing linear trend (slope = -0.03 cm/day/decade, p = 0.19, in Figure 19). There are non-significant decreasing linear trends in total precipitation between snow ablation and monsoon onset in the FC (-0.01 cm/day/decade), NM (-0.02 cm/day/decade) and AZ (-0.01 cm/day/decade) regions (Figure 20).

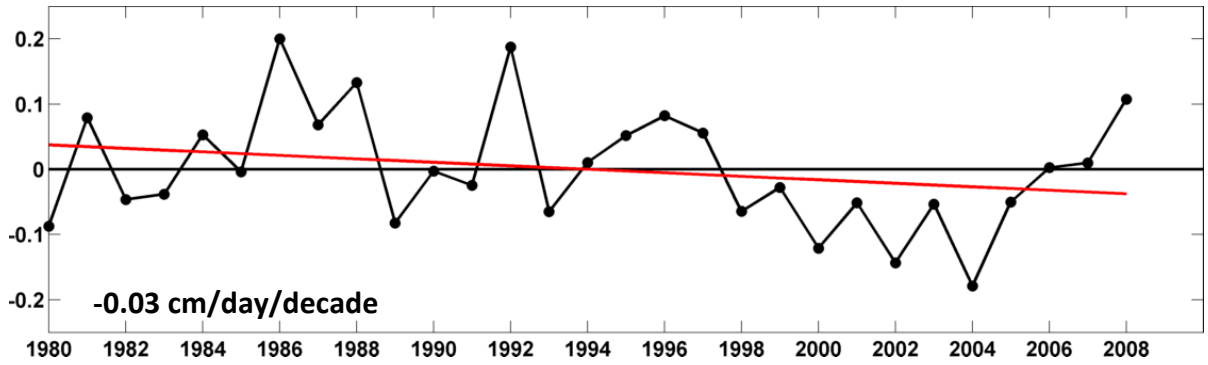

Figure 19. First principal component of NLDAS-2 interim period accumulated precipitation (cm/day) from the FC averaging region. Not statistically significant at α = 0.05 (p = 0.19).

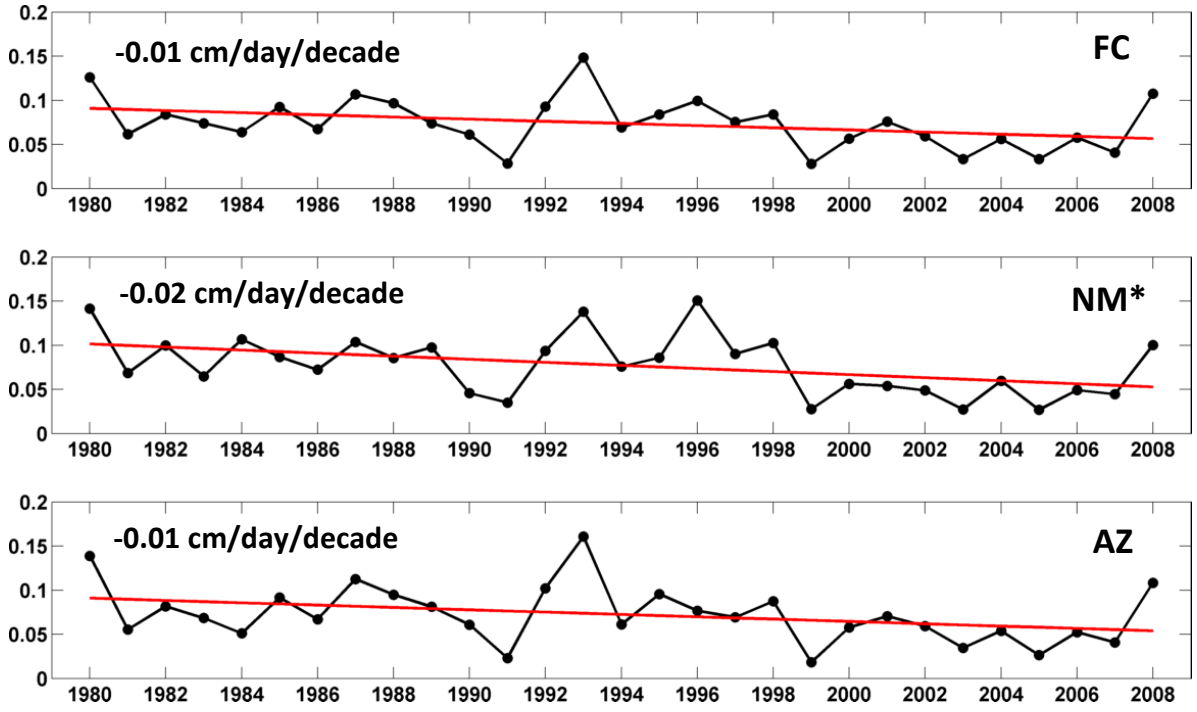

Figure 20. NLDAS-2 post snow ablation and pre monsoon onset mean daily accumulated precipitation (cm/day) for FC, NM* and AZ averaging regions. *Indicates statistical significance at α = 0.05.

Trends in monthly mean accumulated rainfall

In the FC averaging region, the strongest decreasing linear trend in accumulated monthly rainfall occurs in February (-0.39 cm/decade) with the next strongest in April (-0.38 cm/decade, Table 2). In the NM averaging region the strongest decreasing linear trend in accumulated monthly rainfall occurs in March (-0.47 cm/decade), with the next strongest in August (-0.26 cm/decade). In the AZ averaging region the strongest decreasing linear trend in accumulated monthly rainfall occurs in March (-1.2 cm/decade) followed by January (-0.82 cm/decade, Table 2).

In the FC averaging region, March and November trends in rainfall account for the most PCTV in decreasing linear trends in rainfall (15.1% and 12.7%). In the NM averaging region, March and November trends in rainfall account for 15.0% and 12.7% of the variance in the trends, respectively. In the AZ averaging region, 27% of the variance in March rainfall is accounted for by the trend, followed by 13.7% in November (Table 2).

Trends in monthly mean accumulated snowfall

In the FC averaging region January and February have the strongest decreasing linear trends in snowfall (-0.12 cm/decade and -0.11 cm/decade, respectively, in Table 3). In the NM averaging region March and January have the strongest decreasing linear trends in snowfall (-0.39 and -0.29 cm/decade, respectively). In the AZ averaging region, January and February have the strongest linear trends in snowfall (-0.28 cm/decade and -0.18 cm/decade, respectively, in Table 3).

March and February trends account for 22.7% and 9.6% of the variance in snowfall, respectively (Table 3). March and January trends account for 22.1% and 4.5% of the

variance in the snowfall. January and February (22.8% and 15.2%) are the months in which the trend accounts for the most variance in AZ snowfall.

To summarize, AZ has the strongest decreasing linear trends in rainfall and snowfall. The remaining regions and months have decreasing trends in rainfall and snowfall except for June in the FC region and July in the NM and AZ regions, both of which have increasing rainfall trends. January, February and March have the most predominant precipitation trends in our study areas and November is the month in which the greatest PCTV variance in rainfall and snowfall is explained by the trend.

Table 3. Linear trends in NLDAS-2 rainfall and snowfall (monthly cm total/decade) (1979-2009) and percentage of interannual variance explained by the trends in monthly mean NLDAS-2 rainfall and snowfall for the FC, NM and AZ averaging regions.

	FC				**NM**				**AZ**			
	Rain		**Snow**		**Rain**		**Snow**		**Rain**		**Snow**	
	Trend	**PCTV**	**Trend**	**PCTV**	**Trend**	**PCTV**	**Trend**	**PCTV**	**Trend**	**PCTV**	**Trend**	**PCTV**
Jan	-0.04	8.0	**-0.12**	13.8	0.04	0.15	**-0.29**	5.0	-0.82	7.0	**-2.8**	5.0
Feb	**-0.39**	0.10	**-0.11**	9.6	0.14	2.5	-0.20	3.7	-0.19	0.43	**-1.8**	3.7
Mar	-0.04	**15.1**	-0.01	**22.7**	**-0.47**	**15.0**	**-0.39**	**22.1**	-1.15	**26.6**	-1.0	**22.1**
Apr	**-0.38**	0.13	-0.01	0.43	0.07	0.13	0.03	0.24	-0.14	0.87	-0.23	0.24
May	-0.16	7.9	0.00	3.0	-0.18	9.5	0	2.3	-0.27	3.0	-0.01	2.3
Jun	0.06	1.8	0.00	0	-0.18	1.81	0	0.10	-0.06	1.1	0	0.10
Jul	-0.35	0.09	.	.	0.04	0.06	.	.	0.05	0.06	.	.
Aug	-0.35	4.0	.	.	**-0.26**	1.8	.	.	-0.29	1.9	.	.
Sep	0	2.2	0	0.06	-0.02	1.6	0	1.2	-0.03	2.3	0	1.2
Oct	0	0.08	0	0.11	0.00	0.02	0	4.1	-0.01	0.17	0	4.1
Nov	-0.04	**12.7**	-0.01	**15.9**	-0.04	**12.8**	-0.01	**14.1**	-0.06	**13.7**	0	**14.1**
Dec	-0.03	0	0	1.1	-0.04	6.1	0.01	2.9	-0.03	2.0	0.01	2.9

Precipitation Maps

JFM rainfall is highest over the Mogollon Rim in Arizona (Figure 21). Snowfall is the dominant contributor to high elevation precipitation during the same period (Figure 22). Rainfall between snow ablation and monsoon onset is highest in the eastern part of the region, decreasing westward. Negative linear trends in interim precipitation are present in the New Mexico and Colorado high elevations of our analysis region, as well as the southeastern portion of New Mexico (Figure 24).

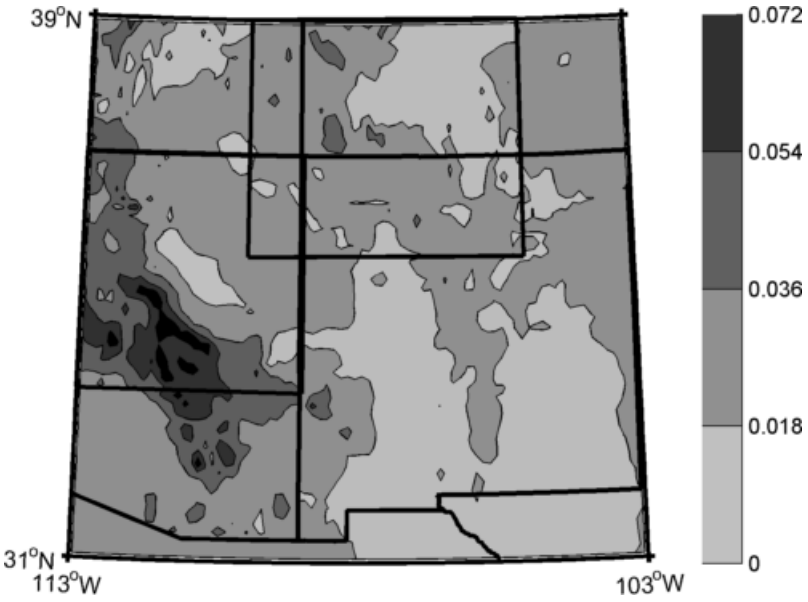

Figure 21. JFM NLDAS-2 rainfall climatology (1979-2009) (kg/m^2).

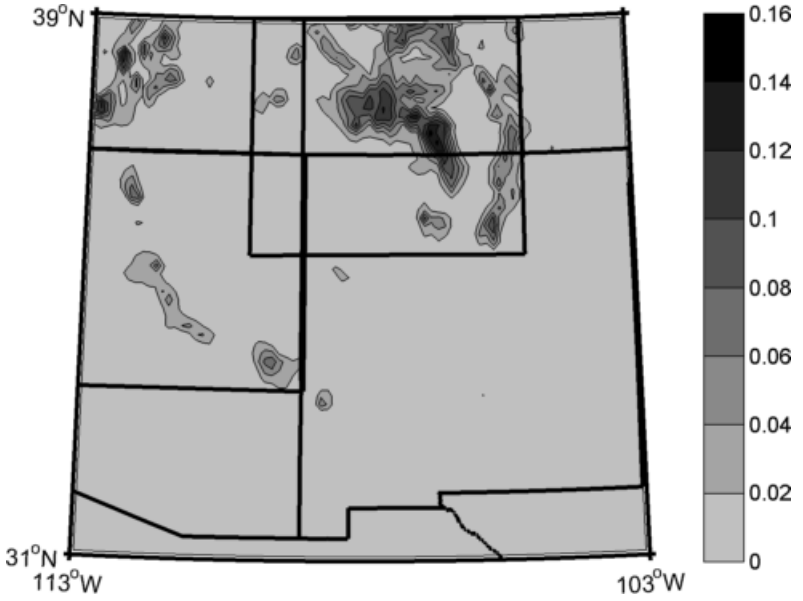

Figure 22. JFM NLDAS-2 total snowfall climatology (1979-2009) (kg/m^2).

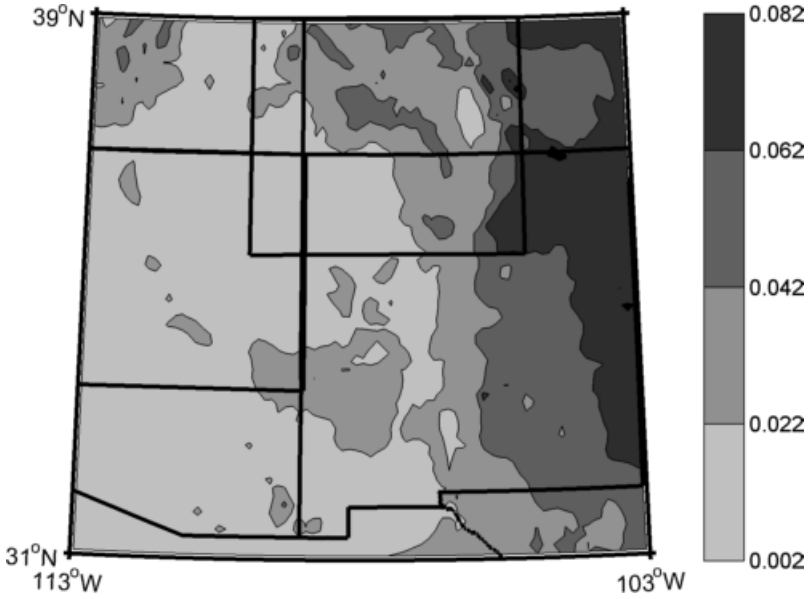

Figure 23. Interim NLDAS-2 rainfall climatology (WY 1980-2008) (kg/m^2).

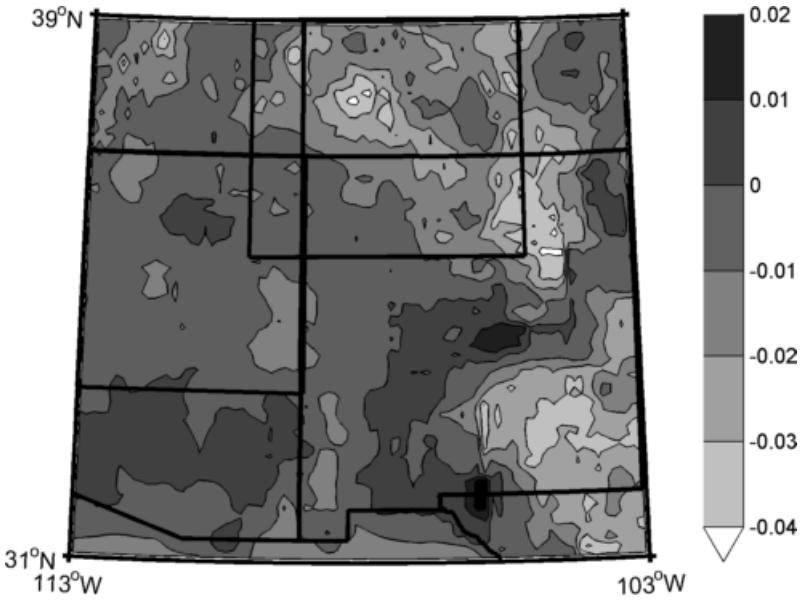

Figure 24. Linear trends in interim NLDAS-2 precipitation (WY 1980-2008) (cm/day/decade).

Total precipitation compared to surface observations

We compared NLDAS-2 monthly total precipitation (rainfall plus snowfall) with monthly mean total precipitation observations from the National Climate Data Center's (NCDC) climate divisions for 1979-2009 (Figure 25, January – April shown). Divisional precipitation data for the state of New Mexico were spatially averaged (area weighted) and compared with spatially averaged values of NLDAS-2 precipitation for New Mexico. Precipitation in the two data sets is well correlated for the months shown here (January – June: r = 0.88 – 0.99, Table 4). NCDC and NLDAS-2 precipitation are better correlated in the spring and summer than in the winter (Table 4). Mean bias in the two data sets is negative in January through April and bias is more negative in the winter. If we assume that NLDAS-2 is a more representative data set, as discussed above, then divisional data may be underestimating precipitation due to the low elevation bias of the co-op stations.

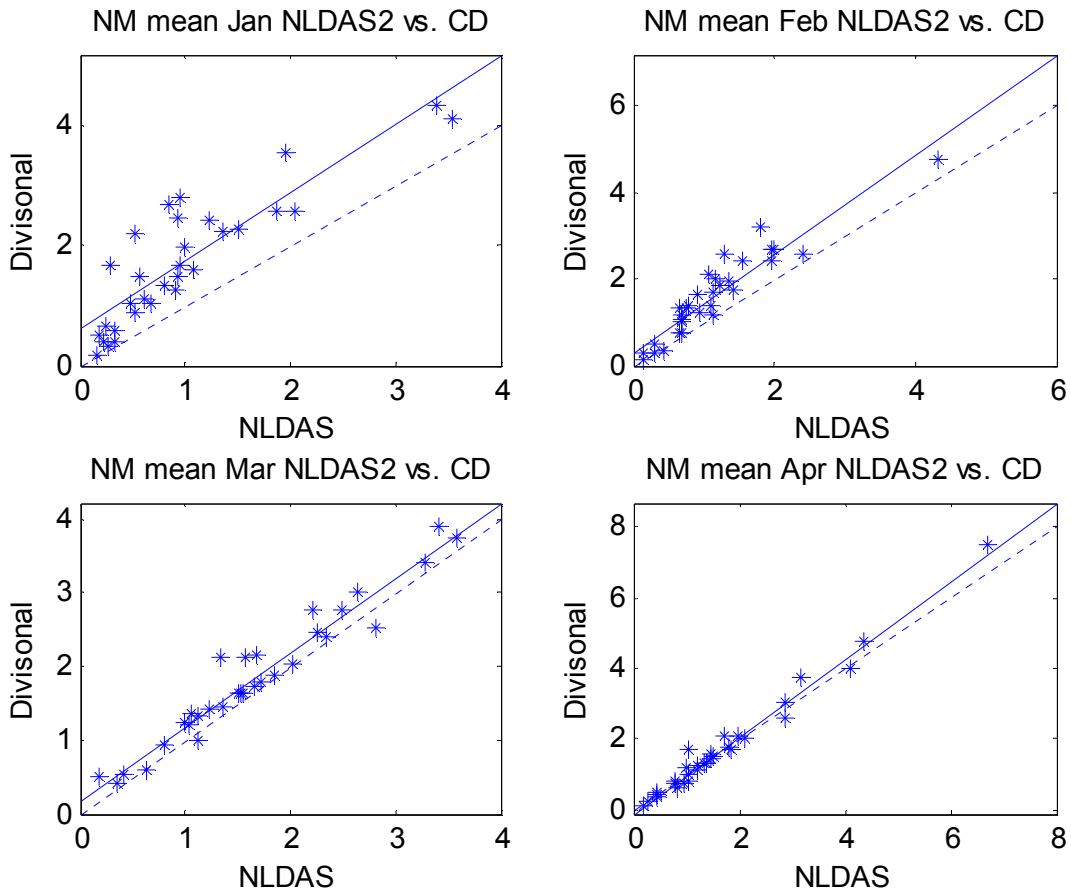

Figure 25. NLDAS-2 monthly accumulated precipitation (abscissa) (cm) versus NCDC climate division monthly accumulated precipitation (ordinate) (cm). Dashed line is a 1:1 line, solid line is a regression line.

Table 4. New Mexico monthly accumulated precipitation values, biases and interannual r-values from NLDAS-2 and NCDC comparisons averaged over 1979-2009.

Month	NCDC Precip (cm total)	NLDAS-2 Precip (cm total)	Mean bias(cm total) (NCDC-NLDAS2)	Pearson's r-value
Jan	0.99	1.74	-0.75	0.88
Feb	1.45	1.63	-0.48	0.94
Mar	1.67	1.87	-0.20	0.97
Apr	1.69	1.76	-0.07	0.99
May	2.88	2.77	0.11	0.99
Jun	3.31	3.15	0.16	0.99

Soil moisture

Interim soil moisture trends

We analyzed mean soil moisture between snow ablation and monsoon onset as well as monthly mean soil moisture for each spatial averaging region. There is a significant decreasing linear trend in PC1 of mean interim soil moisture (slope = -3.5 kg/m^2/ decade, p = 0.03, Figure 26). The trend in the first principal component of mean interim soil moisture accounts for 22.5 PCTV of the data. Spatially averaged soil moisture exhibits a significant negative linear trend in the FC region (slope = -1.3 kg/m^2/decade, p = 0.03) and the AZ region (slope = -2.0 kg/m^2/decade, p = 0.01) but not in the NM region (slope = -1.4 kg/m^2/decade, p = -0.18) (Figure 27).

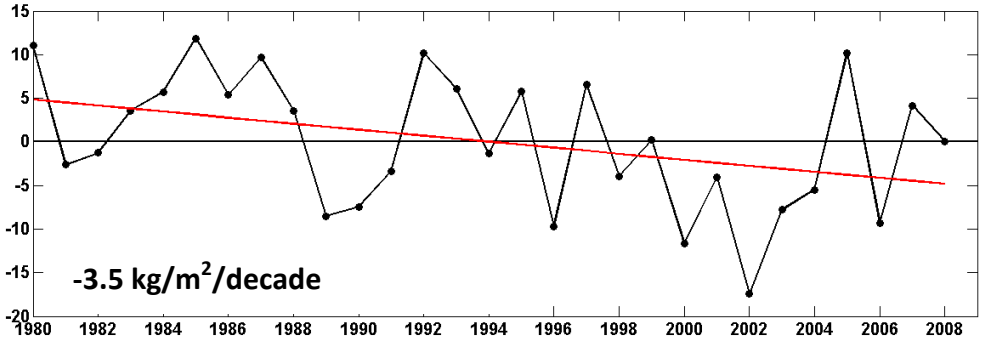

Figure 26. First principal component of interim soil moisture (kg/m^2) for FC region. Slope is significant at α = 0.05 (p = 0.03).

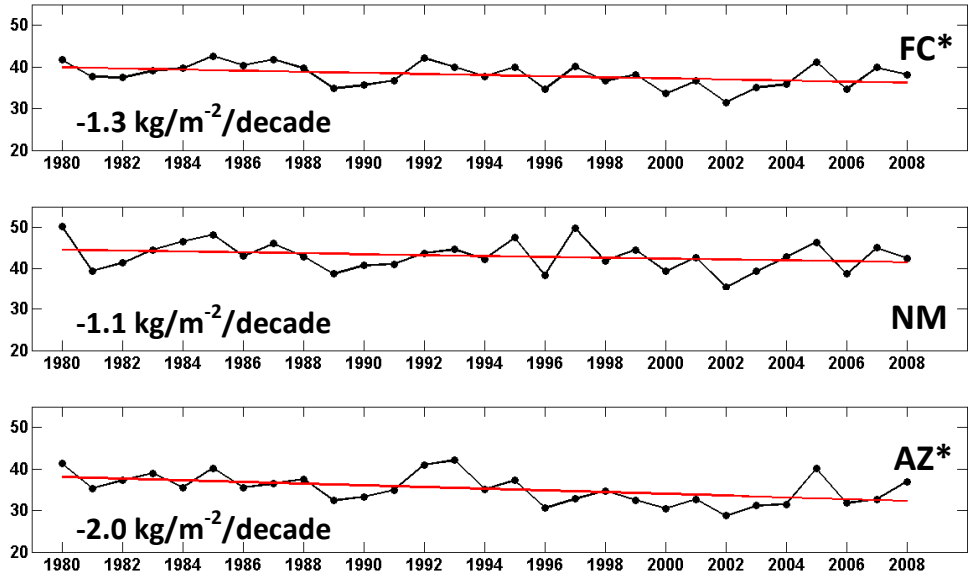

Figure 27. FC, NM and AZ*, NLDAS -2 post snow ablation and pre monsoon onset mean soil moisture (kg/m^2).*Indicates statistically significant linear trend at α = 0.05.*

Monthly mean soil moisture trends

In the FC averaging region, January and February have the strongest negative linear trends in interim soil moisture (-1.1 kg/m^{-2}/decade and -1.0 kg/m^{-2}/decade, in Table 5). Trends in the remaining months range from -0.72 kg/m^{-2}/decade in April to -0.20 kg/m^{-2}/decade in June. The trend in interim FC soil moisture accounts for the greatest percentage of variance (PCTV) in soil moisture in May (20.7%) followed by June (18.2%). The PCTV accounted for by the trend in soil moisture during the remaining months ranges between 17.4% (March) to 1.7% (August).

In the AZ averaging region, March and February have the strongest negative linear trends in interim soil moisture (-2.3 kg/m^{-2}/decade and -2.0 kg/m^{-2}/decade, respectively, in Table 5). Trends in the remaining months range from -1.7 kg/m^{-2}/decade in January to -0.40 kg/m^{-2}/decade in September. The greatest PCTV accounted for by the trend in soil moisture is in April (31.7%), followed by March (26.2%). The PCTV accounted for by the trend in soil moisture ranges between 25.5% (May) to 4.4% (August) in the remaining months.

In the NM averaging region, the strongest negative linear trends in soil moisture occur in March (-0.83 kg/m^{-2}/decade) and May (-0.76 kg/m^{-2}/decade, in Table 5). The trends in the remaining months range between -0.09 kg/m^{-2}/decade (October) to -0.65 kg/m^{-2}/decade (April). The trend in interim soil moisture accounts for the greatest PCTV in soil moisture in May (10.1%) followed by March (8.7%). The PCTV accounted for by the trend in soil moisture during remaining months ranges between 7.1% (April) to 0.04% (September).

At -2.3 kg/m^{-2}/decade, March, in the AZ averaging region has the strongest negative trend in soil moisture (Table 5). April and then March in the AZ region are the two months in which the greatest PCTV in soil moisture is accounted for by the trend. Taking all three averaging regions together, March, April and May are the months in which the strongest trends in soil moisture occur and the greatest PCVT in soil moisture is accounted for by the trends.

Table 5. Linear trends (kg/m^2/decade) (1979-2009) and percentage of interannual variance explained by the trends in monthly mean NLDAS-2 soil moisture.

Soil	FC		NM		AZ	
Moisture(kg/m^2/decade)	Trend	PCTV	Trend	PCTV	Trend	PCTV
Jan	**-1.1**	10.7	-0.13	0.16	-1.7	10.7
Feb	**-1.0**	11.4	-0.26	0.65	**-2.0**	16.3
Mar	-0.66	**17.4**	**-0.83**	**8.7**	**-2.3**	**26.2**
Apr	-0.72	14.7	-0.66	7.08	-1.4	**31.7**
May	-0.50	**20.7**	**-0.76**	**10.1**	-0.98	25.5
Jun	-0.20	18.2	-0.37	5.6	-0.54	24.2
Jul	-0.37	1.7	-0.04	0.07	-0.46	8.5
Aug	-0.37	4.3	-0.14	0.63	-0.44	4.4
Sep	-0.20	2.5	0.09	0.40	-0.40	4.7
Oct	-0.36	2.5	0.07	0.08	-0.80	11.2
Nov	-0.60	5.8	-0.50	2.5	-1.1	9.8
Dec	-0.90	6.7	-0.30	0.99	-1.2	7.41

Soil moisture maps

Climatological (WY 1980-2008) soil moisture in the interim period between snow ablation and monsoon onset generally increases with elevation and most of its interannual variance is in high elevations (Figure 28a,b). The leading EOF of interim soil moisture also has regions of coherent variance in the high elevations of our analysis area (Figure 28c). Forty-three percent of the variance in interim soil moisture is explained by the leading EOF. Linear trends in interim soil moisture are strongest throughout the Mogollon Rim region of

Arizona and in the southern Sangre de Cristo Mountains of New Mexico (-8.0 kg/m^2/decade to -2.0 kg/m^2/decade, in Figure 28d). Soil moisture in the southern Colorado mountains and a small portion of Texas is increasing (+4.0 kg/m^2/decade to +6.0 kg/m^2/decade, in Figure 28d).

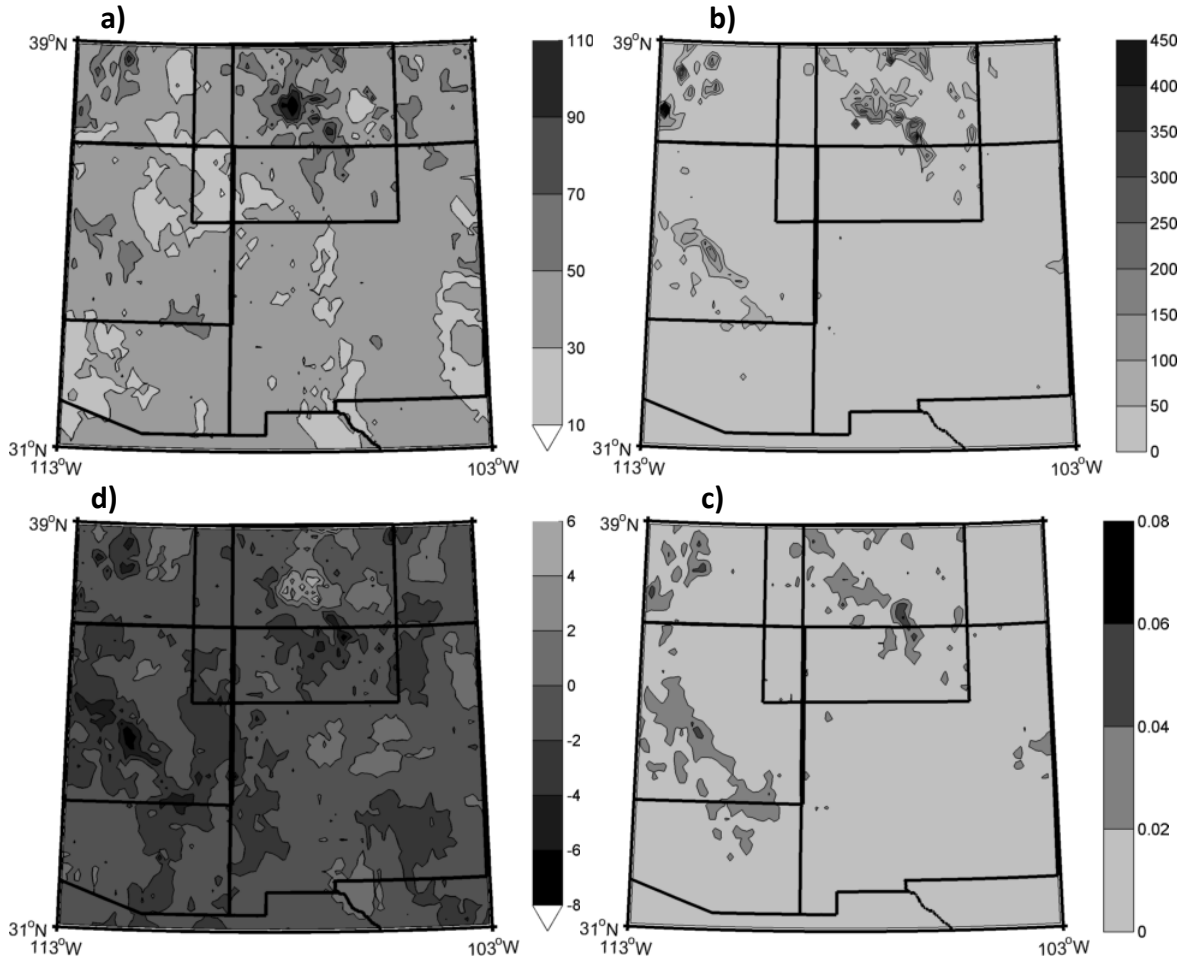

Figure 28. Climatology(kg/m^2) (1979-2009) (a), interannual variance (kg^2/m^4) (b) , the first empirical orthogonal function (unitless) (c) and the linear trend (kg/m^2/decade) (d) of NLDAS-2 surface soil moisture (0-10 cm) between the time of snow ablation and monsoon onset.

Latent Heat Flux

Trends in interim latent heat flux

The first PC of interim latent heat flux has a statistically significant decreasing linear trend (slope = -10 W m^{-2}/decade, p = 0.03, in Figure 29). Spatially averaged time series of latent heat flux have significant negative linear trends for the FC (slope = -3.7 W m^{-2}/decade, p = 0.03), NM (slope = -4.6 W m^{-2}/decade, p = 0.02) and AZ (slope = -4.6 W m^{-2}/decade, p = 0.03) averaging regions (Figure 30).

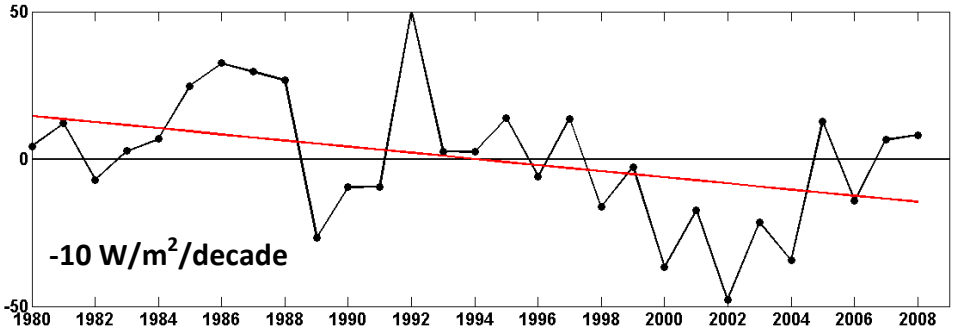

Figure 29. First principal component of interim latent heat flux (W m^{-2}) for FC region. Slope is significant at α = 0.05 (p = 0.03).

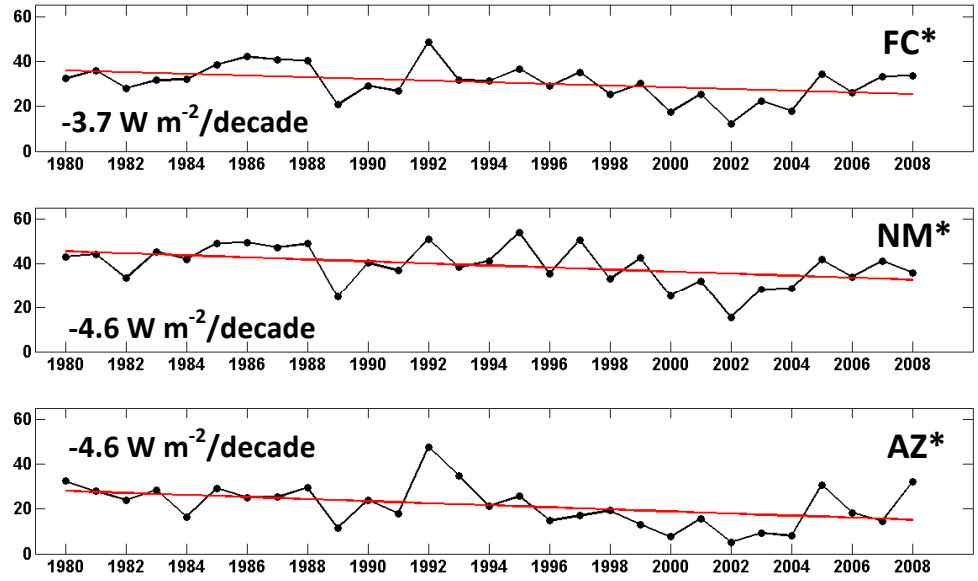

Figure 30. Spatially averaged NLDAS-2 latent heat flux (W m^{-2}) for the FC, NM and AZ averaging regions. *Indicates statistically significant linear trend at α = 0.05.

Monthly mean trends in latent heat flux

In the FC averaging region, April and May have the strongest negative linear trends in interim latent heat flux (-4.1 W/m^2/decade and -3.1 W/m^2/decade, in Table 6). Trends in the remaining months range from -2.7 W/m^2/decade in July to -1.4 W/m^2/decade in October. The trend in FC latent heat flux accounts for the greatest PCTV in latent heat flux in January (19.4 %) followed by May (15.7%). The PCTV accounted for by the trend in latent heat flux during the remaining months ranges between 14% (June) to 1.6% (July).

In the AZ averaging region, May and April have the strongest negative linear trends in interim latent heat flux (-6.2 W/m^2/decade and -5.8 W/m^2/decade, respectively, in Table 6). Trends in the remaining months range from -4.9 W/m^2/decade in March to -1.4 W/m^2/decade in December. The greatest PCTV accounted for by the trend in latent heat flux is in April (22.7%) and the next greatest is in May (17.7 %). The PCTV accounted for by the trend in latent heat flux ranges between 17.3% (March) to 1.2% (September) in the remaining months (Table 6).

In the NM averaging region, the strongest negative linear trends in latent heat flux occur in May (-5.0 W/m^2/decade) and June (-3.5 W/m^2/decade) (Table 6). Trends in the remaining months range from -2.3 W/m^2/decade (August) to 0.1 W/m^2/decade (September). The trend in interim latent heat flux accounts for the greatest PCTV in latent heat flux in May (14.4%) followed by June (9.58 %). The PCTV accounted for by the trend in latent heat flux during remaining months ranges between 8.7% (March) to 0% (September).

Among the three regions, the most negative linear trend in latent heat flux is in the AZ averaging region in May. April, May and June are the months with strongest negative linear trends amongst all three averaging regions. April in the AZ averaging region is the month in

which the highest PCTV in the data is accounted for by the trend (22.7%). May and June follow April for the most PCTV accounted for by the linear trend in the data.

Table 6. Linear trends in NLDAS-2 latent heat flux (W/m^2/decade) (1979-2009) and percentage of interannual variance explained by the trends in monthly mean NLDAS-2 soil moisture for the FC, NM and AZ averaging regions.

Latent Heat(W/m^2)	FC Trend	PCTV	NM Trend	PCTV	AZ Trend	PCTV
Jan	-2.0	**19.4**	-0.23	1.1	-2.3	13.6
Feb	-2.6	10.2	0. 42	2.0	-2.1	7.19
Mar	-2.2	12.4	-1.4	8.7	-4.9	17.3
Apr	**-4.1**	8.5	-1.4	3.3	**-5.8**	**22.8**
May	**-3.1**	**15.6**	**-5.0**	**14.4**	**-6.2**	**17.7**
Jun	-1.5	14.1	**-3.5**	**9.6**	-3.2	17.3
Jul	-2.6	1.6	-1.1	0.75	-2.1	2.6
Aug	-2.8	6.1	-2.2	2.9	-2.2	3.0
Sep	-1.6	3.1	0.08	0.00	-1.5	1.2
Oct	-1.4	2.2	0.40	0.13	-3.5	11.7
Nov	-1.8	8.3	-1.5	7.1	-2.5	8.8
Dec	-1.5	9.0	-0.30	1.7	-1.4	5.0

Latent heat flux maps

Climatological interim latent heat flux is highest in the mountainous regions of our study area but also in the eastern part of the study area, that which receives the heaviest rainfall during the pre-monsoon spring (Figure 31a). Interannual variance in interim latent heat flux is greatest in the high elevation regions of Arizona (Figure 31b). Interim latent heat flux variance is not necessarily high in every high elevation area, such as in Colorado (Figure 31b). The leading EOF of interim latent heat flux explains 47% of the variance in the data (Figure 31c). The leading EOF of latent heat flux is not entirely coherent as there are two concentrated locations in Colorado that are varying oppositely of the rest of the map (Figure 31c). The remaining mountainous areas in the study region vary coherently. Those

regions of coherent variance on the EOF map coincide with the regions of strongest decreasing latent heat flux on the linear trend map (-20 W/m^{-2} to -25 W/m^{2}), the strongest of which is in Arizona (Figure 31d).

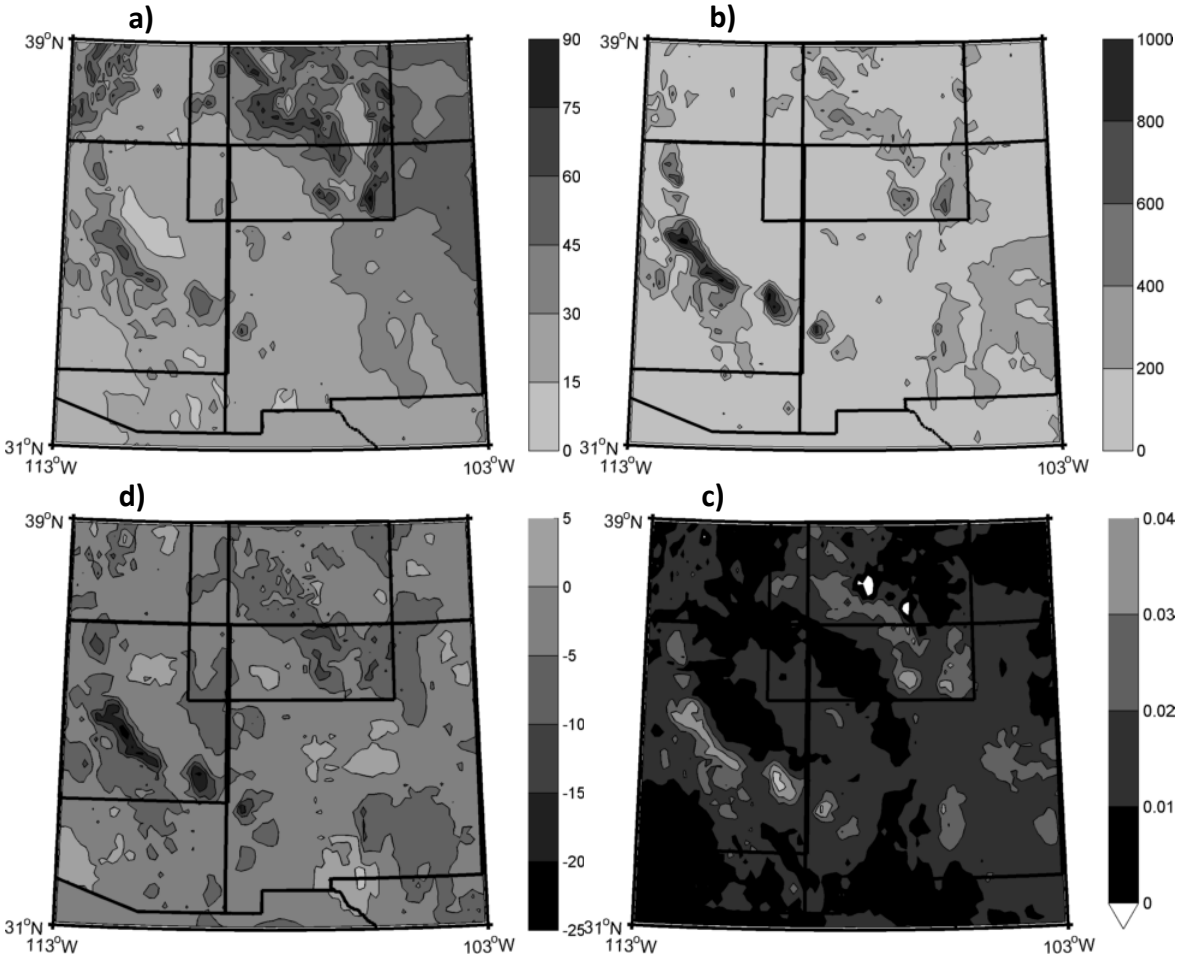

Figure 31. Climatology (W/m^{2}) (1979-2009) (a), interannual variance (W^{2}/m^{4}) (b), the first empirical orthogonal function (unitless) (c) and the linear trend (W/m^{2}/decade) (d) of NLDAS-2 latent heat flux between the time of snow ablation and monsoon onset.

Sensible Heat Flux

Trends in interim sensible heat flux

There is a non-significant positive linear trend in the leading PC of sensible heat flux (slope = +6.9 W/m^2/decade, p = 0.06, in Figure 32). All three averaging region also have non-significant positive linear trends in sensible heat flux (FC: slope = +1.9 W/m^2/decade, p= 0.15; NM: slope = +2.8 W/m^2/decade, p = 0.11; AZ: slope = +2.9 W/m^2/decade, p = 0.08, in Figure 33).

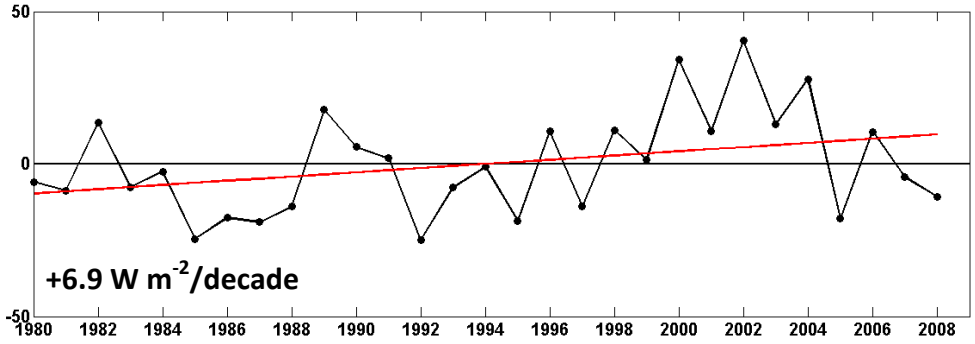

Figure 32. First principal component of NLDAS-2 SWE interim sensible heat flux (W/m^2) for the FC region. (slope = +6.9 W/m^2/decade). Trend is not significant at α = 0.05.

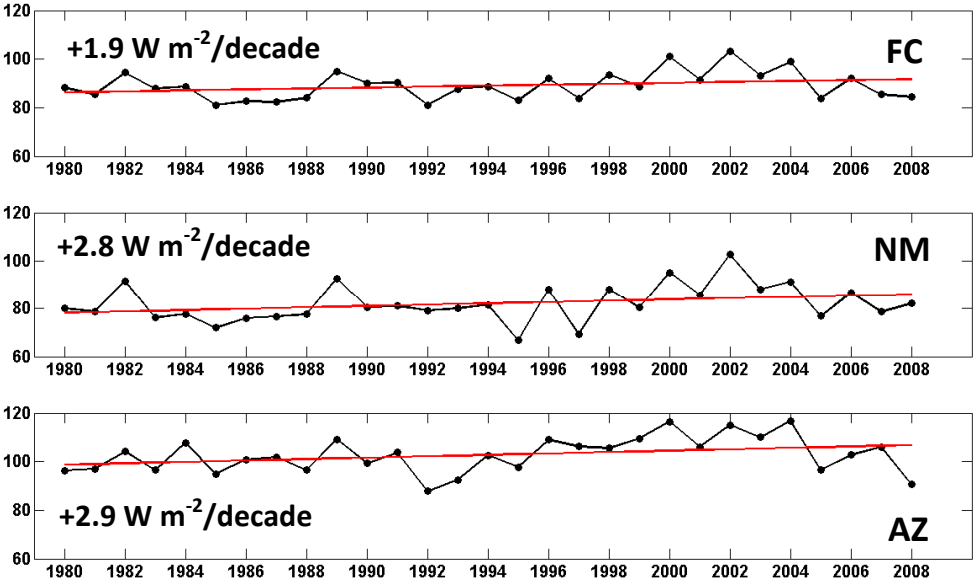

Figure 33. Spatially averaged NLDAS-2 interim sensible heat flux (W/m^2) for FC, NM, AZ regions.

Monthly mean sensible heat flux trends

In the FC averaging region, August and September have the strongest positive linear trends in interim sensible heat flux (+4.5 W/m^2/decade and +3.0 W/m^2/decade) (Table 7). Trends in the remaining months range from +2.3 W/m^2/decade in June to -1.2 W/m^2/decade in July. The trend in interim FC sensible heat flux accounts for the greatest PCTV in sensible heat flux in April (14.6 %) followed by June (10.7%). The PCTV accounted for by the trend in sensible heat flux during the remaining months ranges between 9.1% (February) to 0.3% (August).

In the NM averaging region, the strongest positive linear trends in sensible heat flux occur in May (+3.0 W/m^2/decade) and June (+2.2 W/m^2/decade) (Table 7). Trends in the remaining months range from +1.9 W/m^2/decade (March and April) to -1.3 W/m^2/decade (July). The trend in interim sensible heat flux accounts for the greatest PCTV in sensible heat flux in March (9.7%) followed by May (7.1%). The PCTV accounted for by the trend in sensible heat flux during remaining months ranges between 4.6% (June) to 0.01% (January).

In the AZ averaging region, March and April have the strongest positive linear trends in interim sensible heat flux (+3.6 and +5.8 W/m^2/decade, respectively, in Table 7). Trends in the remaining months range from +2.9 W/m^2/decade in June to +0.02 W/m^2/decade in August. The greatest PCTV accounted for by the trend in AZ sensible heat flux is in April (33.3%), followed by March (17.1 %). The PCTV accounted for by the trend in sensible heat flux ranges between 16.9% (June) to 0% (July), in the remaining months (Table 7).

The positive linear trend in sensible heat flux is strongest in the AZ region in March. Between the three averaging regions, the strongest trends and highest PCTV's explained by the trends are found in March, April, May and June. The exception is the FC averaging

region where the first and second strongest trends in that region are in August and September, though the highest PCTV explained by the trend is in April.

Table 7. Linear trends in NLDAS-2 sensible heat flux (W/m^2/decade) (1979-2009) and percentage of interannual variance explained by the trends in monthly mean NLDAS-2 sensible heat flux for the FC, NM and AZ averaging regions.

Sensible Heat	FC		NM		AZ	
(W/m^2/decade)	Trend	PCTV	Trend	PCTV	Trend	PCTV
Jan	0.56	3.1	-0.04	0.01	1.0	5.3
Feb	0.97	5.3	0.5	0.73	1.3	7
Mar	1.6	9.1	1.9	**9.7**	**3.6**	**17.1**
Apr	2.2	**14.6**	1.9	6.4	**5.8**	**33.3**
May	1.8	5.2	**3.0**	**7.1**	2.9	7.5
Jun	2.3	**10.7**	**2.2**	4.6	2.8	16.9
Jul	-1.2	2.4	-1.3	2	0.07	0
Aug	**4.5**	0.3	0.12	0.02	0.34	0.13
Sep	**4.0**	0.4	-0.81	0.84	0.82	1.1
Oct	0.72	1.7	-0.7	1.3	2.6	12.7
Nov	0.51	1.4	1.3	6.4	0.69	1.6
Dec	0.93	7.2	0.53	1.8	0.82	7.3

Sensible heat flux maps

Interim period sensible heat flux climatology is highest over a large region of central Arizona and much of the New Mexico highlands (Figure 34a). It is lowest in the Colorado and Utah highlands. Interim sensible heat flux variance is very similar to interim latent heat flux variance (Figure 34b, Figure 31b). The leading EOF of interim sensible heat flux explains 45% of the variance in the data (Figure 34c). Most of the high elevation regions of the EOF map vary coherently but portions of the low elevations vary in the opposite direction. Most of the region has increasing linear trends in sensible heat flux (Figure 34b); especially in Arizona where the maximum linear increase in sensible heat flux is between

+15 W/m^2/decade and +18 W/m^2/decade. Some areas have decreasing sensible heat fluxes, specifically those that had declining temperatures (e.g. Colorado high elevations).

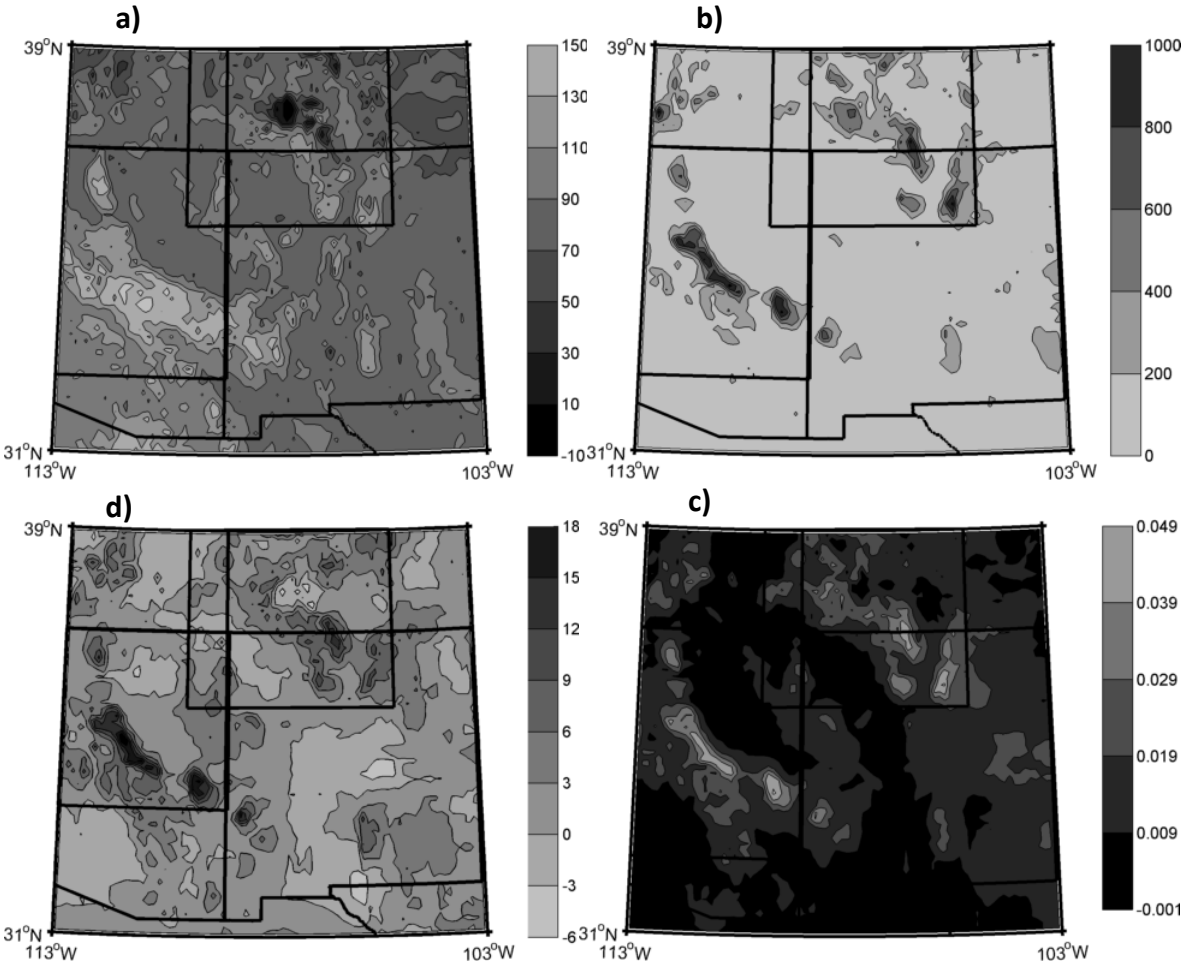

Figure 34. Climatology(W/m^2) (1979-2009) (a), interannual variance (W^2/m^4) (b), the first empirical orthogonal function (unitless) (c) and the linear trend (W/m^2/decade) (d) of NLDAS-2 sensible heat flux between snow ablation and monsoon onset.

Bowen Ratio

Trends in interim Bowen ratio

There is a significant positive linear trend in the leading PC of the Bowen ratio

(slope = +3.1/decade, p = 0.02, in Figure 35). The FC (slope = +1.2 /decade, p= 0.04) and AZ (slope = +2.5/decade, p = 0.02) averaging regions have significant linear trends in the Bowen ratio, while the NM averaging region does not NM (slope = +0.7/decade, p =0.05) (Figure 36).

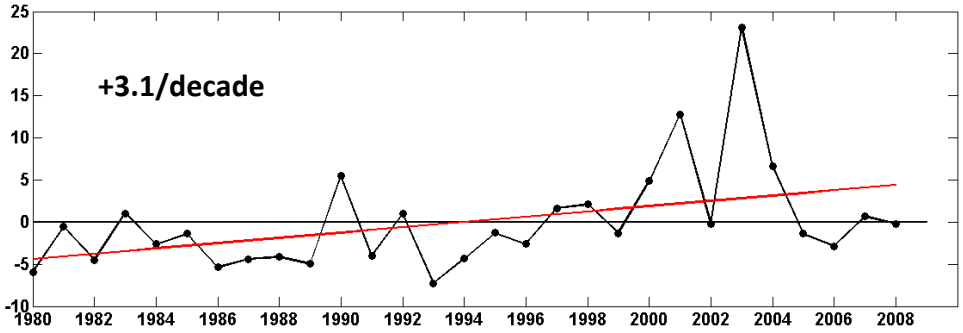

Figure 35. First principal component of NLDAS-2 SWE interim period Bowen ratio (unitless) for the FC region (slope = +3.1 /decade, p =0.02).

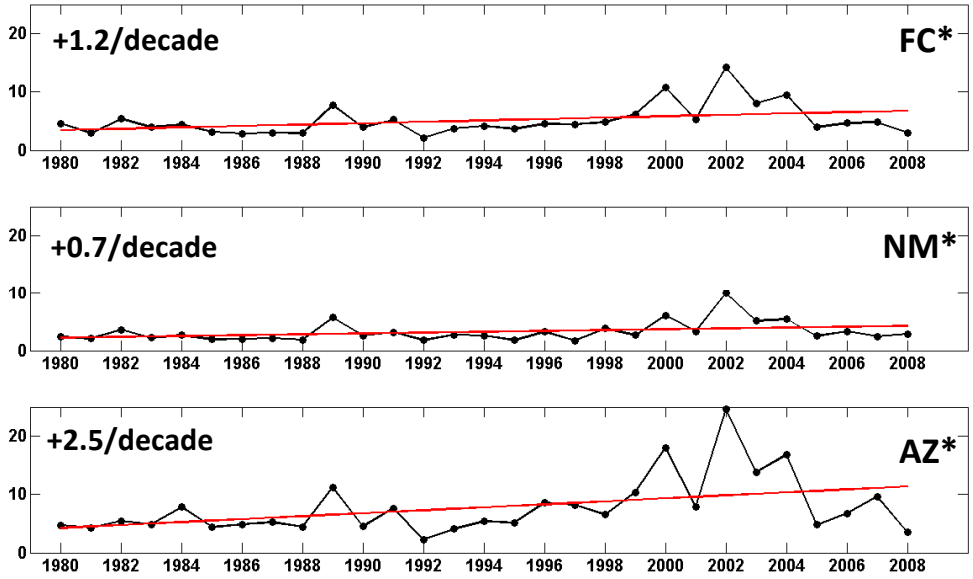

Figure 36. Spatially averaged interim Bowen ratio. Top to bottom: FC*, NM and AZ*. *Indicates statistically significant linear trend at α = 0.5.

Bowen ratio maps

The climatological Bowen ratio during the interim period is highest in the Southwest corner of our study region (12 to 14.5) and becomes weakly negative toward the northeast corner of our study region (-0.5 to 2) (Figure 37a). Interannual variance, however, is greatest in the Mogollon Rim region of Arizona, the mountains of northern New Mexico and parts of the Utah and Colorado high elevations (Figure 37b). Region of high Bowen ratio variance also correspond to areas of high interim period precipitation that fall on eastern edge of our study area, in New Mexico (Figure 37b). There are some areas of opposite covariance on the EOF map, in southern Arizona and in the region of Colorado where temperature and sensible heat flux are decreasing (Figure 37c). The Bowen ratio is not increasing strongly in most high elevation areas, the exception being over a large portion of Arizona that includes the Mogollon Rim (Figure 37d).

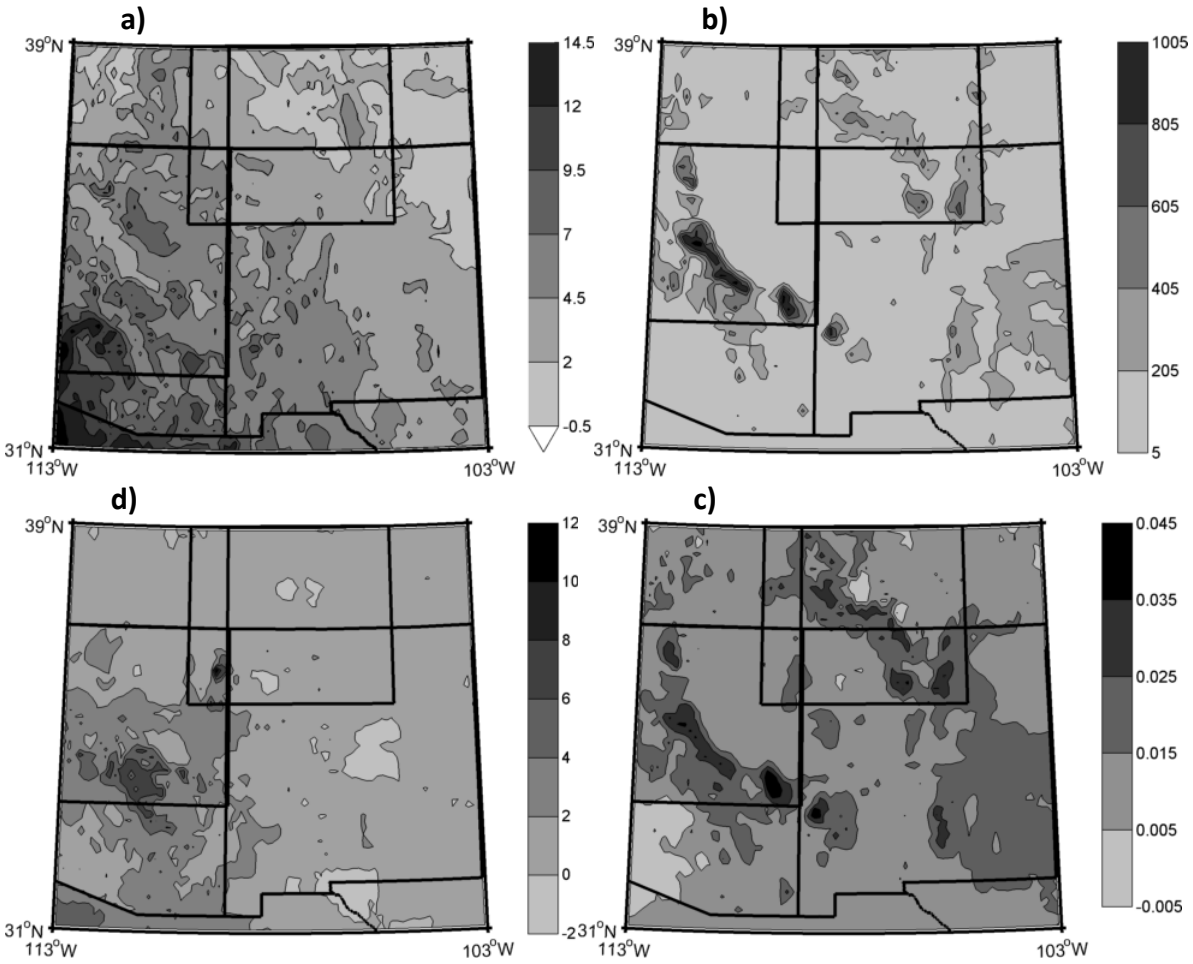

Figure 37. Climatology (unitless) (1979-2009) (a), interannual variance (unitless^2) (b), the first empirical orthogonal function (unitless) (c) and the linear trend (/decade) (d) of NLDAS-2 Bowen ratio between snow ablation and monsoon onset.

Summary of results

Here, we summarize the key features of spring variability in southwestern U.S land surface hydroclimatology. There are non-significant, small, decreasing trends in the maximum amount of SWE (Figure 2c) with the strongest decreasing trends in maximum SWE concentrated entirely in regions with highest snowpack and elevation (Figure 2d).

Trends in the melt day of SWE (up to -28 days/decade) are significant in our study region (Figure 5) and are found in most high elevation regions of the Southwest, in addition to exhibiting large-scale spatial coherence outside of the highest elevations (Figure 6b). The first EOF of SWE melt day shows that the trend in that variable accounts for a large amount of its variance, while the first EOF of maximum SWE is most similar to the variance map of maximum SWE. NLDAS-2 indices of maximum SWE agree reasonably well with observations (Figure 7), but validation of the NLDAS-2 SWE melt date remains elusive, because the regions with greatest trends and variability in that index are sparsely instrumented.

We find large but non-significant positive linear trends in spring temperature and high variability in spring temperature. Positive trends in MAM temperature are present throughout the high elevations of the study region of up to +1.2°C/decade, over the relatively short period of record, with the exception of the highest elevations of Colorado where temperature is decreasing (up to -0.8 °C/decade) (Figure 17d). Over large spatial averages, the effect is still to have positive temperature trends in most months (Table 1). In addition to MAM mean temperature increasing, the predominant temperature trends for different spatial averages occur in March, April, May and July, indicating that spring is the primary season for warming over the period of record (Table 1).

We find decreasing linear trends in post snow ablation and pre-monsoon onset total precipitation that are significant over the NM averaging region (Figure 20). Interim period rainfall is highest in the eastern region of our analysis area with local maxima over the mountains (Figure 23). Monthly mean rainfall and snowfall are decreasing most strongly in

Arizona with the largest rainfall decreases in the spring and the largest snowfall decreases in January and February (Table 3).

High elevations are key regions of coherent variability in soil moisture (Figure 28b). Negative soil moisture trends are strongest over the Mogollon Rim region in Arizona and the southern Sangre de Cristo Mountains in northern New Mexico (Figure 33d). The highest elevations of Colorado and a small area on the Texas border have increasing soil moisture. The strongest trends in soil moisture and highest PCTV explained by the trends in soil moisture occur in the spring (Table 5).

Latent heat flux exhibits spatial coherence over mountainous areas and the strongest negative linear trends are over the Mogollon Rim in Arizona (Figure 31c). Among the three averaging regions, trends in latent heat flux and PCTV explained by the trends are highest among the three regions in April, May and June (Table 6). Climatological sensible heat flux is highest over the Mogollon Rim and much of the New Mexico highlands (Figure 34a). It is lowest in the highest elevations of Colorado. Latent and sensible heat flux variances are similar spatially but they vary oppositely in time.

The Bowen ratio is highest in the southwest corner of the analysis region and decreases towards the northeast (Figure 37a). Increasing Bowen ratio trends in Arizona are the most prominent spatial feature of the Bowen ratio. Areas of decreasing Bowen ratio coincide with decreasing temperature.

In this section we have documented concurrent warming and drying trends in NLDAS-2 land surface hydroclimatology over the 1979-2009 period of record. In the next section, we will examine how snowpack, temperature and precipitation explain variability in soil

moisture and surface turbulent fluxes, with the goal of better understanding how the observed trends may be generated.

4. SNOW WATER EQUIVALENT PREDICTORS

Temperature

The leading PC of January – February – March (JFM) mean temperature is a very weak predictor of SWE melt out date (r = -0.18) or maximum SWE (r = -0.16) (not shown). The leading PC of March – April –May (MAM) mean temperature is a better predictor of SWE melt out day (r = -0.42) and maximum SWE (r = -0.46) (not shown).

To analyze the effects of temperature on SWE indices we used composite analysis with six years each of high maximum SWE or low maximum SWE and late SWE melt or early SWE melt. Figure 38 shows the results of compositing MAM temperature based on extreme years in the SWE indices. In all three averaging regions, low SWE years have a narrower temperature range, and a higher median, compared to high SWE years (Figure 38). High SWE years may have MAM temperatures that are just as high or higher than MAM temperatures in low SWE years, but they may also have temperatures that are lower than the lowest low SWE year temperatures. Late melt years also have a narrower range of temperatures than earlier melt years. However, MAM median temperatures are less similar in late/early melt composites compared to high/low SWE composites, with statistically significant temperature differences between early and late melt years for the FC and NM regions, but not for AZ.

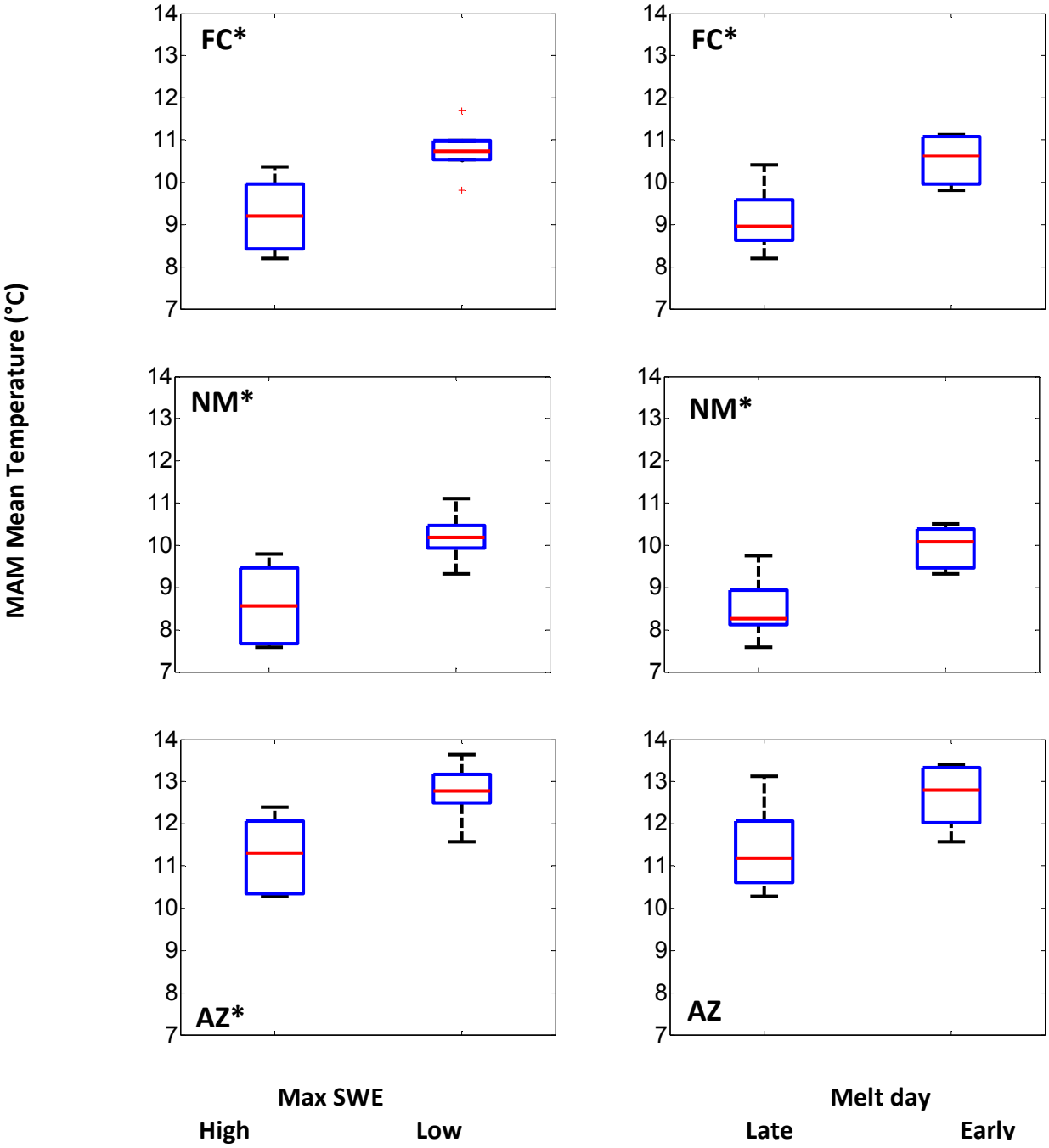

Figure 38. NLDAS-2 MAM mean temperature (°C) composites based on 6 years each late and early SWE melt and 6 years each high and low maximum SWE. *Indicates significant differences between the means at α = 0.05.

Precipitation

We used composite analysis to examine the relationship between JFM precipitation and snowpack in the FC, NM and AZ averaging regions (Figure 39). As expected, median total JFM precipitation is higher in high maximum SWE than in low maximum SWE, with significant differences in JFM precipitation for all averaging regions. High SWE years also have very wide ranges of JFM precipitation compared to low SWE years. Total JFM precipitation has a less predictable influence on the SWE melt date. Late SWE melt years have a higher median but both high and low SWE years have highly variable melt out dates.

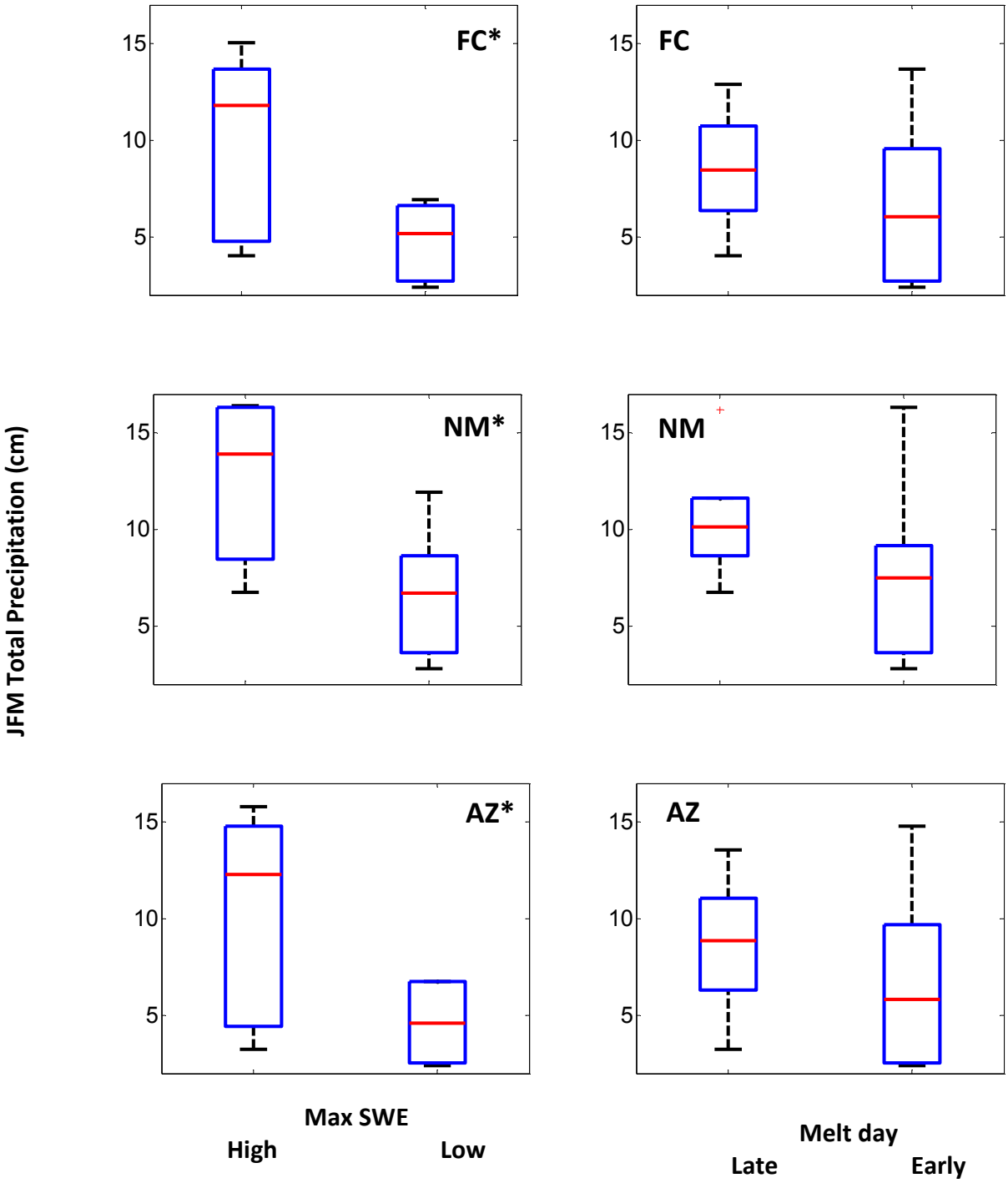

Figure 39. NLDAS-2 total JFM precipitation (cm) composites based on 6 years each late and early SWE melt and 6 years each high and low maximum SWE. *Indicates significant differences between the means at α = 0.05.

Melt date vs. maximum SWE

The first principal components of SWE melt-out day and maximum SWE are weakly positively correlated (r = 0.32) (Figure 40). When the melt day is composited using maximum SWE in the FC, NM and AZ averaging regions, we observe that median melt day has non-significant differences in the NM and FC regions, when composited around high and low maximum SWE. Maximum SWE amount appears to have no influence on SWE melt day in the AZ averaging region. In the NM averaging region, median melt day is later in high SWE years but high SWE years also include a wider range of melt day values than low SWE years. This indicates that in the NM averaging region, any given high SWE year does not reliably lead to a later melt day.

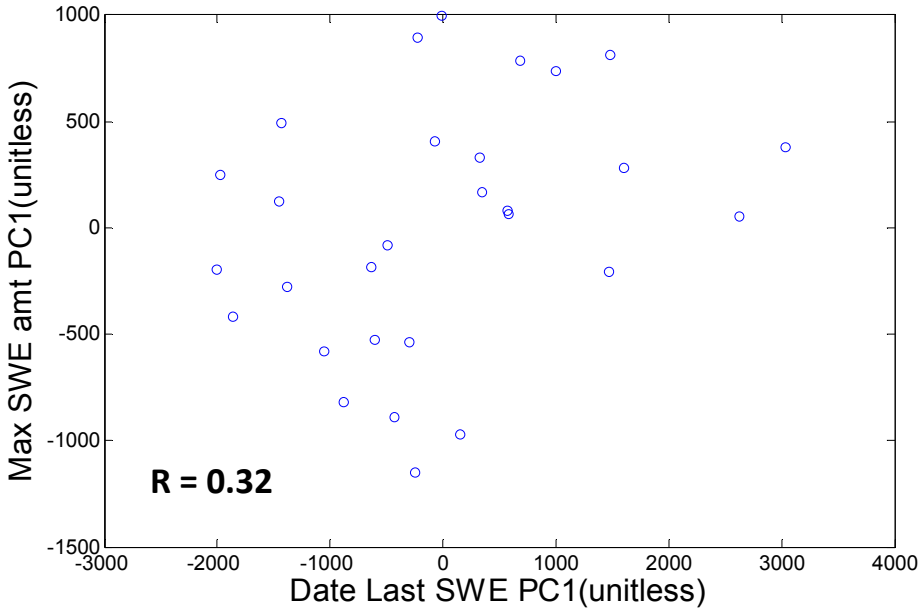

Figure 40. Last day NLDAS-2 SWE PC1 (unitless) (abscissa) versus NLDAS-2 max SWE PC1 (unitless) (ordinate) for 1980-2008 (r = 0.32, p= 0.09, n = 29).

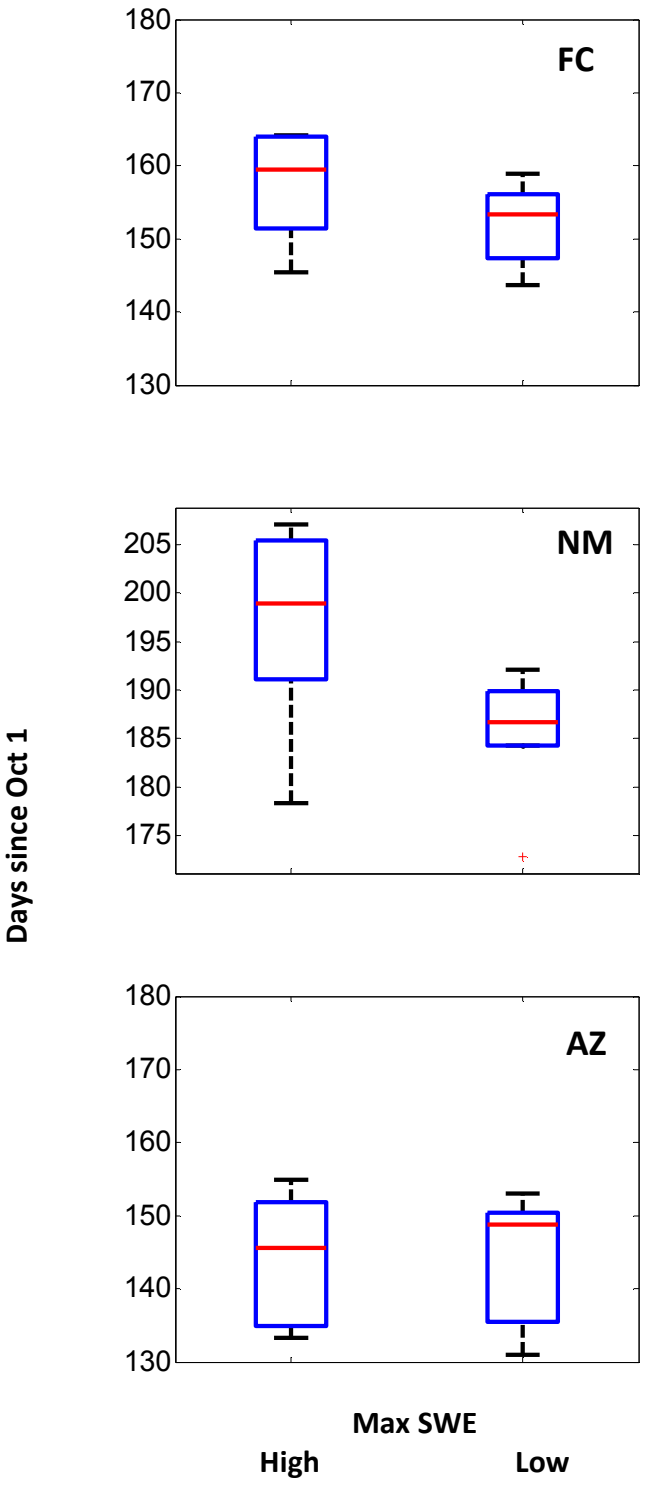

Figure 41. NLDAS-2 SWE melt date composites (number of years into WY) based on 6 years each high (left) and low SWE (right) from the 1980-2008 period.

5. SOIL MOISTURE PREDICTORS

Monthly mean lagged soil moisture

Here, we investigate soil moisture memory using monthly lag correlations of monthly mean NLDAS-2 soil moisture from 1979-2009 (Figure 42). Over the FC averaging region, the ability of previous month's soil moisture to predict soil moisture a month later declines steadily from March to July. By June the relationship with March soil moisture is still moderate (r = 0.42), and is similar to the relationship between April and June soil moisture (r = 0.46). By July the relationship between July soil moisture and March, April and May soil moisture is negative and between r = -0.23 and r=-0.14. Only June soil moisture has a positive correlation with July soil moisture (r = 0.09), but it is very weak (Figure 42).

Relationships between lagged soil moisture in the NM averaging region are very similar to those in the FC averaging region (Figure 40). Lagged soil moisture in the AZ averaging region is distinctive because the lag correlations remain high until June (r = 0.76 to r = 0.87). In the AZ averaging region, the relationship between March, April and May soil moisture and the following months declines sharply in July (Figure 40). March soil moisture has a stronger correlation with August soil moisture than July soil moisture in the AZ region (r = 0.53, r=0.49, respectively). April and May are also slightly better correlated with August moisture than with July soil moisture in the AZ region.

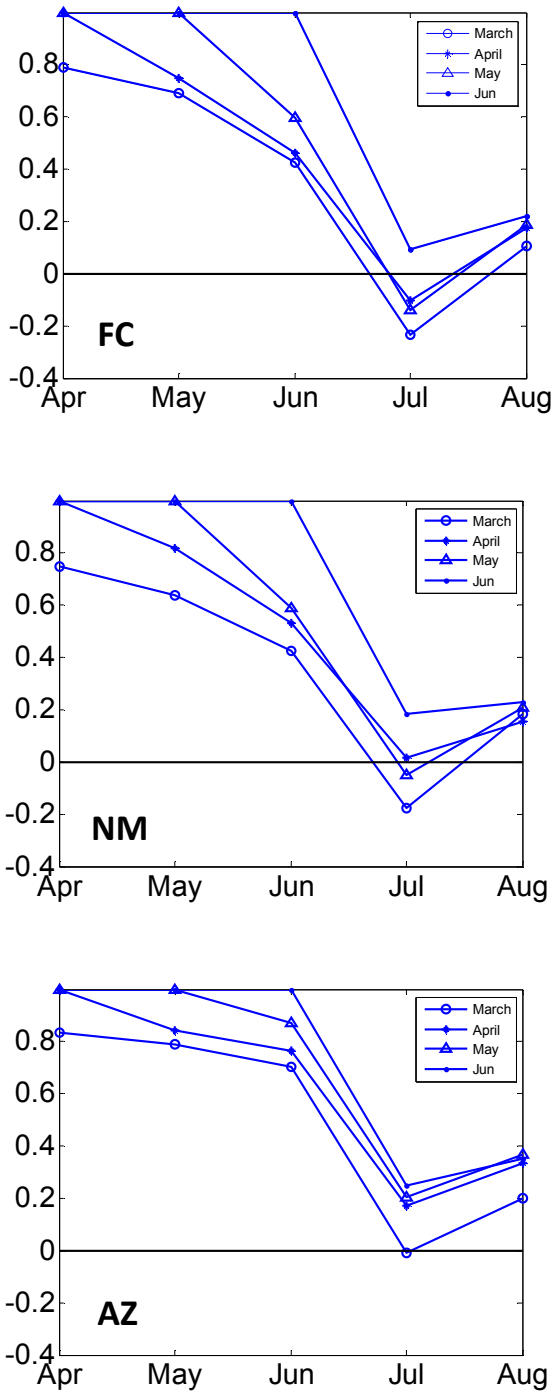

Figure 42. March, April, May and June monthly mean NLDAS-2 soil moisture correlated with monthly mean soil moisture in the following months, at one to five month lags (1979-2009, n = 31).

Temperature vs. soil moisture

Correlations

We analyzed the relationship between temperature and soil moisture as lags between monthly mean soil moisture and temperature (Table 8). We also analyzed the relationship between the leading PC of March – April – May (MAM) mean surface temperature and interim soil moisture. The leading PCs of MAM temperature and of interim soil moisture are moderately correlated (r = -0.54) (not shown).

In the NM averaging region the strongest correlations of spatially averaged monthly mean temperature and soil moisture are between May temperature versus May soil moisture (r = -0.58), April temperature versus April soil moisture (r = -0.56), and April temperature and May soil (r = -0.53) (Table 8).

In the AZ averaging region, temperature is only moderately correlated with soil moisture except for April soil moisture versus April mean temperature (r = -0.56). April temperature and May soil moisture (r = -0.40) and May soil moisture and May temperature (r = -0.42) are moderately correlated. In the FC averaging region, April temperature and April soil moisture are the best correlated (r = 0.50), followed by May temperature and May soil moisture (r= -0.46) (Table 8).

Table 8. r values for NLDAS-2 monthly mean soil moisture versus monthly mean temperature for FC, NM and AZ regions (1979-2009).

Soil Moisture	FC Mar	Apr	May	NM Mar	Apr	May	AZ Mar	Apr	May
Mar Temp	-0.29	-0.18	-0.19	-0.37	-0.22	-0.13	-0.38	-0.33	-0.36
Apr Temp	.	-0.50	-0.35	.	-0.56	-0.53	.	-0.56	-0.40
May Temp	.	.	-0.46	.	.	-0.58	.	.	-0.42

Overall, April and May are the months with the strongest temperature and soil moisture correlations, with April temperature and May soil moisture as the predominant lag relationship. This is likely due to the snowpack enhanced soil moisture in the spring, combined with seasonally increasing spring temperatures.

MAM temperature correlation with interim soil moisture is strongest on border of Colorado and New Mexico as well as in the Arizona high elevations ($r = -0.7$ and $r = -0.85$) (Figure 43).

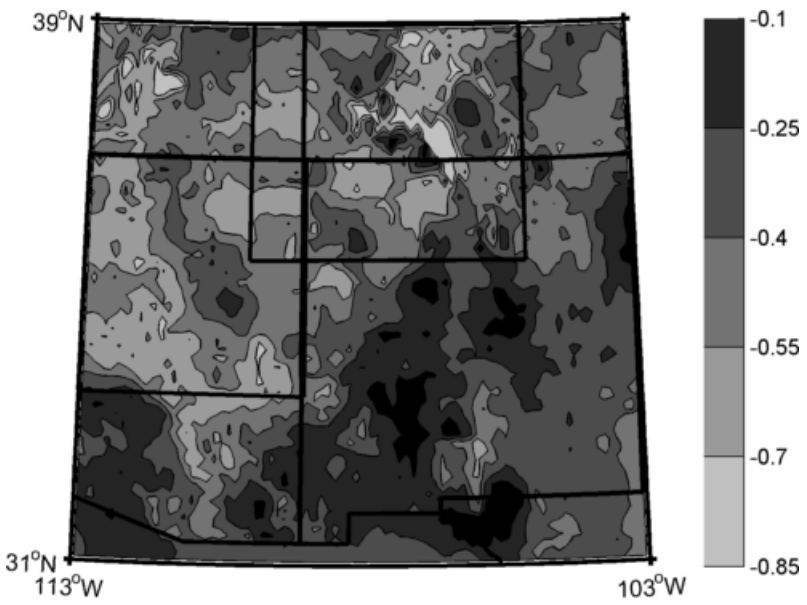

Figure 43. Correlation map of NLDAS-2 MAM mean temperature versus interim soil moisture (1980-2008, n=29). Contours represent r-values.

SWE vs. soil moisture

Correlations

Over the FC region, the first principal component of maximum SWE is a better predictor of soil moisture (r = 0.64) (not shown) than the PC1 of last day of SWE (r = 0.34) (not shown). Breaking the analysis down by region, in the FC averaging region, maximum SWE (r = 0.61) is a better predictor of mean interim soil moisture than SWE melt day (r = 0.52) (not shown). In the NM averaging region, maximum SWE (r = 0.74) is a better predictor of mean interim soil moisture than SWE melt day (r = 0.60) (not shown). In the AZ region, the correlations between maximum SWE and soil moisture and SWE melt day and soil moisture are similarly weak (r = 0.19, r =0.17, respectively) (not shown).

In addition to interim period comparisons, we compared monthly mean, spring and summer soil moisture over the NM, AZ and FC averaging regions, with the SWE indices. In the FC region, maximum SWE is a better predictor of soil moisture than SWE melt date from March to August. Maximum SWE had a moderately strong relationship with soil moisture into June, with the strongest relationship in May (r = 0.59). Last date of SWE had the strongest relationship with soil moisture in April (r = .33).

In the NM region, maximum SWE is a good predictor of March soil moisture (r = 0.72). The relationship decreases from March to June but the maximum SWE relationship with soil moisture is still moderate in June (r = 0.42). In July, maximum SWE and soil moisture have a weak negative relationship (r = -0.23). In the same region, SWE melt day was moderately correlated with monthly mean soil moisture from March to June. The strongest relationship between last day of SWE and soil moisture occurred in April (r = 0.54), followed by June (r = 0.53). The relationship remains weakly positive in July (r= 0.20) and August (r = 0.24).

In the AZ averaging region, both maximum SWE and melt date had weakly positive relationships with March and April soil moisture. Maximum SWE has a much stronger relationship with May soil moisture (r = 0.47) than melt date (r = 0.12). May and June soil moisture had the strongest relationships with maximum SWE (r = 0.47 and r = 0.51, respectively).

Figure 44 shows the spatial distribution of correlation coefficients of maximum SWE and interim soil moisture. The regions of strongest correlation (r = 0.6 - 0.8) between maximum SWE and interim soil moisture coincide with a small portion of the northern New Mexico high elevations, a small portion of the Arizona high elevations and the Utah and Colorado

high elevations represented in this analysis. Some regions of New Mexico that have moderate (r = 0.4 - 0.6) to strong (r = 0.6 - 0.8) correlations between maximum SWE and interim soil moisture do not necessarily have high mean climatological soil moisture, indicating that the relationship is not entirely dependent on mean soil moisture quantity or elevation (Figure 44).

The regions of weak to strongly moderate correlations (r = 0.12 - 0.34, r = 0.34 - 0.56) between the date of last SWE and interim soil moisture are coincident with both the trend map of last date and the climatology map of SWE melt date (Figure 45). While spatial averages of maximum SWE and soil moisture are more strongly correlated than melt date and soil moisture, there are regions of equally strong correlation between SWE melt date and soil moisture. Those regions are in lower elevations, with presumably more marginal snowpack, and they fall partially outside of the spatial averaging domains.

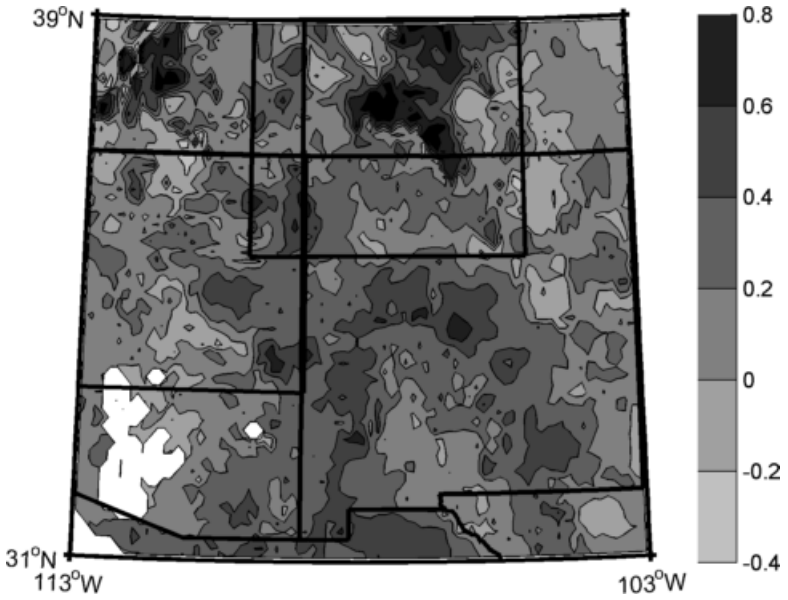

Figure 44. Correlation map of NLDAS-2 maximum SWE (kg/m^2) compared to NLDAS -2 interim soil moisture (kg/m^2)(1980-2008, n=29). Contours represent r-values.

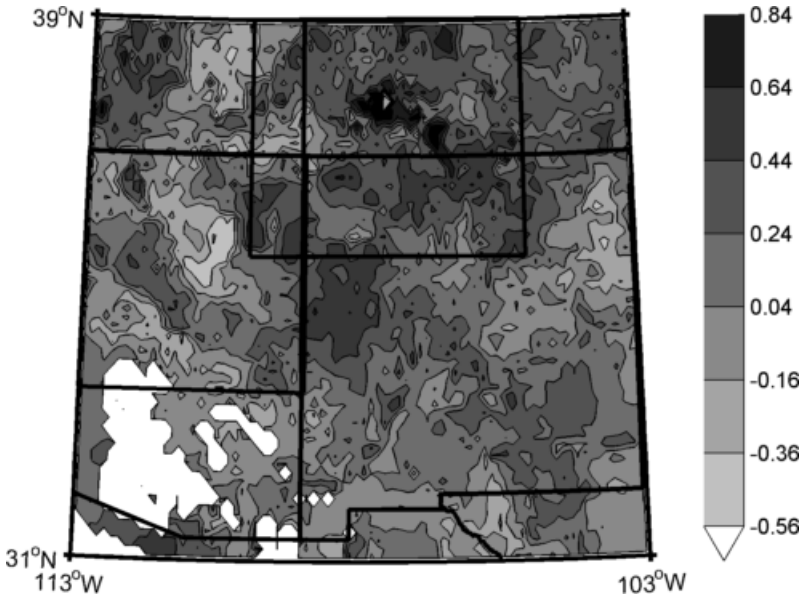

Figure 45. Correlation map of NLDAS-2 last day SWE (days into the WY from Oct 1) compared to NLDAS-2 interim soil moisture (kg/m^2) (1980-2008, n=29). Contours represent r-values.

Precipitation vs. soil moisture

The first PC's of interim precipitation and interim soil moisture are moderately correlated over the FC averaging region (r = 0.41, not shown). Interim soil moisture and total precipitation are weakly to moderately correlated for the FC, NM and AZ averaging regions (r = 0.41, r = 0.44 and r = 0.31, respectively) (not shown).

Over the entire FC averaging region, March rain and March soil moisture (r = 0.64) and May rain and May soil moisture (r = 0.77) have the strongest relationships (Table 9). April rain and April soil moisture have the weakest (r = 0.29). In the NM averaging region, March rainfall is weakly correlated with March soil moisture and subsequent months (r = 0.29). Only May rain and May soil moisture (r = 0.64) and May rain and June soil moisture are strongly correlated (r=0.58) in this region (Table 9). Also, in the NM region, April and May rain and snow are weakly to moderately correlated with May soil moisture. April soil moisture is more strongly related to April snowfall than to April rainfall (r = 0.54 versus r = 0.37, respectively).

Rain and snowfall are better predictors of March soil moisture in the AZ averaging region than in the NM averaging region, while in the NM averaging region March, April and May rain and snowfall are better predictors of May soil moisture. March rain is strongly correlated with March soil moisture in this region (r = 0.71, in Table 9).

Soil moisture and interim period total precipitation are strongly, positively correlated in the lower elevation portions of our study region, especially in the plains of Eastern New Mexico (r = 0.6 - 0.9) (Figure 44). However, soil moisture and interim period total precipitation are weakly, negatively correlated in the high elevation regions of our study

area where interim precipitation is decreasing (Figure 23). The regions where interim period precipitation is decreasing and soil moisture increasing are those with the strongest negative correlations between total interim precipitation and soil moisture.

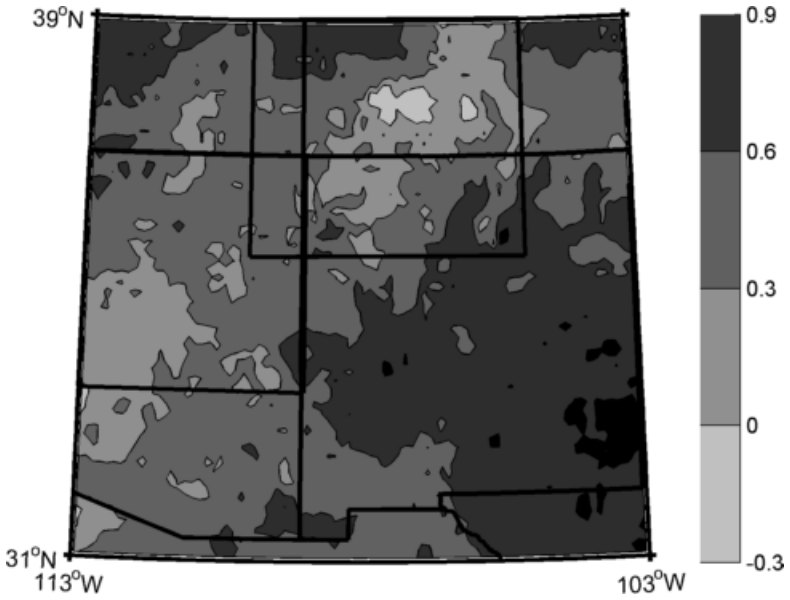

Figure 46. Correlation map of NLDAS interim total precipitation (kg/m^2/day) compared to NLDAS-2 interim soil moisture (kg/m^2) (1980-2008, n=29). Contours represent r-values.

Table 9. r values for NLDAS-2 FC,NM and AZ monthly mean soil moisture versus monthly mean total precipitation, rainfall and snowfall from 1979-2009 (n = 31).

	FC Mar	Soil Moist Apr	May	NM Mar	Soil Moist Apr	May	AZ Mar	Soil Moist Apr	May
Mar Total	0.66	0.50	0.32	0.34	0.27	0.28	0.72	0.58	0.45
Apr Total	.	0.58	0.31	.	0.48	0.45	.	0.33	0.15
MayTotal	.	.	0.78	.	.	0.67	.	.	0.61
Mar Rain	0.64	0.50	0.31	0.29	0.23	0.25	0.72	0.59	0.15
Apr Rain	.	0.29	0.57	.	0.37	0.41	.	0.15	0.32
May Rain	.	.	0.77	.	.	0.64	.	.	0.61
Mar Snow	0.56	0.36	0.27	0.35	0.29	0.28	0.52	0.38	0.13
Apr Snow	.	0.27	0.42	.	0.54	0.51	.	0.16	0.27
May Snow	.	.	0.35	.	.	0.53	.	.	.

Composite analysis of soil moisture

We used composite analysis to examine the relationship between interim period soil moisture and snowpack in the FC, NM and AZ averaging regions (Figure 47). High and low SWE years do lead to statistically significant differences in mean interim soil moisture while early and late melt years do not (Figure 47).

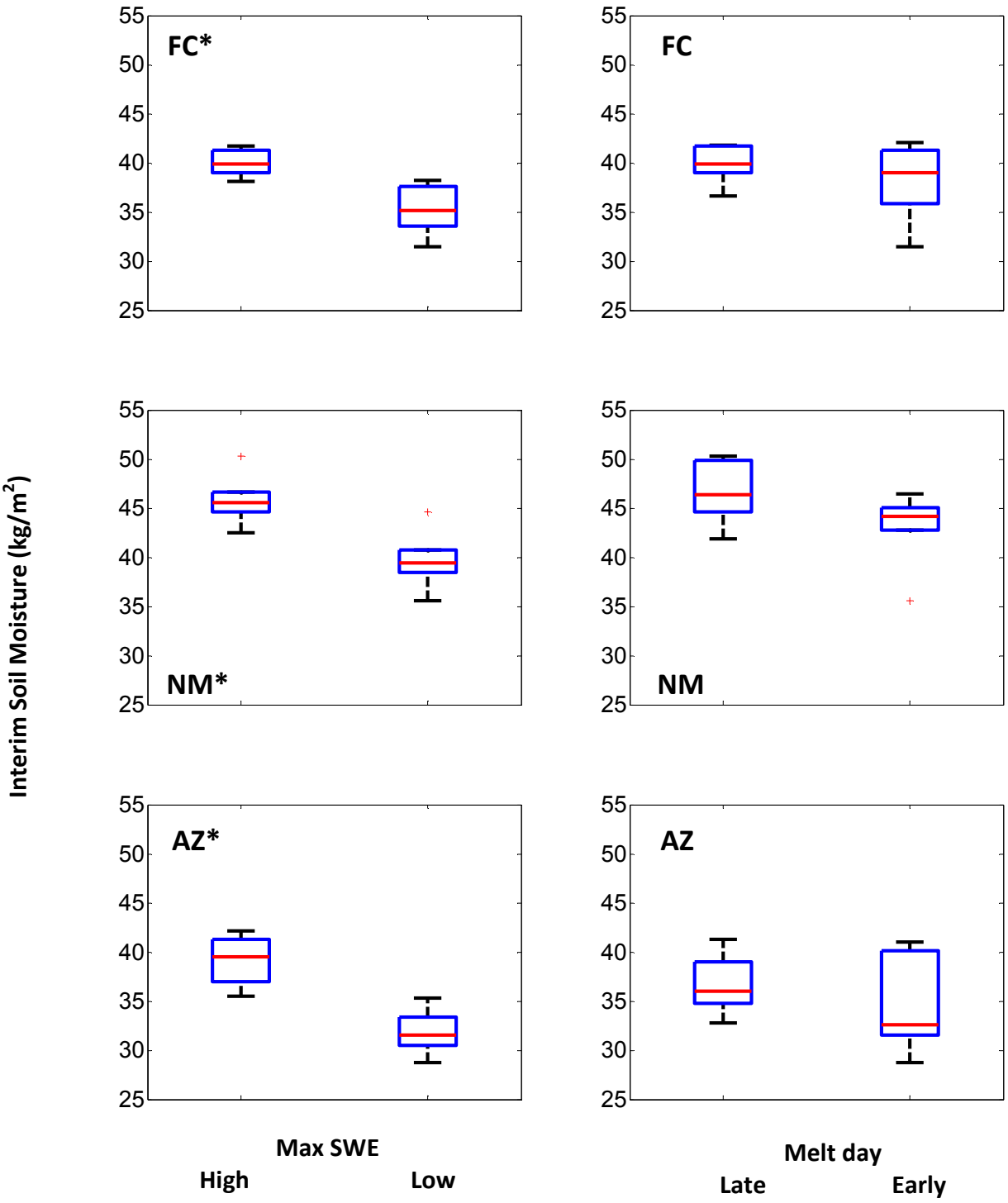

*Figure 47. NLDAS-2 interim soil moisture (kg/m^2) composites based on 6 years each late and early SWE melt (right) and 6 years each high and low maximum SWE (left) from the 1980-2008 period. *Indicates significant differences between the means at α = 0.05.*

We used composite analysis of pentad (5 day averaged) NLDAS-2 soil moisture to compare differences in soil moisture amount and timing between high and low SWE years (Figure 48) and early and late melt years (Figure 49). Soil moisture composited around high SWE in the NM region has an annual mean of 49.4 $\pm$ 5.6 kg/m^2 and soil moisture composited around low SWE has an annual mean of 45.1 $\pm$ 7.4 kg/m^2. Climatological (1979-2009) soil moisture peaks in mid-March for max SWE composites (not shown). Soil moisture composited around low SWE anomalies peaks in mid-March also, but five days earlier. In the NM region, climatological soil moisture peaks in mid-March (not shown) approximately 20 days earlier than low SWE soil moisture and 15 days earlier than climatology. High SWE composite soil moisture reaches its minimum in mid-July and the low SWE composite soil moisture reaches its minimum in late June, approximately 15 days before high SWE soil moisture. The effects of maximum SWE on soil moisture cease to exist in early July (Figure 48).

In the AZ averaging region, soil moisture composited around high SWE in the AZ region has an annual mean of 45.7 $\pm$ 7.4 kg/m^2 and soil moisture composited around low SWE has an annual mean of 38.6 $\pm$ 5.0 kg/m^2. Lower SWE years have greater uncertainty in the NM region, but not in the AZ region. High SWE soil moisture peaks in mid-February and low SWE anomaly soil moisture peaks 20 days later than high SWE soil moisture, in mid-March (Figure 48). The timings of the low points of each composite are similar to those in the NM region. In contrast to the NM averaging region, high SWE composite soil moisture remains higher than low SWE or for almost a month past the low point of soil moisture. The

composites reach the same values in mid-July, after which, moderate differences are maintained through August (Figure 48).

Soil moisture composited around late melt SWE in the NM region has an annual mean of 51.2 $\pm$ 5.0 kg/m^2 and soil moisture composited around early melt SWE has an annual mean of 48.1 $\pm$ 6.3 kg/m^2 (Figure 49). In the AZ averaging region, soil moisture composited around late melt SWE in the AZ region has an annual mean of 46.1 $\pm$ 5.3 kg/m^2 and soil moisture composited around early melt SWE has an annual mean of 43.1 $\pm$ 6.8 kg/m^2. In melt day composites, the differences between the means are smaller than those in the max SWE composites, yet the uncertainties in the means are larger. Therefore, in the NM and AZ regions, maximum SWE extremes have a greater influence on soil moisture than melt date extremes. In both composites, differences in surface (0-10 cm) soil moisture are obliterated once the monsoon starts.

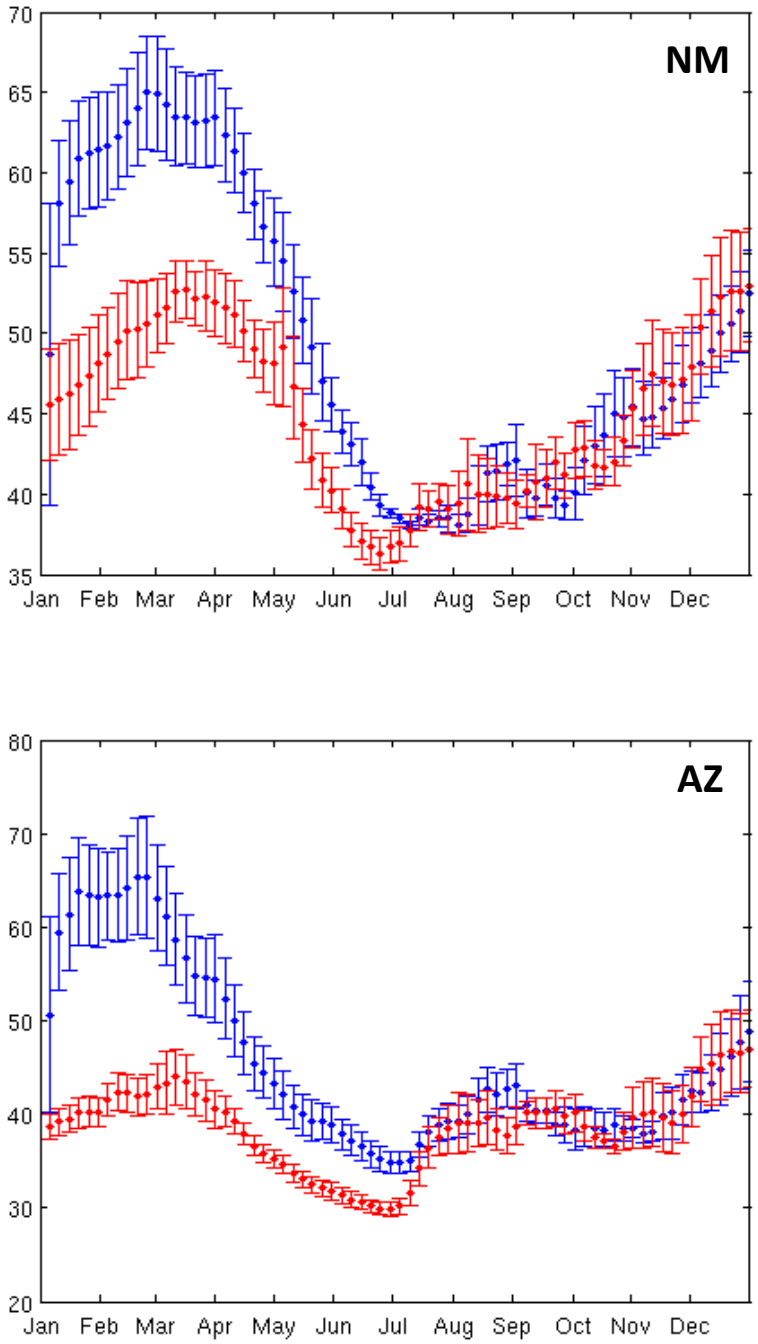

Figure 48. NLDAS-2 NM and AZ averaging region pentad soil moisture (kg/m^2) composites based on 6 years each high and low maximum NLDAS-2 SWE between 1979-2009. Error bars represent one standard error.

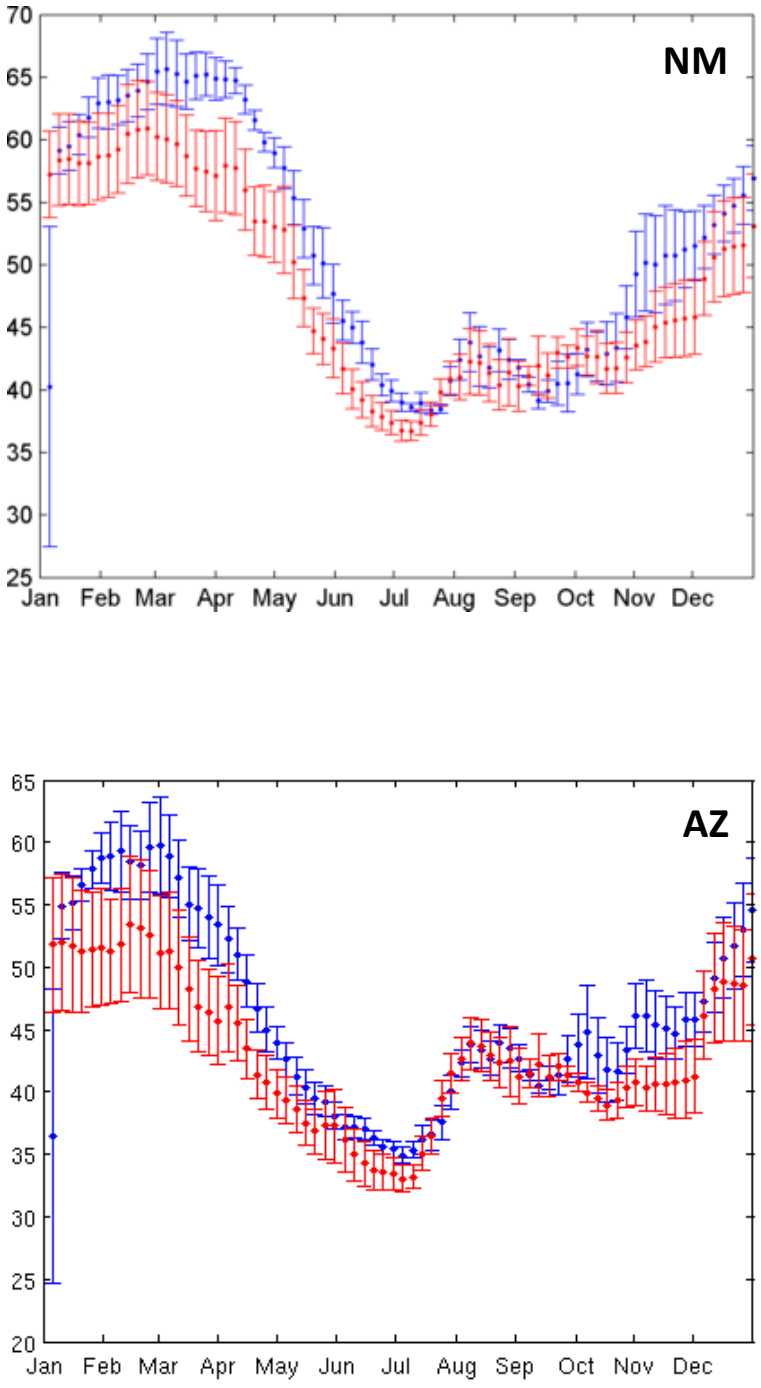

Figure 49. NLDAS-2 NM and AZ averaging region pentad soil moisture (kg/m^2) composites and climatology based on 6 years each of early and late melt day from NLDAS-2 SWE between 1980-2008. Error bars represent one standard error.

Summary of results

Soil moisture persistence is greatest in the AZ averaging region with spring soil moisture memory lasting into June (Figure 42). There are weak negative relationships between July soil moisture and soil moisture from the preceding months. Temperature and soil moisture relationships are strongest in April and May and as lagged correlations between April temperature and May soil moisture (Table 8).

MAM temperature and maximum NDLAS-2 SWE are both strongly correlated with soil moisture (r up to 0.80 and 0.85) (Figure 43 and Figure 44). Temperature is most strongly correlated with soil moisture over the northwest portion of the analysis region (Figure 43) while maximum SWE is most strongly correlated in parts of New Mexico and in the southern Colorado mountains and Utah, where temperature correlations are weak (Figure 44). Temperature, rather than maximum SWE, has the strongest correlation with soil moisture in the Mogollon Rim region of AZ (Figure 42, 44).

SWE melt day correlation with soil moisture reaches a maximum negative correlation at approximately r = -0.84 (Figure 45). The relationship between melt day and soil moisture overlaps with both temperature and max SWE in space. Precipitation also strongly correlates with interim soil moisture (Figure 46), with interim period r-values for the leading principal component of soil moisture and precipitation similar to those for temperature and SWE indices.

Interim period composites of soil moisture based on high and low maximum SWE and early and late melt days show that extreme years in maximum SWE amount influences soil moisture more than extreme years in early and late snow melt (Figure 47). Compositing

pentad soil moisture around maximum SWE yields differences in soil moisture amount that begin in Feb and persist until early July (AZ) or early August (NM). However, our small sample size (n = 6) yields large uncertainties in the means. Maximum SWE yields greater differences in amount and timing of pentad soil moisture composites than SWE melt day (Figures 48, 49).

6. ENERGY BUDGET PREDICTORS

Soil moisture versus latent heat flux

We expect soil moisture to exert a strong influence on latent heat flux and sensible heat flux, and vice versa. There is a strong correlation between the leading PC of interim latent heat flux and the leading PC of soil moisture (r = 0.80, not shown) and a strong correlation between the leading PC of interim sensible heat flux and soil moisture (r = -0.90, not shown).

We analyzed the lagged effect of soil moisture on latent heat flux (Table 10). Over the FC averaging region, the relationships between March, April and May latent heat and contemporaneous soil moisture are strong (r = 0.97 – 0.93). March soil moisture and April latent heat have the strongest lagged relationship (r = 0.75). July latent heat and March, April and May soil moisture all have weak negative relationships (r = -0.17, r = -0.18, r= -0.23).

In the NM averaging region, the strongest monthly mean correlation between latent heat and soil moisture occurs between April soil moisture and May latent heat (r = 0.91) (Table 10). The second strongest correlation is between May soil moisture and May latent heat (r = 0.90). The presence of snowpack likely weakens the relationship between soil moisture and latent heat in March and April.

In the AZ averaging region, latent heat is best predicted by contemporaneous soil moisture in March, April and May (r = 0.95 – 0.98) (Table 10). AZ latent heat has a strong

relationship with soil moisture at a two month lag (April soil moisture versus June latent heat, r = 0.83). March soil moisture also correlates well with April latent heat (r = 0.80).

Table 10. r-values for monthly mean NLDAS-2 latent heat flux versus monthly mean soil moisture for the FC, NM and CO regions (1979-2009).

Soil Moisture	FC Mar	Apr	May	NM Mar	Apr	May	AZ Mar	Apr	May
Mar LH	0.94	.	**.**	0.50	.	**.**	0.95	**.**	**.**
Apr LH	0.75	0.93	**.**	0.43	0.78	**.**	0.80	0.96	**.**
May LH	0.64	0.65	0.97	0.60	0.91	0.91	0.74	0.76	0.98
Jun LH	0.24	0.32	0.46	0.29	0.43	0.46	0.65	0.72	0.83
Jul LH	-0.23	-0.17	-0.17	**.**	-0.06	-0.14	**.**	0.02	0.06
Aug LH	0.14	0.21	0.21	**.**	0.15	0.23	**.**	**.**	0.36

SWE versus latent heat flux

We examine the relationship between NLDAS-2 SWE indices and interim latent heat flux. The leading PCs of interim latent heat and maximum SWE have a weak positive linear relationship (r = 0.33) (not shown). Interim latent heat flux and soil moisture in the FC and NM averaging region are similarly correlated (r = 0.45 for both) (not shown). Interim latent heat flux and soil moisture in the AZ averaging region are weakly correlated (r = 0.34) (not shown).

We compare the effects of both SWE indices on interim latent heat flux using composite analysis with six years each of high SWE/late melt and low SWE/early melt (Figure 49). The only statistically significant difference between mean interim latent heat flux occurs in between high and low SWE years in the AZ averaging region. In high SWE years the FC and NM averaging regions have slightly higher latent heat flux values but they also have much

narrower ranges of values than low SWE years (Figure 47), that are not explained by the ranges in interim soil moisture composites (Figure 50).

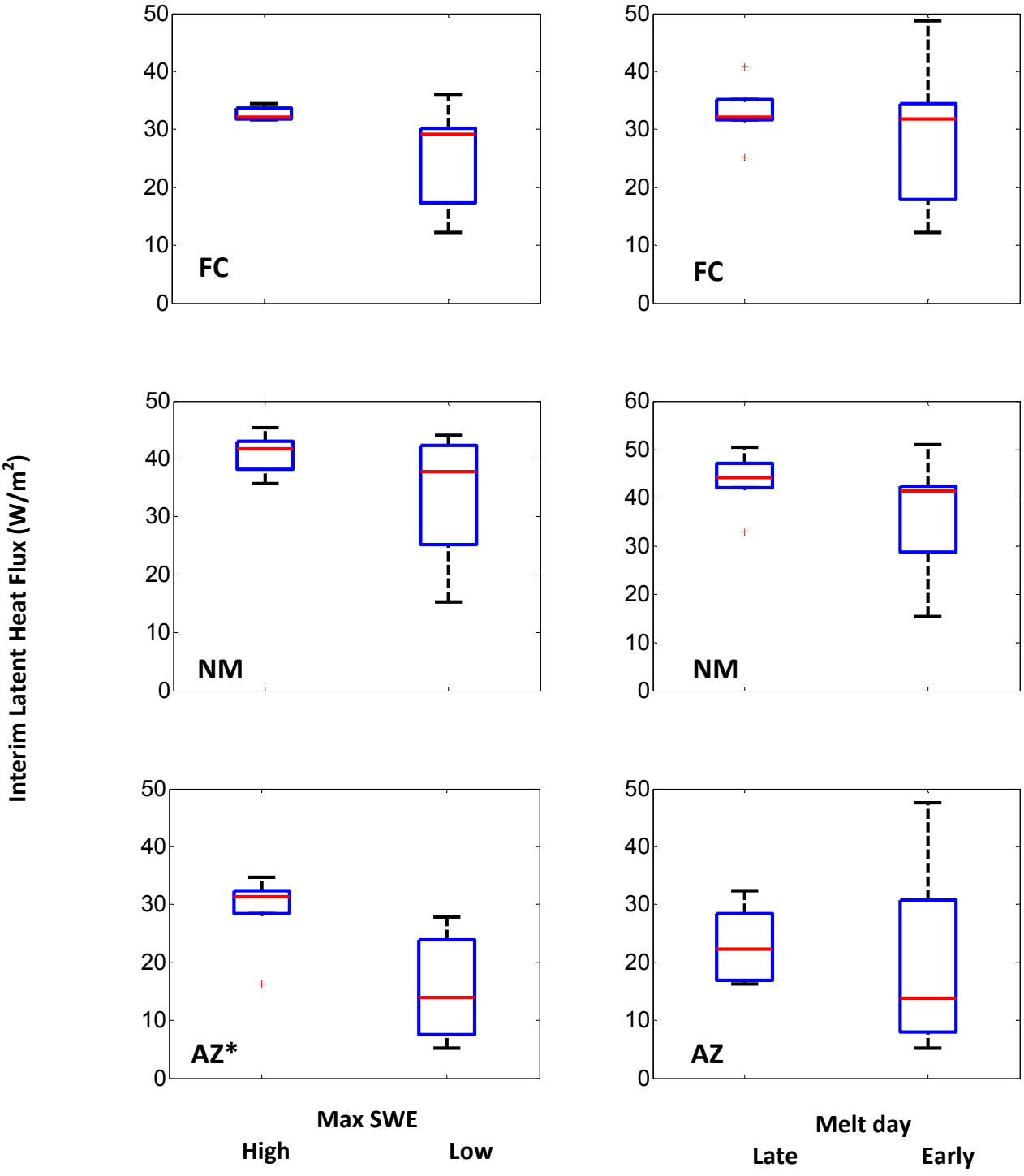

*Figure 50. NLDAS-2 interim latent heat flux (W/m^2) composites based on 6 years each late and early SWE melt (right) and 6 years each high and low maximum SWE (left) from the 1980-2008 period. *Indicates significant differences between the means at α = 0.05.*

SWE versus sensible heat flux

We compare the effects of both SWE indices on interim sensible heat flux using composite analysis with six years each of high SWE/late melt and low SWE/early melt (Figure 51). There are only minor differences between mean sensible heat flux composite values for any averaging region or for either SWE index, and the only significant difference in mean sensible heat flux occurs for the maximum SWE composite in the AZ averaging region. High SWE years, and to a lesser extent, late melt years, do have much narrower ranges of sensible heat flux values than low SWE/early melt years.

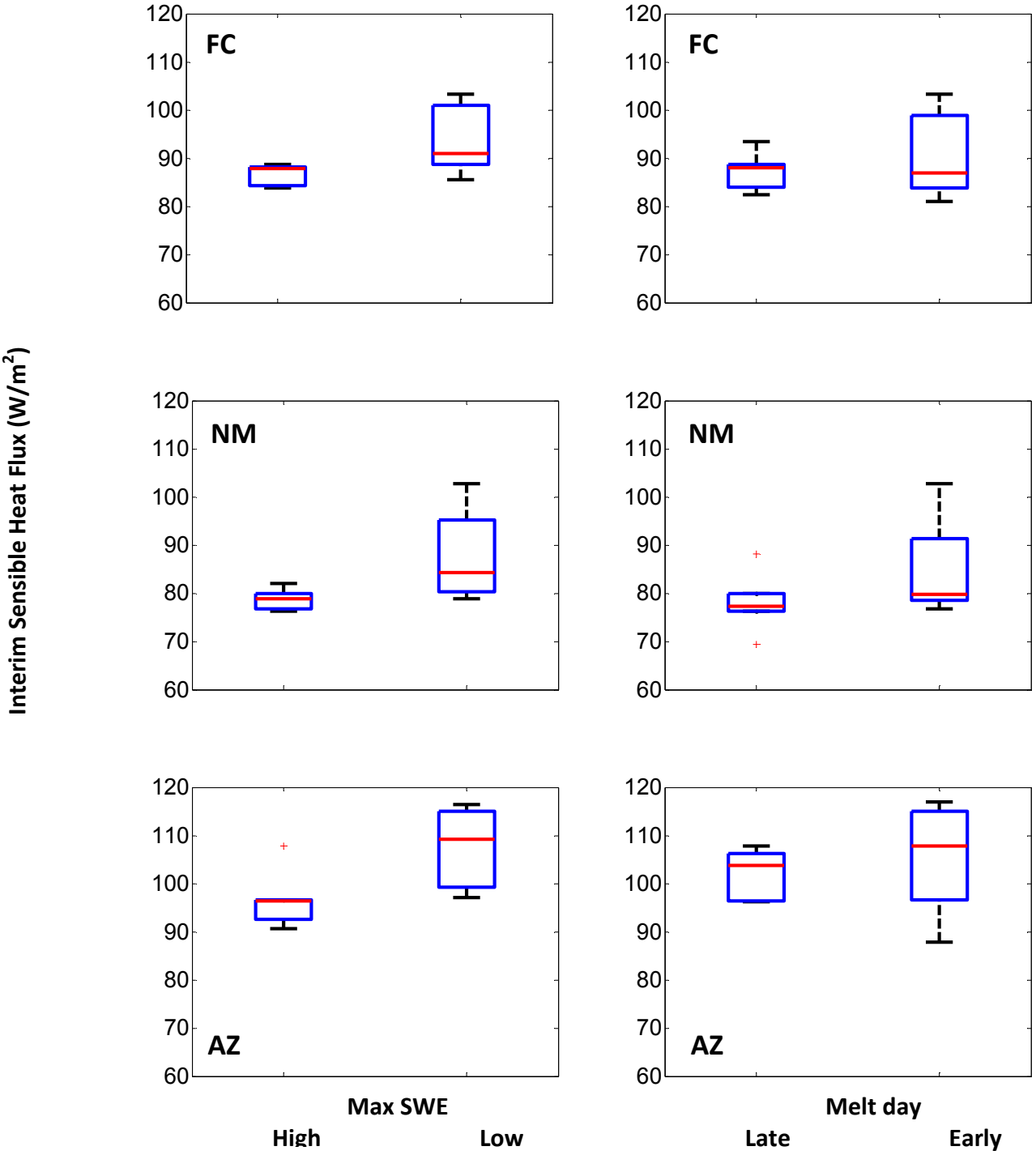

Figure 51. NLDAS-2 interim sensible heat flux (W/m^2) composites based on 6 years each late and early SWE melt and 6 years each high and low maximum SWE from the 1980-2008 period.

Bowen Ratio

We used composite analysis to examine the effect of NLDAS-2 SWE indices on the Bowen ratio during the interim period (Figure 52) and on the pentad Bowen ratio for the annual cycle (Figure 53).

There are no significant differences in mean Bowen ratio composites for either SWE index or for any of the averaging regions (Figure 52). Median Bowen ratio values are only slightly lower in low SWE years in the AZ regions and are very similar in the FC and NM regions. Both SWE indices have much narrower ranges in the Bowen ratio in high SWE/last melt years.

Composites of pentad Bowen ratio values from seven anomalously high and low SWE years during 1979-2009 are different in Bowen ratio amount and timing in the AZ and NM averaging regions (Figure 53). In the NM averaging region, the mean annual Bowen ratio for low SWE years was 1.8 $\pm$ 0.4, in high SWE years it was 1.9 $\pm$ 0.5. In the AZ averaging region, mean annual Bowen ratio for low SWE years was 3.8 $\pm$ 1.2, the Bowen ratio was 3.2 $\pm$ 1.2 for high SWE years. In NM, the Bowen ratio during low SWE years peaks in early June while the Bowen ratio in high SWE years peaks in mid June (Figure 53). In low SWE years, the Bowen ratio falls sharply from its peak until mid July, while the Bowen ratio in high SWE years does not. These two differences in Bowen ratio timing happen near the time of climatological monsoon onset in late June (Figure 53).

We examined the spatial distributions of correlations between interim period Bowen ratio and MAM mean temperature, interim period soil moisture and the two SWE indices. MAM temperature and interim period Bowen ratio have the most strong and coherent

positive relationship in the highest elevations of Arizona (r = 0.5 to 0.7) (Figure 54). Last SWE date has the strongest relationship with the Bowen ratio in northern and eastern New Mexico (r = -0.35 to -0.65), but not in Colorado (Figure 54). Regions of strongest correlation between the Bowen ratio and maximum SWE (r = -0.35 to - 0.65) overlap with the strongest correlations of Bowen ratio and last SWE, but also include some of the Colorado high elevations (Figure 55).

The strongest relationship out of all of the Bowen ratio correlations is soil moisture (Figure 57) (r = -0.8 to - 0.95). There are strong negative relationships between the Bowen ratio and soil moisture throughout New Mexico, include the high elevations and into northern Arizona (Figure 57). The relationship between the Bowen ratio and soil moisture is weaker in a concentrated area of the Arizona high elevations and in the highest elevations of Colorado (r = -0.35 to - 0.65) (Figure 57). Those regions in Colorado are where maximum SWE has the strongest relationship with interim period Bowen ratio (Figure 52).

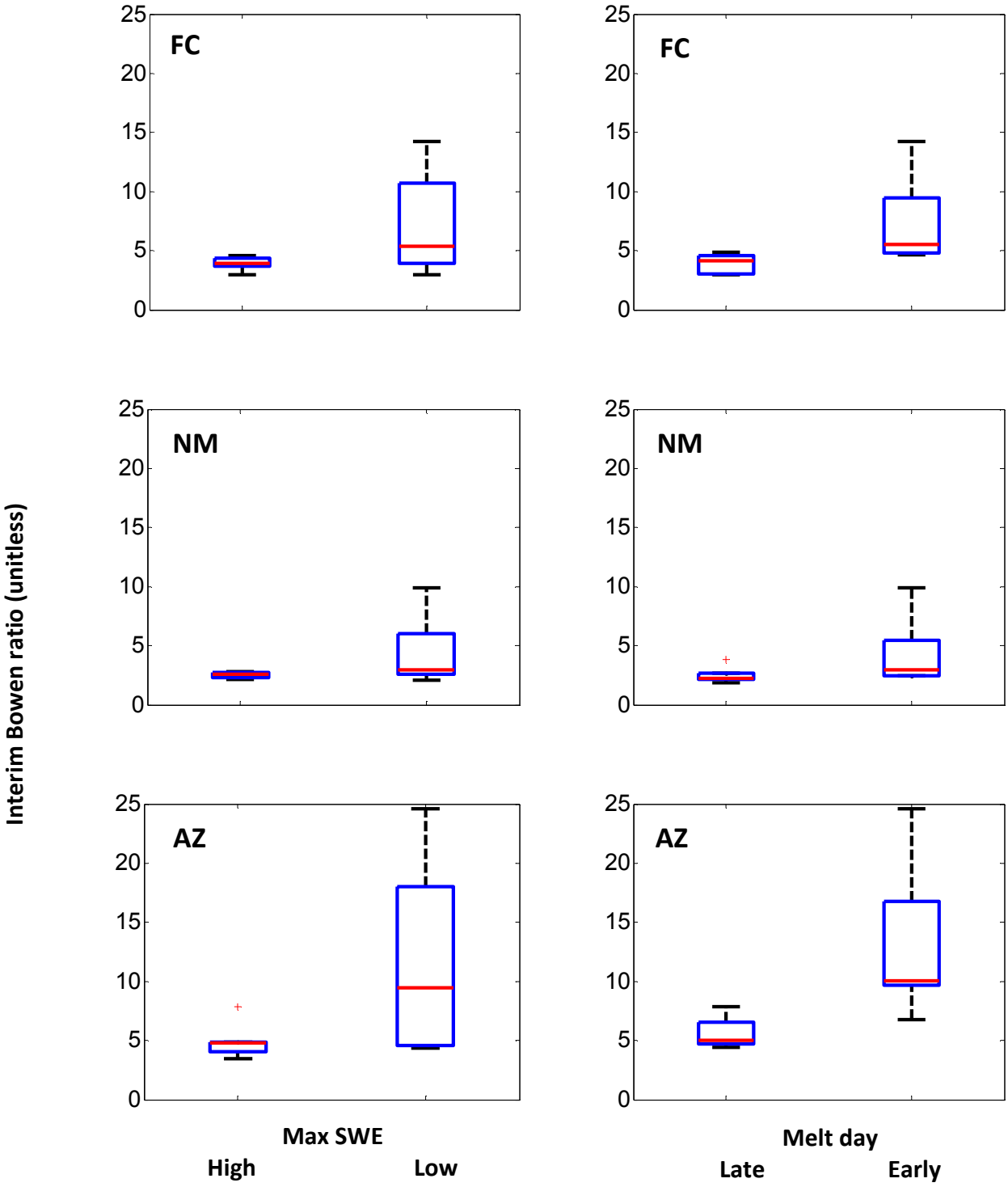

Figure 52. NLDAS-2 interim Bowen ratio composites based on 6 years each late and early SWE melt and 6 years each high and low maximum SWE from the 1980-2008 period.

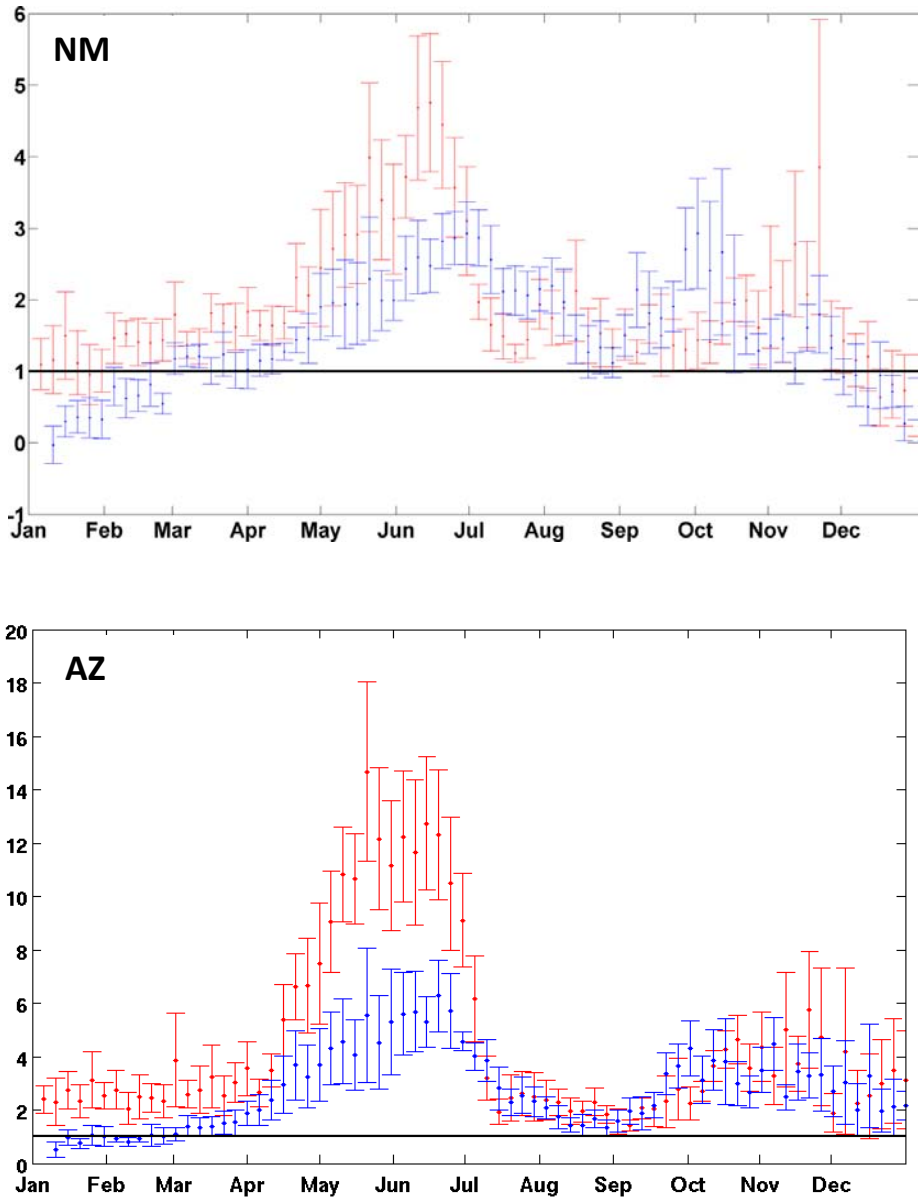

Figure 53. NM and AZ pentad Bowen ratio composited around 6 years of SWE anomalies based on max SWE PC from the 1979-2009 period. (Red = Low SWE, Blue = High SWE).

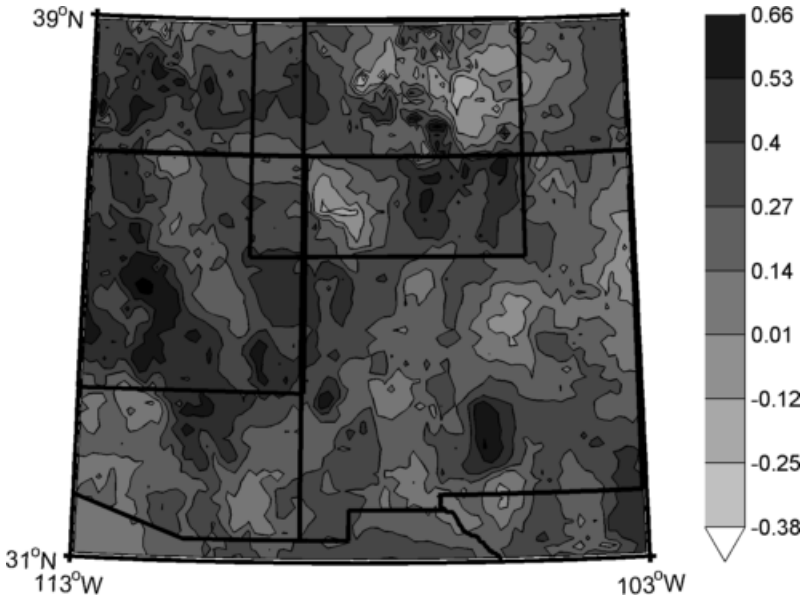

Figure 54. NLDAS-2 MAM mean temperature vs. NLDAS-2 interim Bowen ratio (1980-2008, n=29). Contours represent r-values.

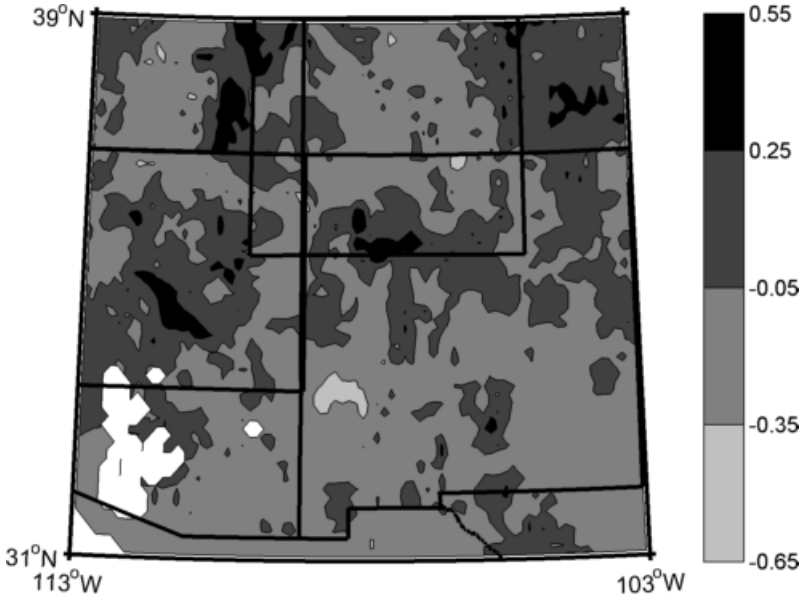

Figure 55. NLDAS-2 max SWE versus NLDAS-2 interim Bowen ratio (1980-2008, n=29). Contours represent r values.

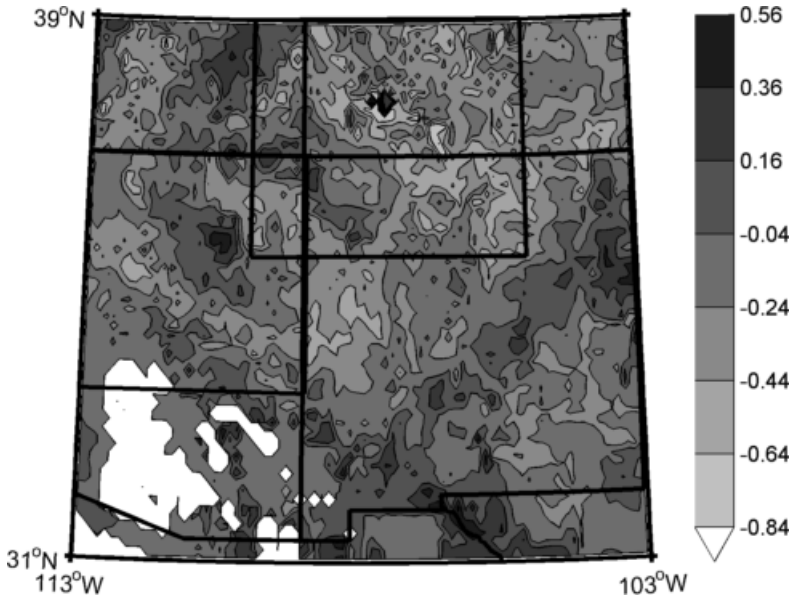

Figure 56. NLDAS-2 last SWE versus NLDAS-2 interim Bowen ratio (1980-2008, n=29). Contours represent r values.

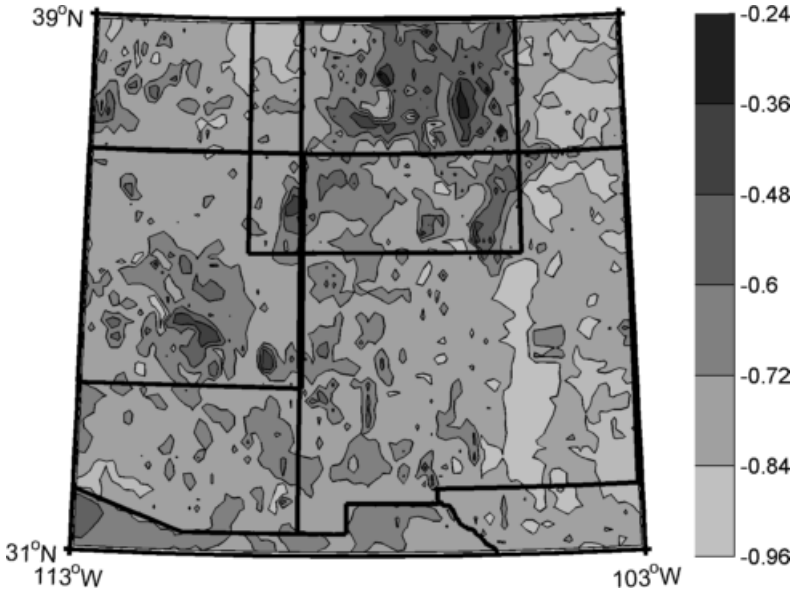

Figure 57. NLDAS-2 interim soil moisture versus interim Bowen ratio. (1980-2008, n=29). Contours represent r values.

Energy budget analysis

We show composite differences in sensible heat flux and latent heat flux for 1979-2009, based on six high and low SWE years (Figure 58, Table 11 and Figure 59, Table 12). In the NM averaging region differences in latent heat associated with extreme maximum SWE years are greatest between mid-May and early June (Figure 58). During this time, differences in latent heat and sensible heat are similar. Differences in latent and sensible heat disappear around the time of monsoon onset, and during July, decreased sensible heat flux is associated with high SWE years and increased heat flux is associated with low SWE years.

In the AZ averaging region, differences in latent and sensible heat flux associated with SWE extremes are larger than those in the NM averaging region, until the time of monsoon onset (Figure 59). Differences in both latent and sensible heat flux begin in January and persist until late June, with the largest differences in both variables occurring in May and June.

In the NM averaging region, mean annual net radiation is 1.3 ± 1.85 W/m^2 higher in high SWE years compared to low SWE years (Table 11) and total turbulent flux to the atmosphere is -2.5 ± 2.3 W/m^2 lower in low SWE years compared to high SWE years (Table 11). In the AZ averaging region, mean annual net radiation is 2.1 ± 1.3 W/m^2 higher in high SWE years compared to low SWE years and total turbulent flux to the atmosphere is 1.7 ± 1.5 W/m^2 higher in high SWE years compared to low SWE years. Due to the small sample sizes used for these composites, the uncertainties in these differences are large.

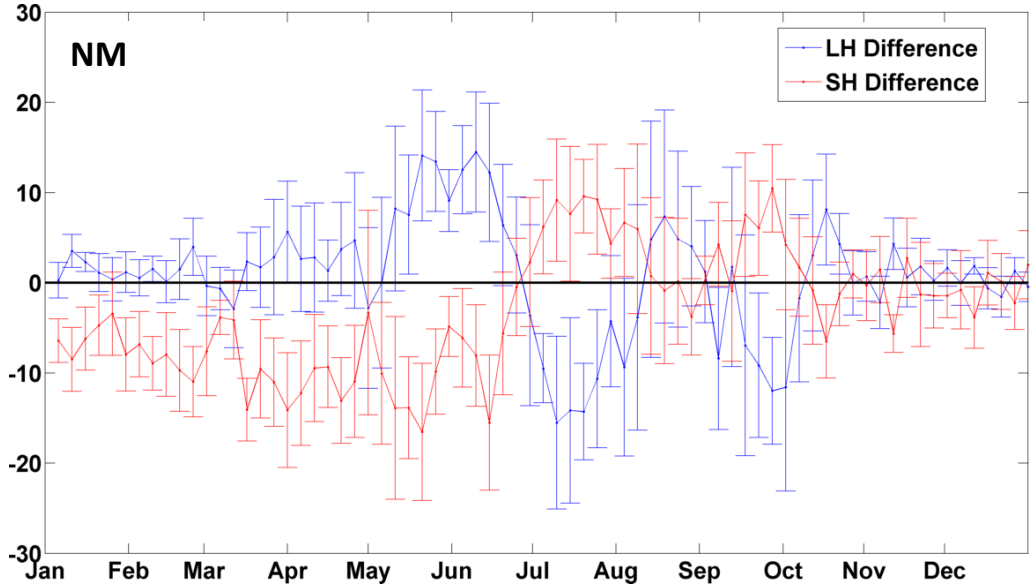

Figure 58. NM averaging region composite difference (high SWE – low SWE) latent heat flux and sensible heat flux, based on 6 years of high and low maximum SWE anomalies. Error bars represent 1 standard error.

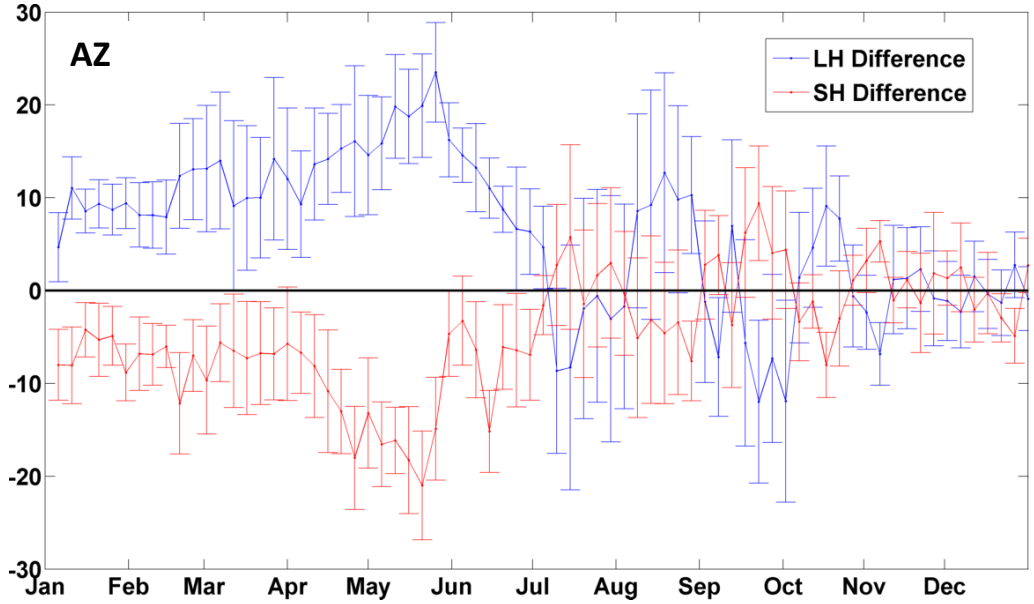

Figure 59. AZ averaging region composite difference (high SWE – low SWE) latent heat flux and sensible heat flux, based on 6 years of high and low maximum SWE anomalies. Error bars represent one standard error.

Table 11. Mean annual values ± 1 standard error (W/m^2) of NLDAS-2 energy budget components for the NM region (figure 58), for climatology, high NLDAS-2 max SWE composites and low SWE composites (7 years each).

NM	Climatol.	High SWE	Low SWE	Difference (High-Low)
Net Rad.	67.1±18.1	67.3±18.2	66.0±18.1	1.3±1.9
LE	29.6±5.9	28.6±5.52	27.9±5.8	0.7±2.6
SH	41.6±16.5	40.8±16.8	44.0±16.4	-3.2±1.8
Bowen	1.28±0.23	1.25±0.26	1.50±0.30	-0.25±0.2
Total SH+LE	71.1±3.18	69.4±16.8	71.9±2.1	-2.5±2.3

Table 12. Mean annual values ± 1 standard error (W/m^2) of NLDAS-2 energy budget components for the AZ region (figure 59), for climatology, high NLDAS-2 max SWE composites and low SWE composites (7 years each).

AZ	Climatol.	High SWE	Low SWE	Difference (High-Low)
Net Rad.	75.8±16.8	76.2±17.0	74.1±16.9	2.1±1.3
LE	26.4±4.5	27.8±4.8	21.8±5.0	6.2±3.4
SH	54.8±12.9	53.1±12.4	57.6±13.5	-4.5±2.6
Bowen	2.19±0.63	2.0±0.45	3.2±1.1	-1.2±0.82
Total SH+LE	80.8±15.0	81.1±15.4	79.4±15.1	1.7±1.5

Summary of results

As expected, both latent heat and sensible heat fluxes are very strongly correlated with soil moisture in NDLAS-2. Composite analysis of the effects of the two SWE indices on interim latent heat flux show that latent heat flux associated with extreme high SWE years is higher than latent heat flux associated with low SWE years, though the differences are only statistically significant in the AZ averaging region (Figure 50). Sensible heat flux differences are minor for any averaging region or for either SWE index, and the only

significant difference in mean sensible heat flux occurs for the maximum SWE composite in the AZ averaging region (Figure 51).

There are no significant differences in Bowen ratio composites based on high/low SWE or late/early melt years in NLDAS-2. However, the ranges of values associated with high/late SWE are much narrower than those associated with low/early SWE. Differences in pentad Bowen ratio values associated with high and low SWE years are much greater in the AZ averaging region, starting in May and persisting until the time monsoon onset in late June (Figure 53).

MAM temperature affects the interim Bowen ratio most strongly over the high elevations of the analysis regions, except for where temperature is increasing in Colorado (Figure 54). Snowpack melt date or amount affects the Bowen ratio most strongly outside of regions with high climatological SWE (Figures 55, 56).

Pentad differences in latent and sensible heat flux associated with maximum SWE are largest in the NM averaging region and peak in mid May (Figure 11). Differences in sensible and latent heat flux disappear around the time of monsoon onset and in the NM averaging region the differences change sign from late June to late July. There are mean annual differences in net radiation and total turbulent flux associated with extreme SWE years but the uncertainties are large (Tables 11, 12).

7. DISCUSSION AND CONCLUSIONS

We have used a new land surface data-product, NLDAS-2, to describe the effects of snowpack on interannual variability and trends in the land surface hydroclimatology of the southwestern U.S. We have analyzed SWE, soil moisture and turbulent fluxes; these variables are notoriously difficult to model and nearly impossible to ground-truth with confidence over large, mountainous regions. Before considering the implications of our results, we review some of the known biases in NLDAS-2 SWE and soil moisture.

Pan et al. (2003) compare NLDAS SWE for all four LSMs to SNOTEL stations in the western United States. NLDAS refers to the Land Data Assimilation System, without specific reference to the time period of system runs, while NLDAS-2 is a specific reference to the second run (1979-present) of the system. Pan et al. (2003) found that all LSMs used in NLDAS underestimate maximum SWE compared to 110 SNOTEL stations in the western United States, with Mosaic underestimating SWE by -59.4% for the entire Pan et al. (2003) study region. However, bias is generally lower (-500mm to 100 mm) in our study area compared to the rest of the regions that Pan et al. (2003) studied. NLDAS precipitation data are also generally low-biased compared to precipitation data from SNOTEL sites.

Schaake et al. (2004) compare simulated soil moisture in the four NLDAS LSM's to in situ soil moisture observations from Illinois. Their focus was largely on intercomparison of the four LSM's rather than validation of any single LSM. Compared to soil moisture data from 17 locations in Illinois, the absolute values of Mosaic total water storage did not agree well with observations, but the linear relationship between the mean water storage values (2 years of data) in the two data sets was strong. Schaake et al. (2004) did find that the Mosaic

LSM has higher and nearly constant values of total water storage capacity, compared to the other three LSMs, over the entire NLDAS domain. This is important because total water storage capacity sets the amount of soil water that can be simulated and Schaake et al.'s (2004) findings suggest that NLDAS-2 is probably not artificially constrained towards modeled soil moisture that is drier than reality.

In chapter 3 of our study, we find that monthly mean NLDAS-2 precipitation and temperature are consistent with surface observations of the same variables over the same time scale (Figures 18 and 25). We also find that NLDAS-2 SWE is biased towards earlier snowmelt when compared to SNOTEL observations, over the averaging regions in this study. However, the bias in melt day and the linear relationship between NLDAS-2 and SNOTEL melt days improves when higher elevation data from NLDAS-2 are compared to SNOTEL (Figure 12). NLDAS-2 captures the trends and variability in cooperative station observations of temperature and an in situ snow course-based index of maximum SWE (Gutzler 2000) (Figures 7 and 18). While there are absolute uncertainties and biases in NLDAS-2, it is still possible to take advantage of the internal consistency among the different variables in NLDAS-2, to examine land surface process in a way that cannot be done with direct observations.

Our first analysis question was: What was the spatial and temporal variability in southwestern U.S. spring land surface conditions during 1979-2009? Chapter 3 of this thesis documented trends and covariability of hydroclimatic variables, emphasizing the period between snowmelt and monsoon onset. We identified numerous linear trends in the NLDAS-2 data set. In general, we observed earlier snowpack melt, increasing temperature,

decreasing precipitation, decreasing soil moisture, decreasing latent heat flux, increasing sensible heat flux and an increasing Bowen ratio over the period of record. These trends were not present in every location in the region, but they were dominant features of large spatial averages. The high elevation regions of Arizona consistently showed the strongest warming and drying trends with the high elevations in Utah and New Mexico susceptible to those trends as well.

Large spring temperature increases (+0.8 °C/decade) and large trends towards earlier snow melt (- 17 days/decade) are concurrent over the 1979-2009 period, when averaged over the southwest United States. The trend towards earlier snowmelt in the Four Corners region is consistent with a number of other studies that have found similar trends elsewhere in the western U.S. (Stewart et al. 2004, Hamlet et al. 2005, Mote et al. 2005). Maximum SWE amount has a small and statistically insignificant decreasing trend (-12 kg/m^2/decade).

The trend towards earlier snowmelt in NLDAS-2 is difficult to corroborate with SNOTEL data because the trend appears most prominently along the margins of climatological snowpack. The existing in situ SNOTEL network is deliberately designed to measure snowpack in locations with high climatological snowpack and is not situated to detect changes in marginal, lower elevation snowpack about which other authors have expressed concern (Hamlet et al. 2005). However, selecting NLDAS-2 spatial averages with elevation distributions that are similar to the SNOTEL network reduces the linear trend towards earlier snowmelt and demonstrates the elevation dependence of snowmelt trends. The presence of trends towards earlier snowmelt in NLDAS-2 suggests that the current in situ

snow monitoring network does not provide sufficient coverage for detecting current climate change signals in the Southwest's marginal snowpack.

As shown in chapter 3, small decreases in total winter precipitation are also present over 1979-2009 (up to -0.39 cm monthly total/decade) but their impacts on snowpack are less than those of temperature. Composite analyses in chapter 4 show that maximum SWE is influenced by both MAM temperature (Figure 38) and JFM precipitation (Figure 39). In composite analyses based on SWE melt day, there are no significant differences between JFM precipitation associated with years having extreme early and late SWE melt days. MAM temperature, however, is associated with significant differences in SWE melt date. The extreme trends in NLDAS-2 SWE melt date are attributed to temperature trends, while temperature effects on maximum SWE are buffered by precipitation variability.

This brings us to the second question in this analysis: How does interannual variability of spring snowpack affect the amount and timing of warm season soil moisture in the southwestern U.S.? Large, decreasing trends in soil moisture are present throughout the study region (-3.5 kg/m^2/decade), as shown in chapter 3. Though there are large trends in the last day of SWE, interim period soil moisture is more strongly correlated with the maximum amount of snowpack, MAM temperature and interim period precipitation, than SWE melt out day. Composite analyses in chapter 5 also show that soil moisture differences are greater in years associated with high or low SWE than in years associated with early or late snowmelt (Figure 47). Therefore, the large post-snowmelt, pre monsoon-onset declines in soil moisture shown in this study are primarily spring temperature-driven, with a significant contribution to variability from the maximum amount of snowpack. The dual

importance of temperature and snowpack in determining spring soil moisture suggests that projected declines in southwest U.S. snowpack will lead to severely depleted soil moisture before monsoon onset.

Soil moisture persistence is an important consideration in the context of this study because in chapter 6 we show that soil moisture influences land memory, to some extent, through latent heat fluxes, at least until monsoon onset. Koster and Suarez (2001) point out that land memory associated with soil moisture can provide the primary source of forecasting skill for summer precipitation. While the land memory that we have identified in the southwestern U.S. would not likely provide a high level of precipitation forecasting skill and is confounded by the North American monsoon, it does raise questions about how land memory could change in the future and whether or not monitoring soil moisture persistence would help us better predict those changes.

The third research question addresses how snowpack anomalies influence the surface energy budget throughout the warm season. In NLDAS-2, soil moisture strongly controls both latent and sensible heat fluxes. Any process that alters SWE-mediated soil moisture will change surface turbulent fluxes as well. As shown in chapter 3, latent heat flux in NLDAS-2 is declining over the southwest U.S (-10 W/m^2/decade), especially in high elevation regions and during the spring season. Sensible heat flux is also increasing over the same region (+6.9 W/m^2/decade), but the trends in sensible heat flux are not significant. Significant increases in the Bowen ratio also occur over the same period, though the largest increasing trends in the Bowen ratio occur primarily in Arizona (Figure 37d). The co-correlation of snowpack, temperature and soil moisture over the interim period in this

study makes it difficult to determine the relative contributions of trends in those variables to turbulent fluxes.

However, in chapter 6, composites based on years of extreme maximum snow water equivalent do yield significant differences in post snow ablation and pre monsoon onset latent heat flux, only for the AZ averaging region (Figure 50). Significant differences in sensible heat flux using the same composites are also found only in AZ (Figure 51). This may be due to the more extreme temperatures that are associated with extreme maximum SWE years in AZ, compared to the other averaging regions (Figure 38). While latent heat flux values associated with extreme maximum SWE years are only slightly higher than latent heat flux values associated with low maximum SWE years, the range of latent heat flux values associated with low SWE is much narrower than those associated with high SWE. The same pattern occurs in sensible heat flux and Bowen ratio composites (Figures 50 and 51). According to the composites, years in which snowpack was low are less predictable with regards to the surface fluxes than years in which snowpack was high.

If the warming and drying trends in NLDAS-2 are real and if they are representative of the future, our composites indicate that snowpack-mediated surface hydrology will be constrained not only towards earlier melt but also towards decreased soil moisture and thus a lower latent heat flux and higher Bowen ratio. High snowpack/late melt years do not promise abundant soil moisture and high evaporation but low SWE anomalies are much more likely to lead to a warmer, drier surface. While monsoon onset negates these effects later in the year, decreased snowpack will likely exacerbate temperature-driven warming and drying months after the complete ablation of snowpack.

While land surface - atmosphere feedbacks cannot be assessed directly from these data, the results from this study provide a data-based starting point for testing hypotheses about potential land surface-atmosphere feedbacks in the southwestern U.S. First, our data seem to suggest that the initial conditions for a positive SWE-mediated soil moisture-rainfall feedback as proposed by Zheng and Eltahir (1998) may be present in high SWE years, at least over part of the region. There are also signals in our analysis that are suggestive of a Gutzler(2000) type feedback where differences in latent and sensible heat fluxes associated with extreme snowpack years become opposite in sign after monsoon onset, relative to pre-monsoon onset. We do not know if soil moisture anomalies in our region are large enough spatially or have if they have sufficient magnitude to generate such a feedback. However, our findings could provide quantitative guidance for modeling experiments in which SWE and soil moisture are manipulated, and the effects on moist static energy and convection are observed. This could provide further insight into whether or not projected long-term SWE declines in the southwestern U.S. will translate into enhanced aridity through a reduction in available moisture for recycling in later months.

The annual incursion of the North American monsoon into the southwestern U.S. means that considerations of soil moisture-rainfall feedbacks are necessarily more complicated than those proposed by Zheng and Eltahir (1998). We have shown that anomalously high SWE years produce the initial land surface conditions (lower surface temperature, higher soil moisture) that are necessary for a negative SWE-monsoon feedback to occur. However, the sizes of the effects that we have found are not tremendous. An interesting question arises from considering both the Zheng and Eltahir (1998) and the Gutzler (2000)

hypotheses: If both of these processes operate to some extent in our region, is there a threshold of snowpack decline that will reduce local, pre-monsoon onset surface moisture to a point that it negatively impacts monsoonal precipitation in the following summer?

A final consideration associated with declining snowpack is ecological in nature. While NLDAS-2 Mosaic represents vegetation, it does not do so interactively. Even so, vegetation is an important component of the land-surface system and merits consideration in the context of our results. Work such as that by Breshears et al. (2005) documents recent vegetation die-offs in the southwestern United States, and associated large-scale drought and high temperature anomalies. Anderson-Teixeira and Litvak (2011) find that temperature and water availability strongly affect the ability of New Mexico ecosystems to sequester and store carbon. While surface soil moisture in this analysis is "reset" during the monsoon season, it is not clear how spring soil moisture depletion affects long-term deep soil moisture storage or how this contributes to ecological drought and the potential for reduced regional carbon dioxide uptake by vegetation.

Using NLDAS -2, we have demonstrated how snowpack changes may alter surface hydroclimatology in the southwestern U.S. Our results are consistent with those of numerous other studies, but it is not possible to fully confirm with in situ observations that the Southwest U.S. has experienced the precise spatial and temporal variability in soil moisture and surface fluxes shown here. However, we do not suggest the expectation of exact quantities of relative soil moisture and surface fluxes based on a specific decrease in spring snowpack.

Rather, this study is a starting point with which to assess how snowpack - modulated changes in the land surface may proceed under trends such as those reported here. NLDAS-2 provides a unique opportunity to consider potential large-scale interactions of land surface hydrologic variables. With additional quantification of how the land surface behaves under changing climate conditions, we may be better able to anticipate future land surface variability and feedbacks and assess model projections with a better foundation of results from current climate change.

REFERENCES

Anderson-Teixeira, K. J.**,** and M. Litvak, 2011: Differential responses of production and respiration to temperature and moisture drive the carbon balance across a climatic gradient in New Mexico. ***Global Change Biology,*** 17, **410-424.**

Barnett, T. P., et al., 2008: Human-Induced changes in the hydrology of the Western United States, *Science*, **319,** 1080-1083.

Breshears D*,* Myers O*,* Meyer C.W. **et al**., 2009*:* Tree die-off in response to global change-type drought*:* mortality insights from a decade of plant water potential measurements. *Frontiers in Ecology and the Environment***, *7*,** 185–189*.*

Cayan, D. R., 1996: Interannual climate variability and snowpack in the western United States. *J. Climate,* **9**, 928–948.

Cayan, D. R., T. Das, D. W. Pierce, T. P. Barnett, M. Tyree, and A. Gershunov, 2010: Climate change and water in Southwestern North America special feature: Future dryness in the southwest US and the hydrology of the early 21st century drought. *Proc. Natl. Acad. Sci. USA*. **107,** 21271-21276*.*

Eltahir, E. A. B. and R. L. Bras, 1996: Precipitation recycling, *Rev. Geophys.*, **34,** 367-379.

Fischer, E. M. and S. I. Seneviratne, 2007: Soil moisture–atmosphere interactions during the 2003 European summer heat wave, *J. Climate,* **20,** 5081-5099.

Guttman, N. B. and R. G. Quayle, 1996: A historical perspective of U. S. climate divisions, *Bull. Amer. Met. Soc.,* **77,** 293-303.

Gutzler, D. S. and J. W. Preston, 1997: Evidence for a relationship between spring snow cover in North America and summer rainfall in New Mexico. *Geophys. Res. Lett.,* **24,** 2207-2010.

Gutzler, D. S., 2000: Covariability of spring snowpack and summer rainfall across the Southwest United States. *J. Climate*, **13**, 4018–4027.

Gutzler, D.S., and T.O. Robbins, 2010: Climate variability and projected change in the western United States: Regional downscaling and drought statistics, *Climate Dynamics*, DOI 10.1007/s00382-010-0838-7, 2010.

Hamlet, A. F., P. W. Mote, M. P. Clark, D. P. Lettenmaier, 2005: Effects of temperature and precipitation variability on snowpack trends in the Western United States. *J. Climate*, **18,** 4545-4561.

Hansen, M.C., R.S. DeFries, J.R.G. Townshend, and R. Sohlberg, 2000: Global land cover classification at 1km spatial resolution using a classification tree approach, *International Journal of Remote Sensing*, **21,** 1331-1364.

Higgins, P., 2008: An index of the onset of the North American monsoon season in central New Mexico. B.S. thesis, Dept of Earth & Planetary Sciences, Univ of New Mexico, 35 pp (unpublished).

Knowles, N., M. D. Dettinger, and D. R. Cayan, 2006: Trends in snowfall versus rainfall in the western United States. *J. Climate*, **19**, 4545–4559.

Koster, R. D., and M. J. Suarez (1996), Energy and water balance calculations in the Mosaic LSM, NASA Tech. Memo., 104606, vol. 9, 58 pp.

Koster, R. D., M. J. Suarez, 2001: Soil Moisture memory in climate models. *J. Hydrometeor.*, **2**, 558–570.

Lo, F. M.P. Clark, 2002: Relationships between spring snow mass and summer precipitation in the Southwestern United States associated with the North American Monsoon system. *J. Climate*, **15**, 1378–1385.

Mitchell, K. E., et al., 2004: The multi-institution North American Land Data Assimilation System (NLDAS): Utilizing multiple GCIP products and partners in a continental distributed hydrological modeling system. *J. Geophys. Res.*, **109,** D07S90.

Molotch, N. P., P. D. Brooks, S. P. Burns, M. Litvak, R. K. Monson, J. R. McConnell, and K.Musselman, 2009: Ecohydrological controls on snowmelt partitioning in mixed-conifer sub-alpine forests. *Ecohydrology*, **2,** 129–142.

Mote P. W., A. F. Hamlet and D.P. Lettenmaier. 2005: Variability and trends in mountain snowpack in Western North America. *Bulletin of the American Meteorological Society*, **86**, 39-49.

Pal, J. and E. A. B. Eltahir, 2001: Pathways relating soil moisture conditions to future summer rainfall within a model of the land-atmosphere system, *J. Climate*, **14,** 1227-1242.

Pan, M., et al., 2003: Snow process modeling in the North American Land Data Assimilation System (NLDAS): 2. Evaluation of model simulated snow water equivalent, *J. Geophys. Res.,* **108,** 8850.

Schaake, J. C., et al., 2004: An intercomparison of soil moisture fields in the North American Land Data Assimilation System (NLDAS), *J. Geophys. Res.*, **109**, D01S90.

Serreze, M. C., M. P. Clark, R. L. Armstrong, D. A. McGinnis, R. S. Pulwarty, 1999: Characteristics of the western United States snowpack from snowpack telemetry (SNOTEL) data. *Water Resources Research,* **35,** 2145-2160.

Stewart, T., D. R. Cayan, M. D. Dettinger, 2004: Changes toward Earlier streamflow timing across western North America. *J. Climate*, **18,** 1136–1155.

Zheng, X. and E. A. B. Eltahir, 1998: A soil moisture - rainfall feedback mechanism, 2. Numerical experiments, *Water Resources Research*, **34,** 777-786.

Zhu, C., D. P. Lettenmaier, T. Cavazos, 2005: Role of antecedent land surface conditions on North American monsoon rainfall variability. *J. Climate*, **18**, 3104–3121.